Design And Control Of A Two-column Distillation Process For The Separation Of Homogeneous Binary Azeotropic Mixtures.

INFORMATION TO USERS

This reproduction was made from a copy of a document sent to us for microfilming. While the most advanced technology has been used to photograph and reproduce this document, the quality of the reproduction is heavily dependent upon the quality of the material submitted.

The following explanation of techniques is provided to help clarify markings or notations which may appear on this reproduction.

1. The sign or "target" for pages apparently lacking from the document photographed is "Missing Page(s)". If it was possible to obtain the missing page(s) or section, they are spliced into the film along with adjacent pages. This may have necessitated cutting through an image and duplicating adjacent pages to assure complete continuity.

2. When an image on the film is obliterated with a round black mark, it is an indication of either blurred copy because of movement during exposure, duplicate copy, or copyrighted materials that should not have been filmed. For blurred pages, a good image of the page can be found in the adjacent frame. If copyrighted materials were deleted, a target note will appear listing the pages in the adjacent frame.

3. When a map, drawing or chart, etc., is part of the material being photographed, a definite method of "sectioning" the material has been followed. It is customary to begin filming at the upper left hand corner of a large sheet and to continue from left to right in equal sections with small overlaps. If necessary, sectioning is continued again–beginning below the first row and continuing on until complete.

4. For illustrations that cannot be satisfactorily reproduced by xerographic means, photographic prints can be purchased at additional cost and inserted into your xerographic copy. These prints are available upon request from the Dissertations Customer Services Department.

5. Some pages in any document may have indistinct print. In all cases the best available copy has been filmed.

University Microfilms International
300 N. Zeeb Road
Ann Arbor, MI 48106

Abu-Eishah, Samir Ibraheem

DESIGN AND CONTROL OF A TWO-COLUMN DISTILLATION PROCESS FOR THE SEPARATION OF HOMOGENEOUS BINARY AZEOTROPIC MIXTURES

Lehigh University PH.D. 1983

DESIGN AND CONTROL OF A TWO-COLUMN DISTILLATION PROCESS FOR THE SEPARATION OF HOMOGENEOUS BINARY AZEOTROPIC MIXTURES

by

Samir I. Abu-Eishah

A Dissertation

Presented to the Graduate Committee

of Lehigh University

in Candidacy for the Degree of

Doctor of Philosophy

in

Chemical Engineering

Lehigh University

1982

In the Name of God, Most Gracious, Most Merciful

"O my Lord! Expand me my breast; Ease
my task for me; and remove the impediment
from my speech, so they may understand
what I say"

The Glorious Quráan
(Sura 20)

CERTIFICATE OF APPROVAL

Approved and recommended for acceptance as a dissertation in partial fulfillment of the requirements for the degree of Doctor of Philosophy.

10/19/82
(date)

William L Luyben
Professor in Charge

Accepted 10/19/82
(date)

Special committee directing the doctoral work of Mr. Samir I. Abu-Eishah

William L Luyben
Chairman
Dr. W. L. Luyben

Robert B. Akell
Mr. R. B. Akell

C W Clump
Dr. C. W. Clump

Fred P. Stein
Dr. F. P. Stein

Robert E. Vallerschamp
Dr. R. E. Vallerschamp

ACKNOWLEDGEMENTS

I would like to thank Dr. W. L. Luyben for his invaluable advice and encouragement during the course of this work. I would also like to thank the members of my special committee for their helpful advice and comments.

I am especially grateful to my parents, my wife and my children, Mojahed, Hidayah, Moayyad and my newborn daughter, Manal for their love and continued encouragement, without which the completion of this dissertation would have been impossible.

I would like to express my gratitude to Yarmonk University (Jordan) for providing me with the full scholarship which made it possible for me to continue my graduate studies and complete this work.

TABLE OF CONTENTS

LIST OF FIGURES

LIST OF TABLES

NOMENCLATURE

A	Heat transfer area, cm^2
A_i	1st constant in Antoine equation for component i
A_{ij}	Parameter in Wilson equation
A_t	Tray area, m^2
b	Difference point on enthalpy-composition diagram
B	Bottom product flow rate, gmol/hr
B_i	2nd constant in Antoine equation for component i
C_c	Cost of cooling water $/1000 gal.
C_{cw}	Annual cost of cooling water, $/year
c_i	1st constant in heat capacity equation
C_i	3rd constant in Antoine equation for component i
C_p	Heat capacity at constant pressure, cal/gmol°C
C_s	Cost of steam, $/1000 lbs.
C_{st}	Annual cost of steam, $/year
C_v	Heat capacity at constant volume, cal/gmol°C
d_i	2nd constant in heat capacity equation
D	Distillate flow rate, gmol/hr
D_c	Column diameter, cm
E_j	Efficiency of joints, Equation (7-5), fraction

F	Feed flow rate, gmol/hr
FC	Flow controller
FT	Flow transmitter
h	Liquid enthalpy, cal/gmol
h_B	Bottom product enthalpy, cal/gmol
h_D	Distillate enthalpy, cal/gmol
h_F	Feed enthalpy, cal/gmol
h_I	Difference point used in Equations (4-12) and (4-13)
H	Vapor enthalpy, cal/gmol
H_{NT}	Top tray vapor enthalpy, cal/gmol
H_{VB}	Bottoms vapor enthalpy, cal/gmol
H_y	Operation period per year, hr/year
K_c	Controller gain, dimensionless
K_i	K value for component i
K_p	Process gain, dimensionless
L	Liquid flow rate, gmol/hr, Log modulus in Bode plots
LC	Level controller
M	Tray holdup, gmol
M_{Wi}	Molecular weight of component i
$\bar{M}_W$	Average molecular weight of a mixture
M_V	Volumetric tray holdup, m^3

N_F	Feed tray
N_T	Total number of trays
P	Pressure
p_i^s	Vapor pressure of component i, mmHg
P_d	Compressor discharge pressure, atm.
P_r	Reduced pressure
P_s	Compressor suction pressure, atm.
P_u	Ultimate period, min.
PC	Pressure controller
Q	Heat duty, cal/hr
Q_C	Condenser heat duty, cal/hr
Q_R	Reboiler heat duty, cal/hr
Q_T	Total energy required by the system, cal/hr
Q_{Tm}	Minimum total energy required by the system, cal/hr
r_i	Inside radius of the shell before corrosion allowance is added, in.
R	Reflux flow rate, gmol/hr
RC	Ratio controller
R_{min}	Minimum reflux flow rate, gmol/hr
RR	Reflux ratio
RR_{min}	Minimum reflux ratio
S	Maximum allowable working stress, psi

t,T	Temperature, °C and °K, respectively
t_c	Corrosion allowance, in.
t_s	Shell thickness, in.
T_b	Boiling point, °K
T_c	Critical temperature, °K
T_d	Compressor discharge temperature, °K
T_F,T_{FP}	Feed temperature before and after preheaters, °C
T_r	Reduced temperature
T_s	Compressor suction temperature, °K
TC	Temperature controller
TT	Temperature transmitter
U	Overall heat transfer coefficient, cal/hr cm^2°C
U_{VN}	Net vapor velocity, cm/sec
v^{ℓ}	Molar liquid volume, cm^3/gmol
V	Vapor flow rate, gmol/hr
V_B	Vapor flow rate from bottom of the column, gmol/hr.
W	Work required by the compressor, cal/hr
WEP_i	Wilson energy parameter for component i
W_h	Weir height, m
W_{ℓ}	Weir length, m
x	Liquid composition, mole fraction
x_B	Bottoms composition, mole fraction
x_D	Distillate composition, mole fraction

y Vapor composition, mole fraction

y_B Vapor composition from bottom of the column, mole fraction

y_D Vapor composition of distillate, mole fraction

Z_F Feed Composition, mole fraction

Other Symbols

β RR/RR_{min}

γ Activity coefficient

ε Convergence tolerance

θ Phase angle, degrees

κ $= C_p/C_v$

λ Latent heat of vaporization, cal/gmol

π $= 3.14156$

ρ_ℓ Liquid density, g/cc

ρ_v Vapor density, g/cc

Δ Difference

$\sum$ Sum

τ_I Time constant of controller, min.

τ_p Time constant of process, min.

τ_Z Time constant of a lead function, min.

ω Ultimate frequency, rad/min.

ABSTRACT

The steady-state design and the dynamics and control of a two-column distillation system operating at two different pressures have been studied through digital simulation. Tetrahydrofuran-water azeotrope separation was used as an example.

The effect of various design parameters on the two-column system and its energy requirement have been studied. The low-pressure column was found to be more sensitive to changes in reflux ratio and distillate composition than the high-pressure column. Reducing the first column pressure and/or increasing that of the second column was found to require less energy.

Energy integration, using the second column overhead vapor to reboil the first column, has been explored at various pressures and found to save up to 30% of the total energy required. It was also found that there is always a combination of the pressures of the columns that minimizes the total energy required by the system. Preheating the feeds of the columns via hot product streams was found to save up to 10% of the total energy required. Operating the first column at P_1 = 350 mmHg and the second column at P_2 = 150 psig was found to be the optimum pressure case. Applying energy integration and heat economizers on this case was found to save up to 55% of the energy used in the standard industrial configuration, using pressures of P_1 = 760 mmHg and P_2 = 100 psig and preheating feed with the

bottoms product of the first column. Optimum reflux ratios were found to lie in the range of 1.2 to 1.5 times the minimum reflux ratio.

A dynamic model for the heat integrated system was developed and used to study the dynamic behavior of the system. A control scheme to control indirectly the two-bottom product compositions has been developed. The temperature on a control tray was controlled by manipulating the heat input to the reboilers. The ratios of the reflux to distillate and reflux to feed were used in the first and second columns, respectively, to minimize energy consumption. The performance of that scheme was examined for various disturbances in feed rate and composition. Its dynamic effectiveness was found to be as good as or better than a constant reflux scheme and Shinskey's material-balance scheme. It also was the most energy efficient.

CHAPTER 1

INTRODUCTION

1.1 Dissertation Outline

This chapter gives a brief introduction about pressure distillation and the scope of this work. Chapter 2 deals with the background of azeotropic separation while Chapter 3 includes the physical and thermodynamic properties of the THF-water system. Chapters 4-7 deal with the steady-state aspects of the system in the same order outlined in Section 1.3. Chapters 8 and 9 cover the simulation and control part of this work and Chapter 10 gives conclusions and recommendations.

1.2 Pressure Distillation

Pressure distillation, using two columns operating at two different pressures, is one of the simplest and most economical techniques for the separation of homogeneous binary azeotropes [5,45], provided that a substantial shift in the composition of the azeotrope occurs when the pressure is changed. In this case, the distillate from the low pressure column is fed to the high pressure column whose distillate is recycled to the first column. The products are taken from the bottom of the columns. The specific system studied as an example was tetrahydrofuran-water system.

Tetrahydrofuran (THF) forms a homogeneous, minimum boiling azeotrope with water. As the pressure is raised, for example, from

0 to 100 psig, the concentration of water in the azeotrope will increase from 5.3 to 12.0 wt. % [5,37].

While pressure distillation is capable of producing drier solvent than any other common drying methods, the degree of dryness obtained is determined by the design of the high pressure column [5]. Therefore, in order to have a good design of the separation units, very accurate physical and thermodynamic data are required. In this work, we propose the use of Wilson's equations [46] to predict the vapor-liquid equilibrium data for the THF-water system as a function of pressure, based on the available VLE data at 0 and 100 psig. Other physical properties are available in literature.

Yoshida et al [47], du Pont [5] and Shinskey [37] proposed the use of two columns to separate the THF-water system at two different pressures, ranging from 200 mmHg to 1 atm. in the first column and from 55 to 150 psig in the second. For the design of this system, each column is essentially a binary distillation column where the relationships usually used for conventional columns design are applicable [1,37].

For the THF-water system, Shinskey [37] states that the material balances for the two columns are very sensitive to the actual overhead compositions of each column. In order to avoid positive feedback effect on both columns due to changes in distillate composition, he proposed to set reboilers heat duties in proportion to their respective feeds.

For energy integration, Shinskey [37] proposed the use of the overhead vapor of the high-pressure column to reboil the low-pressure column. In order to keep constant pressure in the second column, he proposed to throttle either the vapor entering or condensate leaving the condenser/reboiler. In this case the flow of the high-pressure steam is set proportional to the system-feed flow rate.

Additional saving in energy can be achieved by preheating the columns' feeds via other hot streams in the system. Buckley [3] expects the control of the columns, in this case, to be more difficult than control of conventional columns.

1.3 Scope of Work

In this work, it is intended to cover the following:

(1) Steady-state design of both columns to estimate the total number of trays, optimun feed-tray(s) location and heat loads as a function of system variables, such as feed rate, feed composition, products purities, distillate composition and columns pressure.

(2) Steady-state rating study of the above designed system to explore the effect of changes in feed composition, products purities and columns pressure on the total energy required by the system.

(3) Steady-state energy conservation schemes, such as heat integration, heat economizers and vapor recompression.

(4) Steady-state economic evaluation of various heat conservation schemes.

(5) Simulation of a dynamic model for the system to solve the material and energy balance equations for both columns, simultaneously. This will include tray hydraulics and inefficiencies.

(6) Study of the dynamic behavior of the system for small disturbances, e.g., in feed rate or composition, as a function of time. This will include a comparison of several control schemes.

CHAPTER 2

AZEOTROPIC SEPARATION

2.1 Definitions and Background

An azeotrope is a mixture of two or more liquid compounds whose boiling point does not change as vapor is generated and removed [30]. For an azeotrope, the pressure, for an isothermal section, or the temperature, for an isobaric section, attains a maximum or minimum.

Due to the attraction between a non-ideal mixture molecules, there will be negative deviations from Raoult's law ($\gamma < 1.0$) and the azeotrope will give a higher-temperature boiling mixture than the boiling point of the heavier component. This is known as maximum azeotrope and the pressure will be minimum.

On the other hand, dissimilar molecules repel each other which will result in positive deviations from Raoult's law ($\gamma > 1.0$). In this case, the azeotrope will give a lower-temperature boiling mixture than the boiling point of the lighter component. This is termed as "minimum azeotrope" and the pressure will be maximum.

Smith [40] said that deviation from Raoult's law is not in itself sufficient to cause the occurrence of an azeotrope. The boiling points of the pure components must be sufficiently close together to permit a maximum or minimum to occur.

If the vapor and liquid of a constant-boiling mixture are of the same composition, the two-phase mixture is called a homogeneous azeotrope. Constant-boiling mixtures that occur with a vapor and two or more liquid phases are called heterogeneous azeotropes [11]. With two-component systems at constant pressure, a vapor phase may coexist with two other phases; with a three-component system, a vapor phase may coexist with three other phases.

For homogeneous azeotropes, the relative volatility is unity and separation processes such as simple distillation becomes impossible [1,26,43]. Robinson and Gilliland [34] classify the separation methods of binary azeotropic mixtures into either (1) distillation plus other separation processes, such as decantation, extraction, crystallization or absorption, to get past the azeotropic composition or (2) a modification of the relative volatility by changing the total pressure or adding other components to the mixture.

Treybal [43] said that if the relative volatility of a binary mixture is very low (close or equal to 1.0), the continuous rectification of the mixture to give nearly pure products will require high reflux ratios and correspondingly high heat requirements, as well as towers of large cross section and number of trays. In other cases the formation of a binary azeotrope may make it impossible to produce nearly pure products by ordinary fractionation. Under these circumstances a third component, sometimes called an "entrainer", may be added to the binary mixture to form a new low boiling azeotrope

with one of the original constituents. The entrainer should be volatile relative to the original components so that it may be easily separated. This method is known as "azeotropic distillation".

Sometimes, a third component, termed a "solvent", is added to alter the relative volatility of the original constituents, thus permitting the separation. The added solvent is, however, of low volatility and is itself not appreciably vaporized in the fractionator. This method is known as "extractive distillation".

However, adding an extraneous substance such as an entrainer or solvent to a process is undesirable. Since it can never be completely removed, it adds an undesirable impurity to the products [43]. There are inevitable losses in solvent. An inventory and source of supply must be maintained. Solvent recovery cost can be large, and new problems in choices of materials of construction are introduced. It follows that these processes, i.e., azeotropic and extractive distillation, can be considered only if, despite their drawbacks, the resulting process is less costly than conventional distillation.

By changing the conditions of the distillation process and by using two distillation columns, azeotropes may be separated economically by straight fractional distillation [45]. These are classified as follows:

(1) Homogeneous azeotropes whose compositions are highly sensitive to pressure changes, i.e., the composition of the azeotrope

between two key components changes as the pressure on the system changes.

(2) Heterogeneous azeotropes between components in the mixture which form two liquid phases and one vapor phase at the azeotropic temperature.

2.2 Separation of Homogeneous Azeotropes by Fractionation

If the azeotrope composition varies sufficiently with change in pressure, it is possible to use a two-column fractionation schemes such as shown in Figures (2-1) and (2-2).

The minimum boiling azeotrope may be separated by feeding the mixture of composition Z_F to a column at P_1 and recovering one component (the less volatile), as a bottom product and, essentially, the azeotrope as a distillate product. The distillate is then fed to the other column maintained at a total pressure P_2. The other component (the more volatile) is obtained as a bottom product from the second column. The distillate product from this column, essentially the azeotrope at P_2, is recycled to the first column. See Figure (2-1).

For a maximum azeotrope the pure components are recovered as distillate products. Bottom products, essentially the azeotropes, from one column is fed to the other, as shown in Figure (2-2).

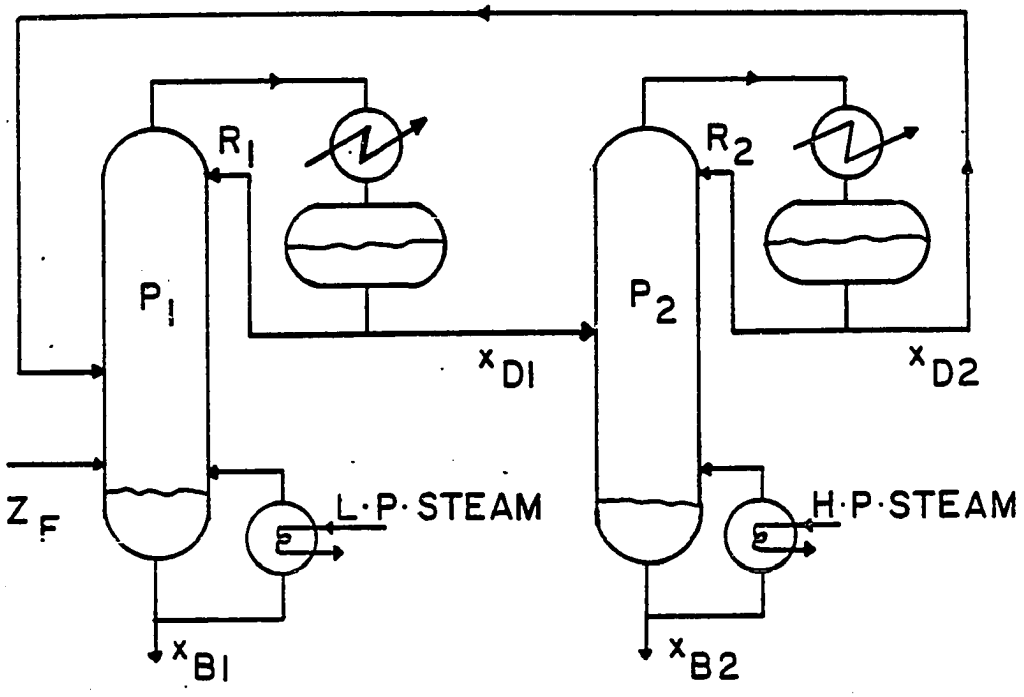

Figure (2-1) - Separation Scheme for Minimum Boiling Azeotrope

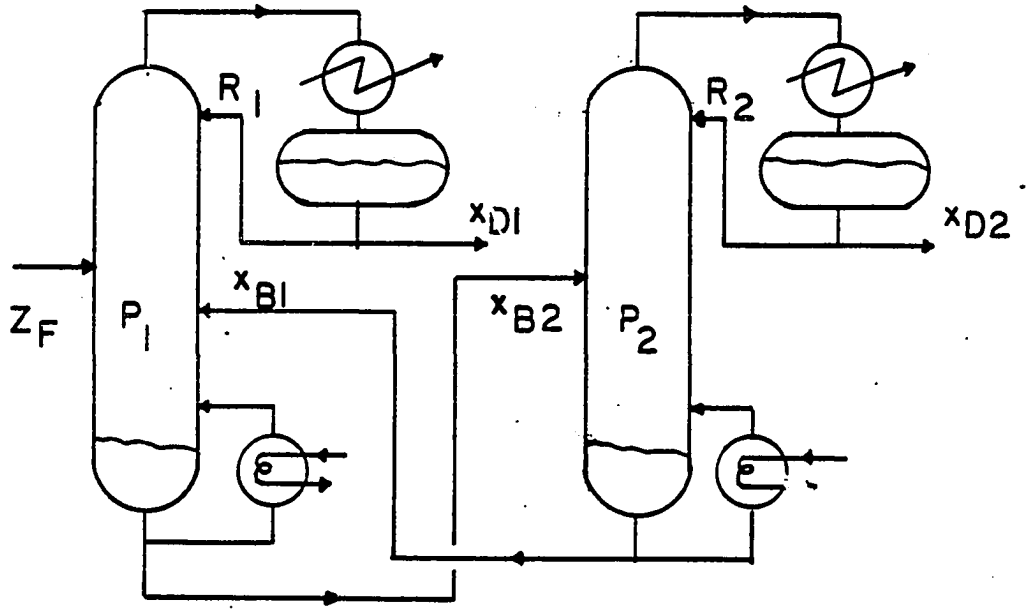

Figure (2-2) - Separation Scheme for Maximum Boiling Azeotrope

2.3 Separation of Heterogeneous Azeotropes by Fractionation

Case I. The feed consists of two liquid phases.

The scheme in this case, as shown in Figure (2-3), consists of introducing the feed into the separator if it is in the composition range such that it forms two liquid phases at the temperature of the separator.

Case II. Single-phase feed.

If the feed is of such a composition that it consists of a single phase, it is fed to the column distilling the material nearest the composition of the feed. This is illustrated, schematically, in Figure (2-4).

Where homogeneous minimum boiling azeotropes occur between the two components, it may be feasible to lower the pressure with the corresponding reduction in temperature to such a level that liquid-liquid phase separation occurs. If this case can be caused, a simple two-column distillation may be utilized to make essentially complete separation [45]. On the other hand, if the azeotrope composition can be shifted far enough with change of pressure, it might be possible to recover material of satisfactory purity or even get essentially pure products by using only a single-column distillation [45].

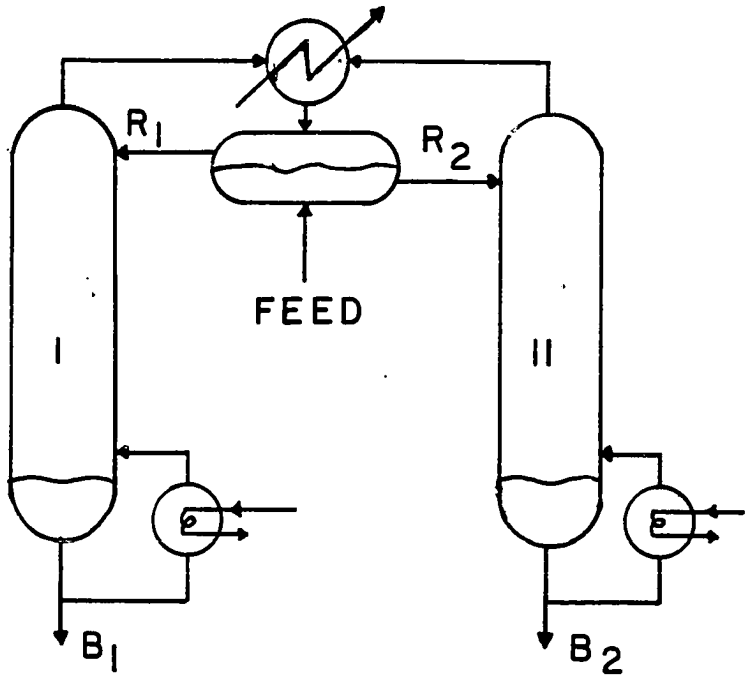

Figure (2-3) - Separation Scheme for a Heterogeneous Azeotrope (Two-phase liquid feed)

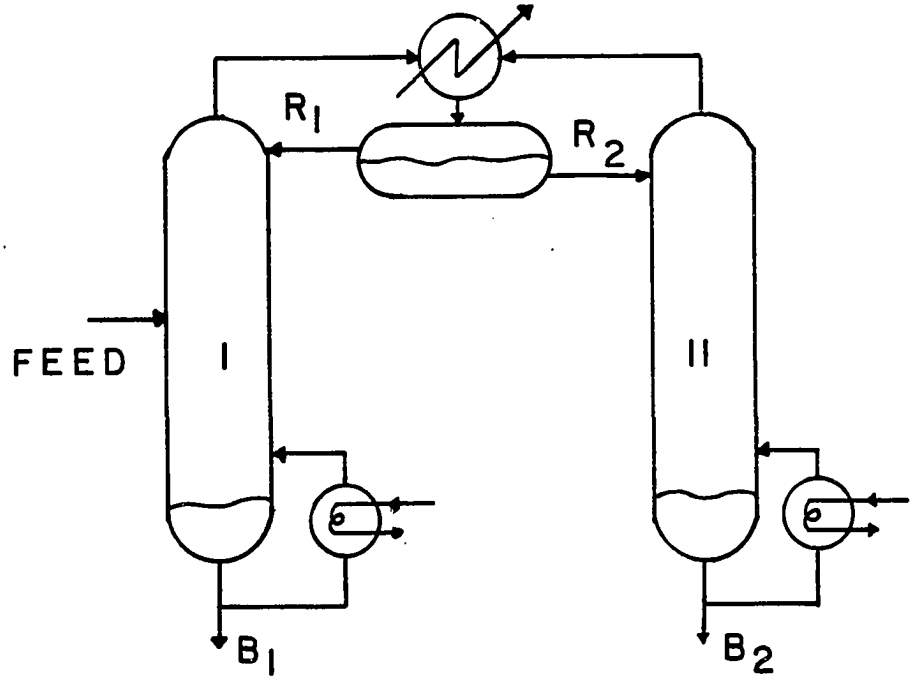

Figure (2-4) - Separation Scheme for a Heterogeneous Azeotrope (Single-phase liquid feed)

2.4 THF-Water Binary Azeotrope

Tetrahydrofuran (THF) forms a homogeneous, minimum-boiling azeotrope with water. It can be recovered safely and efficiently on an industrial scale by conventional methods from operations such as top-coating, printing, film casting, and chemical processes in which it is used as a reaction medium. It may be recovered alone or in mixtures with other solvents.

THF recovery methods, such as adsorption on activated carbon and absorption, usually yield a mixture of THF and water that cannot be separated by simple distillation because it forms an azeotrope containing 5.3 wt.% water at atmospheric pressure. Since most operations require dry THF, a number of separation methods have been developed and several are in commercial use. These methods are classified as follows:

1. Brine extraction
2. Solvent extraction
3. Pressure distillation
4. Other techniques such as
    a. dehydration with caustic soda or calcium chloride
    b. liquid phase adsorption.

It was suggested by du Pont [5] and Shinskey [37] to handle the THF-water separation using two columns operating at two different pressures. This is based on the fact that a shift in the composition of the azeotrope occurs when pressure is changed. For example, as the

pressure is increased from 0 to 100 psig, the concentration of water in the THF-water azeotrope increases from 5.3 to 12.0 wt. %. Some physical properties of pure THF and water are shown in Tables (1) and (2) in the Appendix. Thermodynamic properties of the THF-water system required for this study, will be discussed in the next chapter.

CHAPTER 3

PHYSICAL AND THERMODNYAMIC PROPERTIES OF THE THF-WATER SYSTEM

This chapter deals with the prediction of the physical and thermodynamic properties of the THF-water system, by correlating available experimental data or using an existing equation to fit such data. For both THF and water compounds, the following were covered.

(1) Heat capacities and enthalpies
(2) Liquid molar volumes
(3) Vapor pressures
(4) Activity coefficients prediction
(5) Vapor-liquid equilibrium
(6) Liquid-liquid equilibrium
(7) Thermodynamic consistency test

3.1 Heat Capacities and Enthalpies

The enthalpies of pure tetrahydrofuran and water were calculated using the du Pont [33] data for the heat capacity constants and latent heats of vaporization. The heat capacity is given by

$$C_{p_i} = c_i + d_i(T - 273.15) \qquad (3.1)$$

where C_{p_i} is the molar heat capacity of component i, cal/gmol °K, and T is the absolute temperature in degrees Kelvin. The constants c_i

and d_i, as well as the latent heats of vaporization, ΔH_v, are listed in Table (3-1). References [13&18] give the values of C_p for THF

TABLE (3-1): Heat Capacity Constants and Latent Heats of Vaporization for THF and water [33]

	Vapor		Liquid		ΔH_v, cal/gmol
Component	c_i	d_i	c_i	d_i	(at 1 atm.)
THF	25.579	0.02800	32.517	0.032400	7073.8
H_2O	8.910	0.00144	17.988	0.000825	9720.5

for a wide range of temperature. The enthalpy of pure components were calculated as follows:

a. Liquid:

$$h = \int_{T^\circ}^{T} c_p^{\ell} \, dT \qquad (3\text{-}2)$$

where T° is a reference temperature (273.15 °K).

b. Vapor at 1 atm.:

$$H = \int_{T^\circ}^{T_b} c_p^{\ell} \, dT + \Delta H_v + \int_{T_b}^{T} c_p^{v} \, dT \qquad (3\text{-}3)$$

where

T_b = normal boiling point, °K

ΔH_v = latent heat of vaporization at 1 atm., cal/gmol.

c. Vapor at other pressures: The new boiling points of pure components were calculated from the vapor pressure equation

$$T_{b,i}^{new} = B_i/(A_i - \log P) - C_i + 273.15 \ , \ °K \qquad (3\text{-}4)$$

where A_i, B_i, C_i are the Antoine constants for component i, and P is the total pressure of the system in mmHg.

The latent heat of vaporization was corrected by

$$\Delta H_v^{new} = \Delta H_v \left(\frac{1-T_r^{new}}{1-T_r}\right)^{0.38} \tag{3-5}$$

where

$T_r = T_b/T_c$ = reduced temperature at normal boiling point

$T_r^{new} = T_b^{new}/T_c$ = reduced temperature at new boiling point

and

T_c is the critical temperature in °K.

Here, we assumed that the enthalpy of liquid is not a function of pressure. Only, the enthalpy of vapor was corrected for pressure change. Thus, at pressure other than 1 atm. , the enthalpy of vapor was given by

$$H = \int_{T^\circ}^{T_b^{new}} c_p^{\ell}\, dT + \Delta H_v^{new} + \int_{T_b^{new}}^{T} c_p^{v}\, dT \tag{3-6}$$

As a function of temperature, the liquid and vapor enthalpies are shown in Figure (3-1) for both THF and water.

On the other hand, the data available on the excess thermodynamic properties of the THF-water system are only at atmospheric pressure and low temperatures of 10 and 25°C [7,14,27,28,39]. There is no certain method to predict these properties, namely, excess

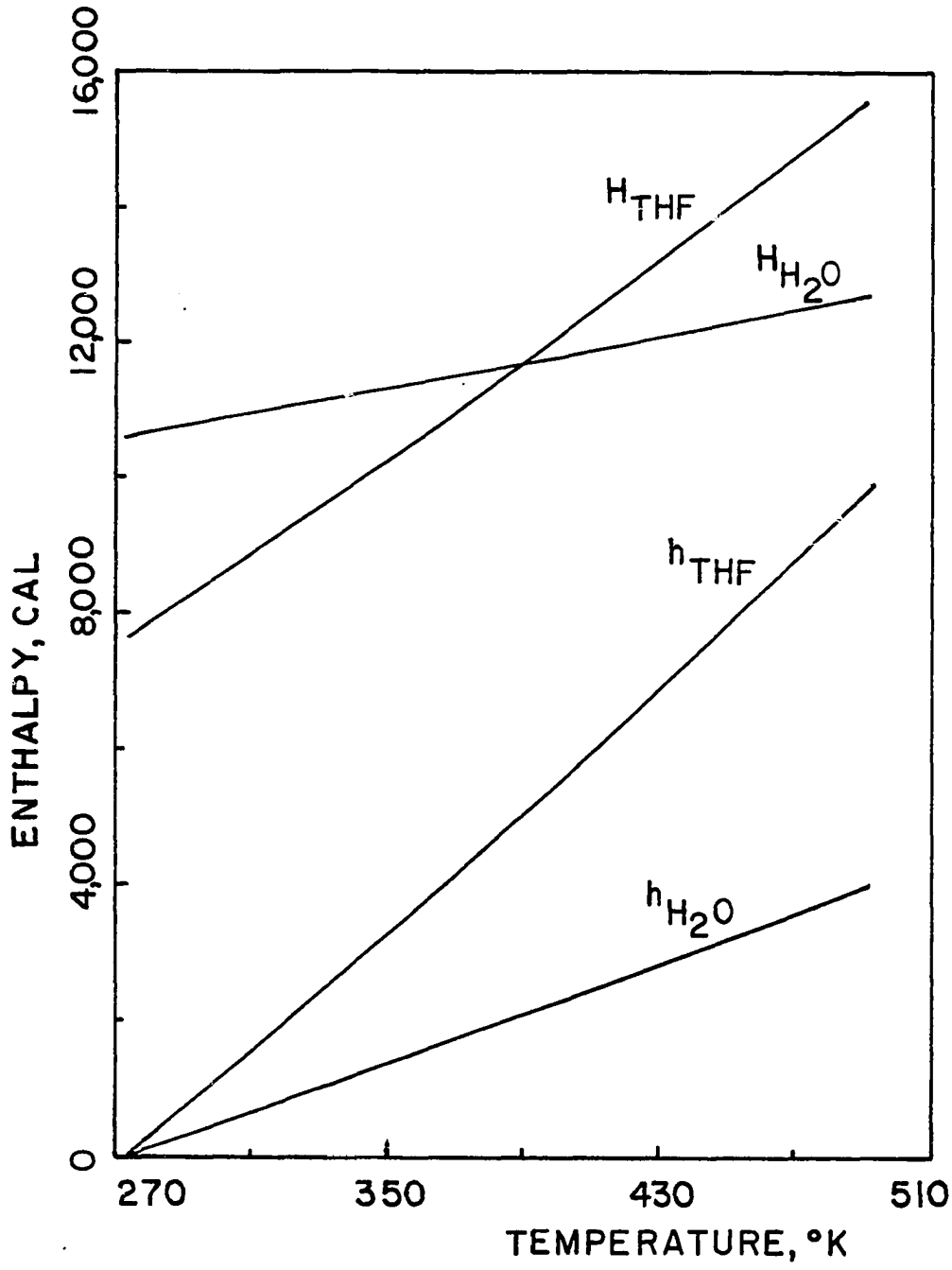

Figure (3-1) - Enthalpy vs. Temperature for Pure THF and Water at 1 atm.

enthalpy and excess molar volume, at high temperatures and/or pressures.

Since our system is going to be operated at above 25°C, and those values of excess enthalpies at 25°C are a very small fraction of the total enthalpy (< 2%); these excess properties will not be considered in this study.

3.2 Liquid Molar Volumes

The liquid molar volume data for pure tetrahydrofuran and water, as a function of temperature, were correlated by

$$v^{\ell}_{THF} = 80.75 + 0.102567\ (T - 288.15) \qquad (3\text{-}7)$$

$$v^{\ell}_{H_2O} = 22.3624 - 0.0333831\ T + 6.42 \times 10^{-5}\ T^2 \qquad (3\text{-}8)$$

and plotted in Figure (3-2), where v^{ℓ}_i is in cc/gmol and T in °K.

Other correlations, for the calculation of the density and pure liquid molar volume of THF and water, are available in literature [5,15,16,36].

3.3 Vapor Pressures

The vapor pressures of pure THF and water were represented by the Antoine equation

$$\log_{10} P^s_i = A_i - B_i/(t + C_i) \qquad (3\text{-}9)$$

where P^s_i is the vapor pressure in mmHg and t is the temperature in °C.

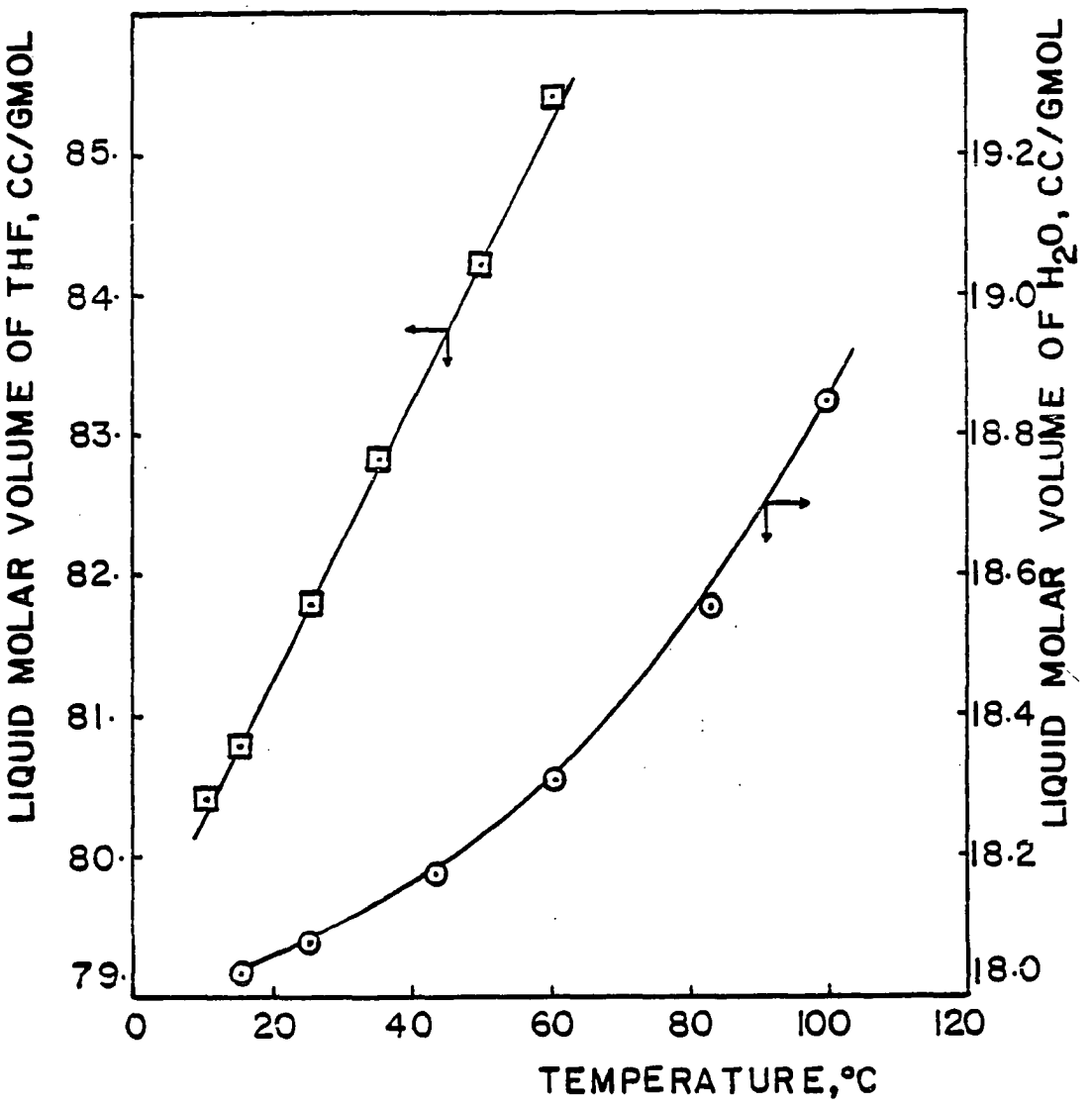

Figure (3-2) - Liquid Molar Volumes vs. Temperature for Pure THF and Water

The values of the Antoine constants used in this study are listed in Table (3-2).

TABLE (3-2): Antoine Constants for THF and Water [8,10,22]

Component	A	B	C
THF (23-100°C)	6.99515	1202.290	226.254
H_2O (60-150°C)	7.96680	1668.210	228.000

Some other values of the Antoine constants of tetrahydrofuran are available in literature. Table (3-3) shows a listing of these constants for THF and the temperature range of applicability. Table (3-4) shows a comparison between the vapor pressure values using these constants.

TABLE (3-3): Antoine Constants For the THF Vapor Pressure in mmHg

Temperature range, °C	A	B	C	Reference
0-66	6.38924	948.251	204.299	[21]
0-100	7.15376	1342.784	248.899	[21]
0-120	7.15906	1306.654	238.599	[21]
23-100	6.99515	1202.290	226.254	[8,10]
-20-120	4.11628	1200.260	226.038	[16]*

*Vapor pressure in bars (1 bar = 0.986923 atm.)

For temperatures above 120°C, the following correlation is available [16] for the temperature range 120-267°C,

TABLE (3-4): Vapor Pressure Data for THF From Different Sources

T,°C	Quaker Oats P,mmHg	duPont P,mmHg	Kobe P,mmHg	Key Chem. Data Book P,mmHg	VLE Data Book, mmHg
0	56	57.3	48.2	48.02	48.00
10	92	92.3	80.0	80.63	80.57
20	145	145.0	127.0	129.76	129.67
30	220	221.	197.0	201.17	201.08
40	322	320.	294.4	301.83	301.70
50	458	461	428.1	439.76	439.57
60	633	640	606.9	624.05	623.83
B.P.*	760	-	-	750.06	760.85
70	-	880	841.3	864.82	865.65
80	-	1185	1142.4	1173.10	1173.16
90	-	1540	1522.8	1561.63	1561.32
100	-	2040	1995.6	2041.67	2041.81
110	-	-	2575.0	2627.60	2627.90
120	-	-	3275.7	3307.77**	3333.29
140	-	-	-	5122.92**	5158.02
160	-	-	-	7575.62**	7628.82

* Normal boiling point of THF

** Calculated from Equation (3-10)

$$\log_{10} p_r = 10.53913 - \frac{4.63102}{T_r} - 12.10658\, T_r + 8.20212\, T_r^2 - 2.00179\, T_r^3 - 0.00362181 \log_{10} (T_r + 8. - T_r\, T_c) \quad (3\text{-}10)$$

where

$$p_r = p^s/p_c$$

$$T_r = T/T_c.$$

It is obvious from Table (3-4) that the Quaker Oats and du Pont data agree closely. The data of Kobe, Key Chemicals Data Book [16] and those calculated using the Antoine constants given by Gmehling and Onken [8] and Hirata et al [10]; agrees well but are offset below the others.

For the ease of calculation, we used the Antoine constants available for the temperature range 23-100°C and extended that for the calculation of THF vapor pressure at higher temperatures.

3.4 Activity Coefficients Prediction

Assuming perfect gas behavior at low pressures (up to 10 atm.) the activity coefficients γ_i, at equilibrium, are related to the vapor pressure p_i^s of component i, total pressure P, liquid composition x_i, and vapor compositions y_i by

$$\gamma_i = y_i P / x_i p_i^s \quad (3\text{-}11)$$

and at the azeotropic point, where $y_i = x_i$,

$$\gamma_i = P/p_i^s \tag{3-12}$$

These relationships were used for the calculation of the activity coefficients, γ_i, from the available experimental data at various pressures.

The calculated values of the activity coefficients then used to calculate Wilson's constants, A_{12} and A_{21}, using the Wilson's equations [29,46]

$$\ell n\ \gamma_1 = -\ \ell n\ (x_1 + A_{12}x_2) + x_2\left(\frac{A_{12}}{x_1+A_{12}x_2} - \frac{A_{21}}{A_{21}x_1+x_2}\right) \tag{3-13}$$

$$\ell n\ \gamma_2 = -\ \ell n\ (x_2 + A_{21}x_1) - x_1\left(\frac{A_{12}}{x_1+A_{12}x_2} - \frac{A_{21}}{A_{21}x_1+x_2}\right) \tag{3-14}$$

by trial and error. These Wilson constants are related to the interaction energy between components 1 and 2 as follows:

$$A_{12} = \frac{v_2^\ell}{v_1^\ell} \exp\left(-\frac{\lambda_{12}-\lambda_{11}}{RT}\right) \tag{3-15}$$

and

$$A_{21} = \frac{v_1^\ell}{v_2^\ell} \exp\left(-\frac{\lambda_{21}-\lambda_{22}}{RT}\right) \tag{3-16}$$

where $\lambda_{12} = \lambda_{21}$ and v_i^ℓ is the molar volume of pure liquid i at temperature T. If we denoted

$$WEP_1 = \lambda_{12} - \lambda_{11} \quad \text{and} \quad WEP_2 = \lambda_{21} - \lambda_{22}, \tag{3-17}$$

then

equations (3-15) and (3-16) can be rearranged as follows

$$WEP_1 = - \ell n(A_{12} \cdot \frac{v_1^\ell}{v_2^\ell}) \cdot RT \qquad (3\text{-}18)$$

and

$$WEP_2 = - \ell n(A_{21} \cdot \frac{v_2^\ell}{v_1^\ell}) \cdot RT \qquad (3\text{-}19)$$

These parameters, WEP_1 and WEP_2, were calculated for each experimental point and averaged for each set of data at that pressure. As a function of pressure, these parameters were correlated by

$$WEP_1 = 1865.2097 + 0.1034391\ (P-760) \qquad (3\text{-}20)$$

$$WEP_2 = 1927.6307 + 0.03133\ (P-760) \qquad (3\text{-}21)$$

where P is the total pressure in mmHg. These correlations will be used to calculate the interaction parameters at any pressure of interest throughout this study.

The interaction parameters, WEP_1 and WEP_2, and the Wilson's constants, A_{12} and A_{21}, were used, as will be shown later, for the prediction of vapor-liquid equilibrium data for the THF-water system.

Table (3-5) shows the literature and the calculated values of WEP_1 and WEP_2 at various temperatures and pressures. These parameters are plotted as a function of pressure on the semi-log graph shown in Figure (3-3).

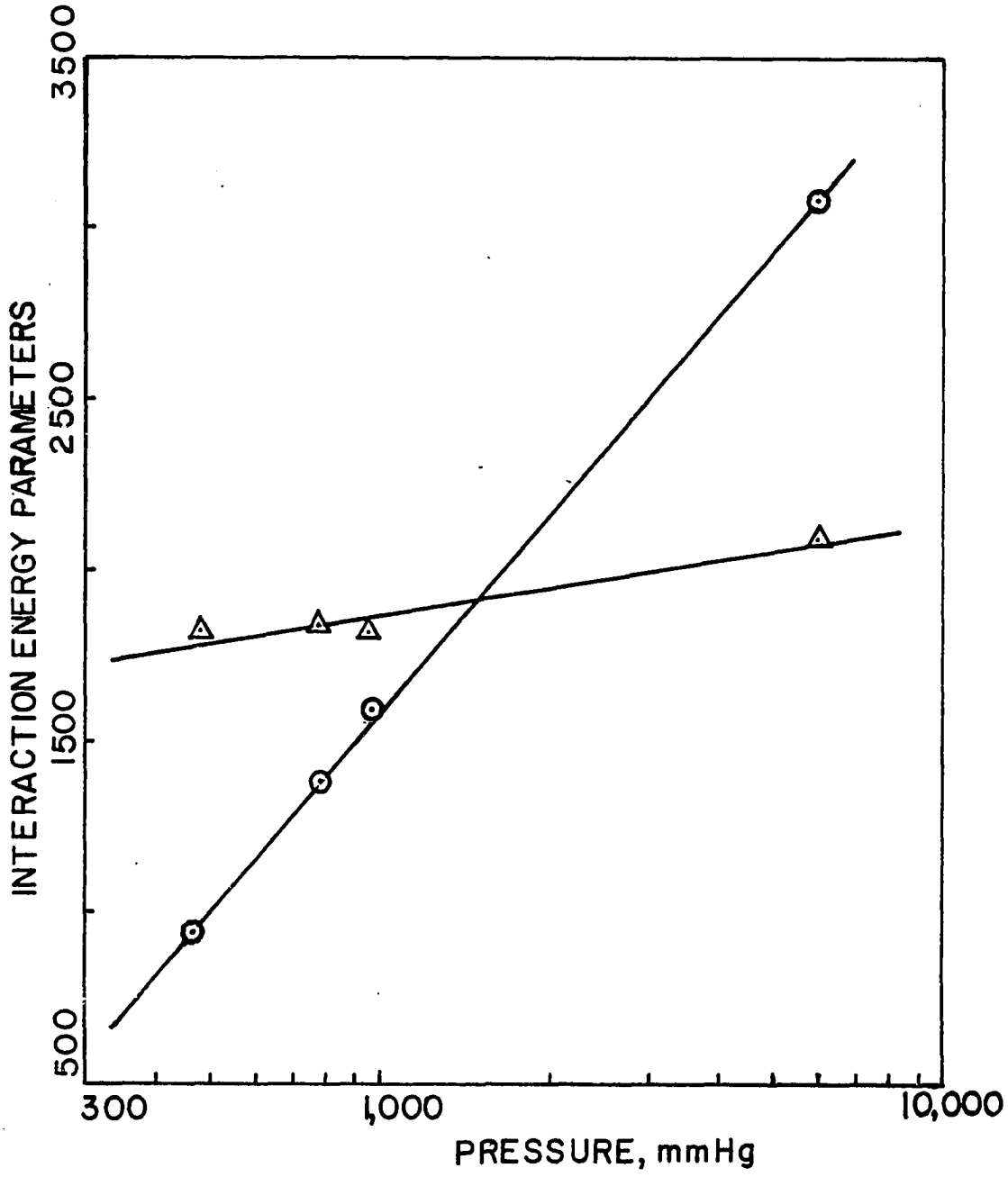

Figure (3-3) - Interaction Energy Parameters vs. Pressure for Wilson Equation

TABLE (3-5): Interaction Energy Parameters for the Wilson Equation at Various Temperatures and Pressures [18]

Azeotrope temp.,°C	Azerotrope pressure, mmHg	WEP_1	WEP_2	Remarks
25.00	174	534.4253	1894.1086	
50.00	464	946.5471	1839.2552	
63.41	760	1386.2870	1891.0566	
63.80	760	1475.2583	1844.7926	
63.80	760	1865.2097	1927.6307	
63.56	760	1518.5800	1888.9900	Calculated
70.00	947	1519.5859	1815.7141	
135.85	5930	3085.0600	2089.6100	Calculated

On the other hand, the experimental and predicted values of the activity coefficients are shown in Figures (3-4) and (3-5) at 0 and 100 psig, respectively. From these figures, it is clear that the predicted values of the activity coefficients agree well with the experimental values except at low concentrations of either THF or water. We also calculated the activity coefficients for the THF-water system from experimental data at 25, 50 and 70°C and found that γ is independent of temperature.

3.5 Vapor-Liquid Equilibrium

As mentioned earlier, this study deals with the separation of the THF-water mixture by pressure distillation. So, it is necessary to have exact vapor-liquid equilibrium data at the separation

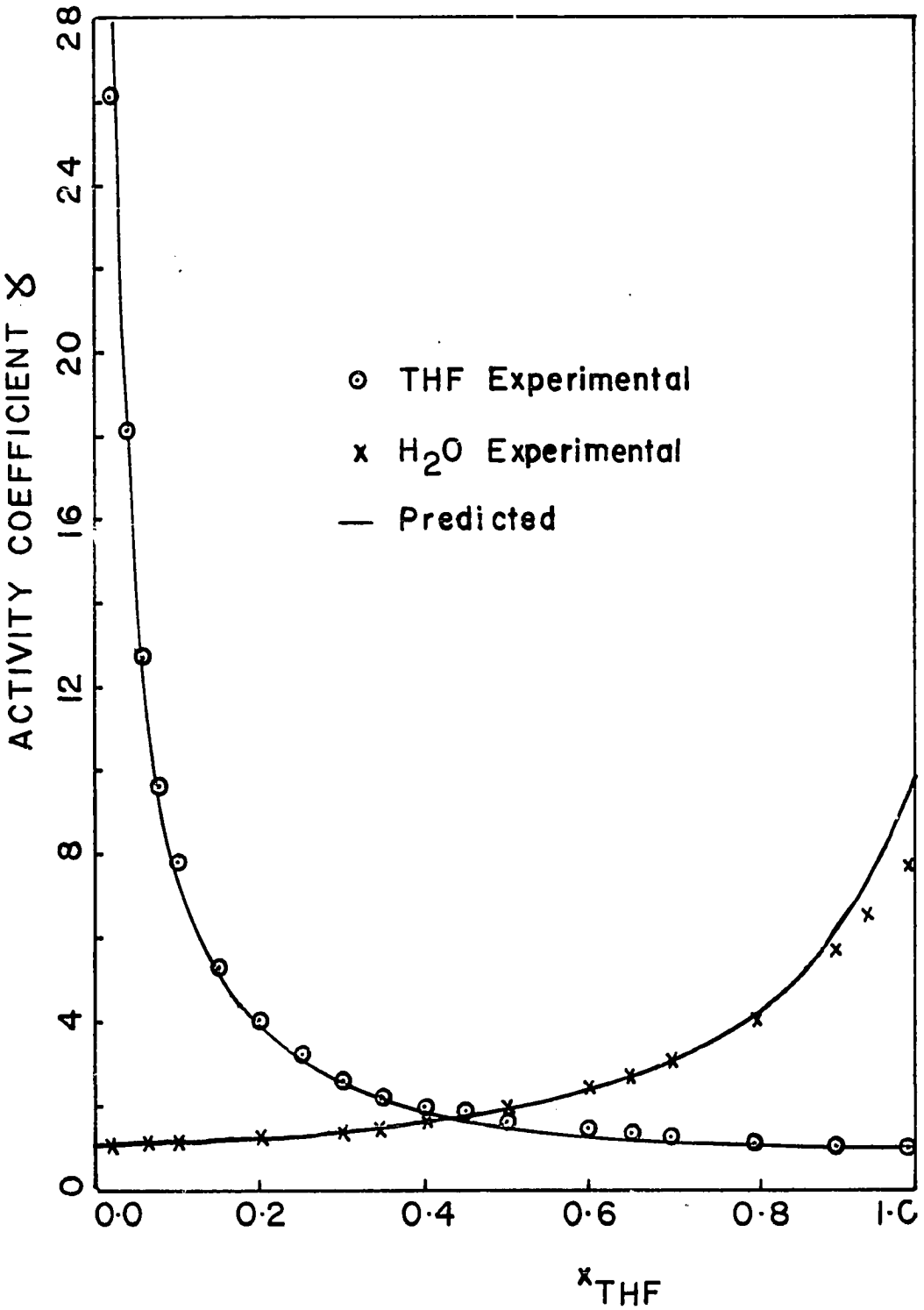

Figure (3-4) - Experimental and Predicted Activity Coefficients vs. Composition at 1 atm.

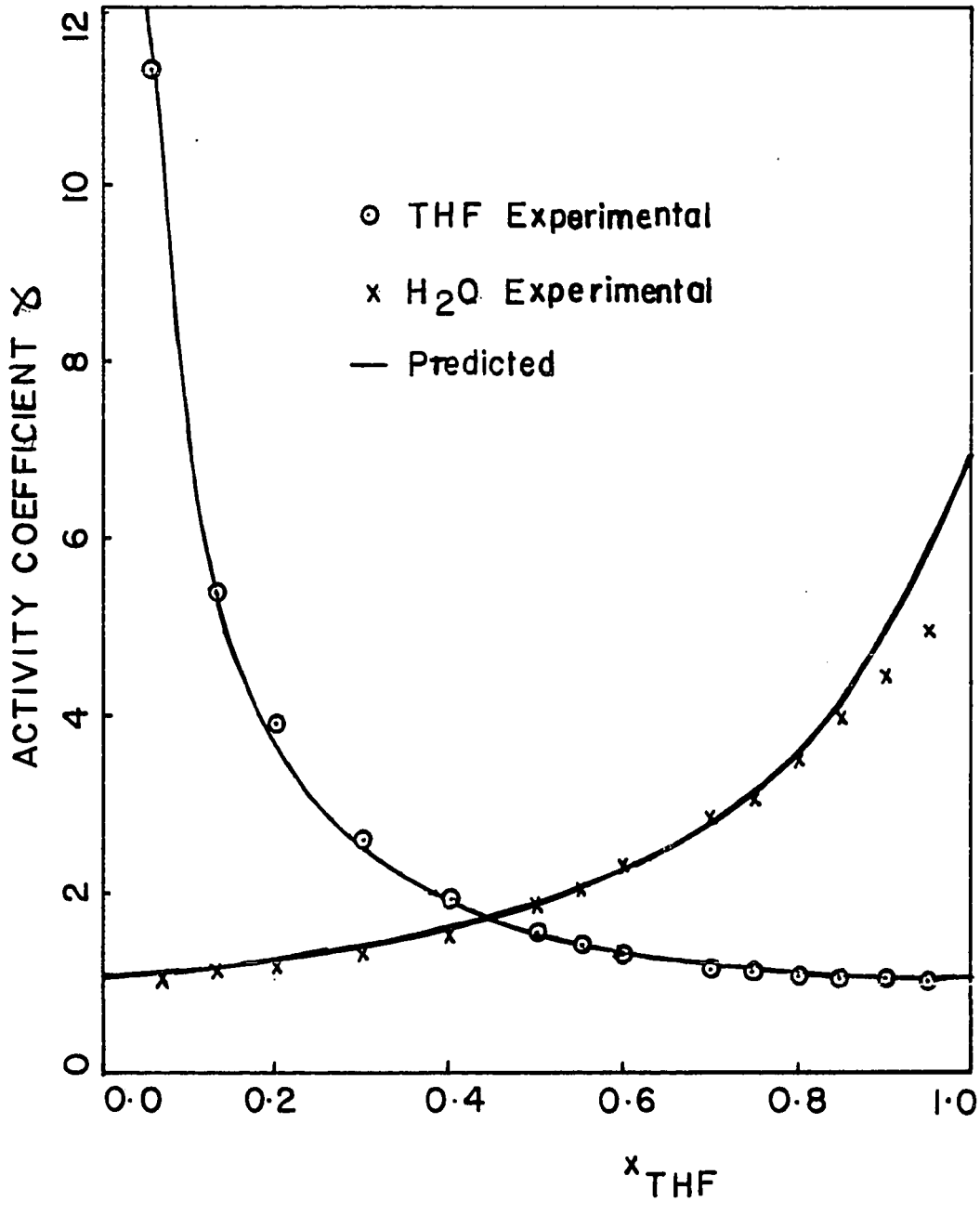

Figure (3-5) - Experimental and Predicted Activity Coefficients vs. Composition at 100 psig

pressures. Most of the VLE data for this mixture are available at atmospheric pressure [4,9,17,32,38]. The only available data at high pressure is from du Pont [5,33], at 100 psig. Other data are available at 25, 50 and 70°C [23,39].

The recorded boiling point and composition of the THF-water azeotrope at 1 atm. vary from one reference to another, as shown in Table (3-6), by up to 0.3°C and 0.04 mole fractions, respectively. At 100 psig, the azeotrope was at 136.0°C and 0.6327 mole fraction THF [33].

TABLE (3-6): Boiling Point and Composition of the THF-Water Azeotrope at 1 atm.

Boiling Point, °C	Composition Mole Fraction	Reference
63.41	0.8000	[32]
63.52	0.8172	[21]
63.80	0.8090	[9]
63.80	0.8400	[38]
63.56	0.8207	Calculated

In correlating the vapor-liquid equilibrium data, the data of Shnitko and Kogan [38] at 1 atm., and du Pont data [5,33] at 100 psig were used. The experimental VLE data of Shnitko and Kogan and the predicted data, using the Wilson Equations, are shown in Figures (3-6.a) and (3-7.a) for atmospheric pressure. The du Pont experimental data at 100 psig and the predicted data at the same pressure are shown in Figures (3-6.b) and (3-7.b). From these Figures, it is

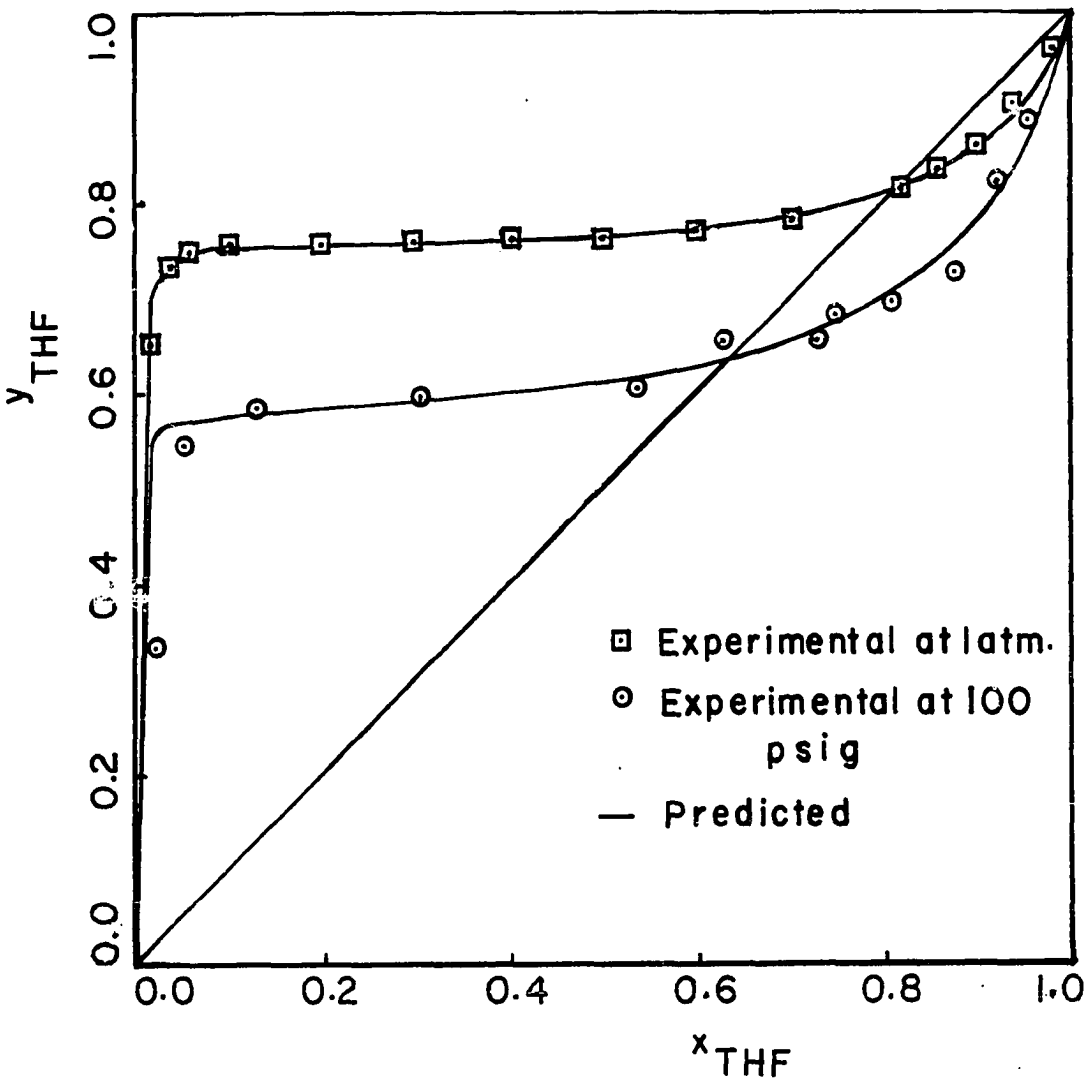

Figure (3-6) - Experimental and Predicted Vapor-Liquid Equilibria for the THF-Water System at 1 atm. and 100 psig

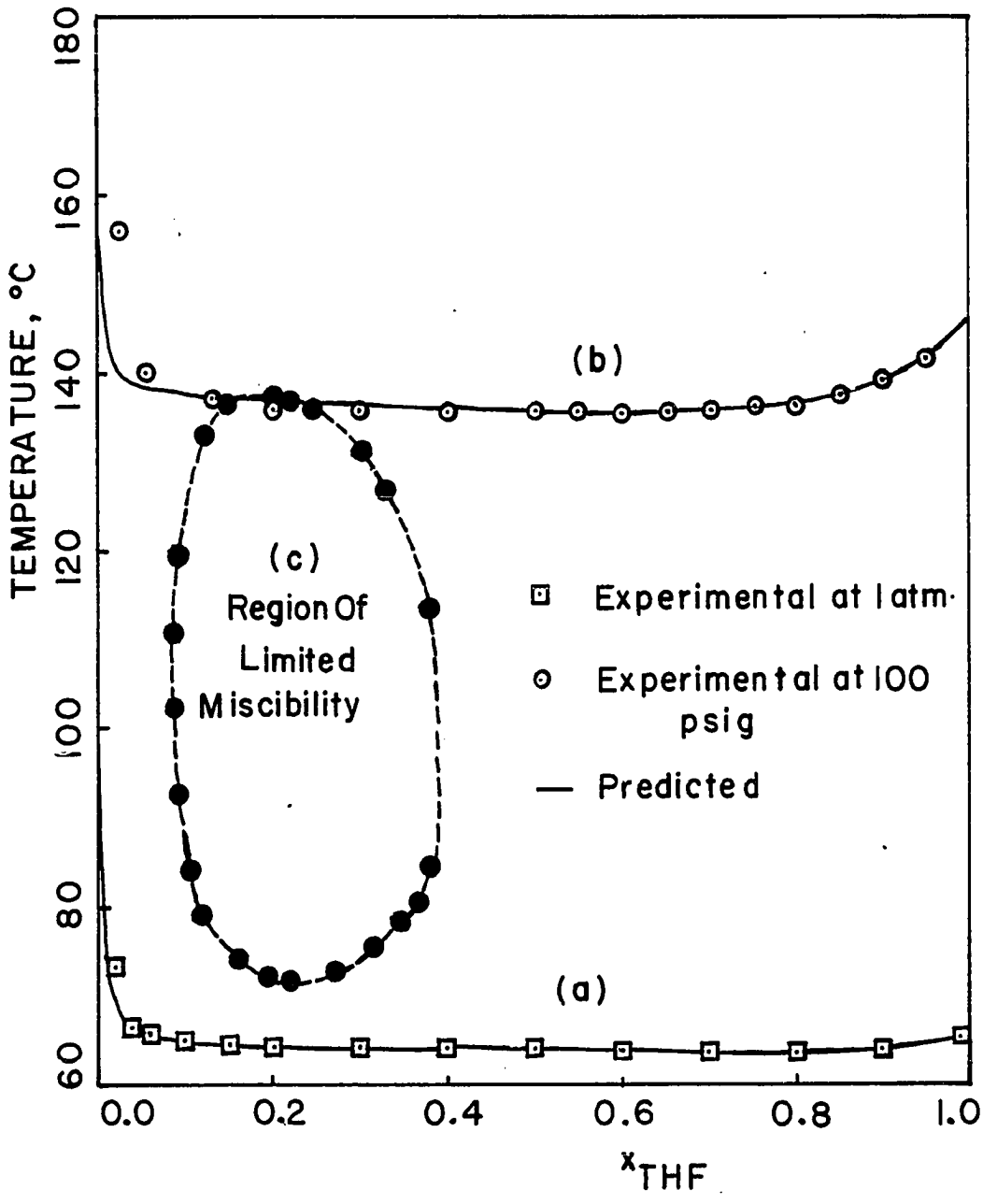

Figure (3-7) - Experimental and Predicted Boiling Point vs. Composition for the THF-Water System at 1 atm. and 100 psig [Curves (a) and (b)], and Region of limited Miscibility [Curve (c)].

clear that Wilson equation predicts VLE data for the THF-water system in good agreement with the experimental data, except at very low concentrations.

3.6 Liquid-Liquid Equilibrium

Matous et al [23,24] found that there is a region of limited miscibility for the THF-water mixture. This region lies between 71.8 ± 0.15°C (at 22.33 mol.% THF), and 137.1 ± 0.15°C (at 18.74 mol.% THF), as shown in Figure (3-7.c). The two-parameter Wilson equation cannot predict such partial immiscibility; Wilson [46] suggested the use of a third parameter in his equation to predict such a region. Tsuboka and Katayama [44] have modified the Wilson's equation, without any additional parameters, which can be applied for both miscible and partially immiscible systems.

3.7 Thermodynamic Consistency Test

The vapor-liquid equilibrium data were checked for thermodynamic consistency at constant pressure. Neglecting the excess enthalpy term in Equation (3-22), the sum of the areas above and below the zero line of $\ell n(\frac{\gamma_1}{\gamma_2})$ vs. x_1 plot was calculated. Thermodynamic consistency was then calculated as the percentage of the difference between the

$$\text{Area} = \int_0^1 \ell n(\frac{\gamma_1}{\gamma_2})\, dx_1 - \int_{x_1=0}^{x_1=1} \frac{h^E}{RT}\, dT \qquad (3\text{-}22)$$

positive and negative areas divided by the sum of the absolute areas. These results are shown in Table (3-7) for the integration interval, $\Delta x_1 = .01$, at various pressures. As shown in Table (3-7), the difference varies from .81 to 1.77%, depending on pressure. These

TABLE (3-7): Thermodynamic Consistency Test Results

P,mmHg	$\Delta x_1 = 0.01$ Difference,%
350	0.81
760	0.88
3345.1	1.24
5930.1	1.53
8515.1	1.77

results might be acceptable since the excess enthalpy term was neglected.

CHAPTER 4

STEADY-STATE DESIGN FOR NON-EQUIMOLAR OVERFLOW, NON-IDEAL BINARY SYSTEMS

4.1 Introduction

By non-equimolar overflow, we mean that the molar heat of vaporization varies with composition. Thus the liquid and vapor flow rates in any section of the distillation column can no longer be assumed constant. Non-ideal systems, such as THF-water mixture, deviate strongly from ideality (Raoult's law), giving activity coefficients that are not unity.

For non-ideal binary systems the graphical methods; based on the use of an enthalpy-composition chart, can be applied. Computers can be used to carry out the plate-to-plate calculations, provided suitable material and energy balance equations, as well as physical properties and vapor-liquid equilibrium correlations are available. In this chapter the following topics will be covered:

(1) Description of Process

(2) Calculation of Trays - Inputs and Outputs

(3) Material Balance

(4) Minimum Reflux Calculation

(5) Design Program for Tray-to-Tray Calculation

(6) Adiabatic Flash Calculations

(7) Feed Tray Location

(8) Top Tray Location

(9) Body of the Design Program

(10) Presentation of the Design Program Results

4.2 Description of the Process

As mentioned earlier, the separation of the THF-water mixture requires two continuous distillation units. The first unit, column 1, will be operated at low pressure (up to 1 atm).

The second unit, column 2, will be operated at a higher pressure (up to 150 psig). A schematic representation of the system is shown in Figure (4-1).

Column 1 operates with a feed F of composition Z_F and temperature T_F, and gives a top product D_1 (near the low pressure azeotrope) of composition x_{D1} and a bottom product B_1 (mainly water) of composition x_{B1}. A recycle stream D_2 of composition x_{D2} comes from the top of column 2 and is recycled to column 1.

Column 2 operates with the top product from column 1 as a feed, and gives a top product D_2, near the azeotrope at high pressure, of composition x_{D2} and a bottom product B_2 (mainly THF) of composition x_{B2}. Flow rates of vapor and liquid streams are in gmol/hr, and the compositions of the streams in mole fraction THF; x referring to the liquid composition and y to the vapor composition.

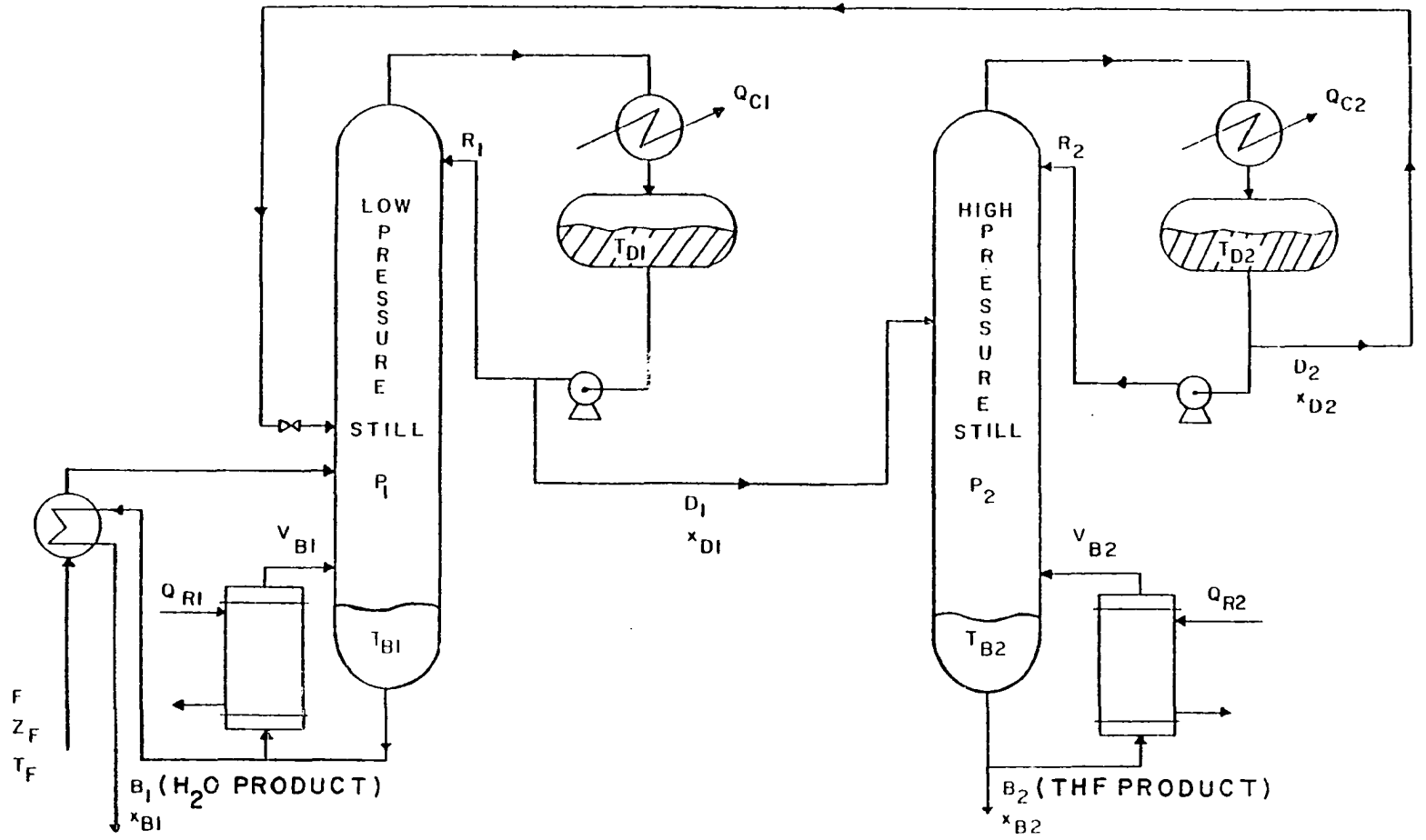

Figure (4-1) - Schematic Representation of the Two-Columns System for the Separation of THF-Water Azeotrope

Plates are numbered from the bottom upward. H and h represent the molar enthalpies of vapor and liquid streams, respectively. Q_C is the heat removed in the overhead condenser. Q_R is the heat input to the reboiler.

4.3 Calculation of Trays-Inputs and Outputs

I. Variables specified:

- Feed rate, composition, enthalpy to first column.
- Products purities required.

II. Other parameters that should be selected:

- Pressure (affects vapor-liquid equilibrium)
- Reflux ratio: (requires minimum reflux calcuations)
- Criterion for feed tray location - "optimum", i.e minimizes total number of trays.

III. Data required:

- Vapor-liquid equilibrium data
- Physical properties such as molecular weight, enthalpy, density for both vapor and liquid species.

IV. Design procedure: The computer plate-to-plate calculations require the following equations:

- Total material balance 1 per tray
- Component material balance (Nc-1) per tray

- Energy balance — 1 per tray
- Vapor-liquid equilibrium — 1 per component
- Enthalpies — 1 per tray

$h = f(x_i, T)$ $\quad i = 1, Nc$

$H = f(y_i, T, P)$ $\quad i = 1, Nc$

where Nc is the number of components in the mixture.

V. Results:

- Total number of trays, N_T
  - height of the column (after specifying tray spacing and top and bottom space).
- Feed tray location(s), N_{Fj}, $j = (1,n)$ where n is the number of feed streams
- Liquid and vapor flow rates, L, V
  - Column diameter (vapor load limiting)
  - Reboiler duty, Q_R
  - Condenser duty, Q_C
- Top and bottom temperatures
  - Area of condenser and reboiler (after specifying heat transfer coefficients)
  - Design temperature and pressure
  - Column shell thickness

4.4 Material Balance

The material balances for the two columns are very sensitive to

the actual overhead compositions of each [37]. The overall and component material balances for both columns are given by

$$F = B_1 + B_2 \tag{4-1}$$

$$F \cdot Z_F = B_1 \cdot x_{B1} + B_2 \cdot x_{B2} \tag{4-2}$$

From Equations (4-1) and (4-2)

$$B_1 = \frac{x_{B2} - x_{B1}}{x_{B2} - Z_F} \tag{4-3}$$

For column 1,

$$F + D_2 = D_1 + B_1 \tag{4-4}$$

$$F \cdot Z_F + D_2 \cdot x_{D2} = D_1 \cdot x_{D1} + B_1 \cdot x_{B1} \tag{4-5}$$

and for column 2,

$$D_1 = D_2 + B_2 \tag{4-6}$$

$$D_1 \cdot x_{D1} = D_2 \cdot x_{D2} + B_2 \cdot x_{B2} \tag{4-7}$$

Eliminating B_2 from Equations (4-6) and (4-7) gives

$$D_2 = D_1 \cdot \frac{x_{B2} - x_{D1}}{x_{B2} - x_{D2}} \tag{4-8}$$

Substituting for B_1 and D_2 from Equations (4-3) and (4-8) into Equation (4-5) and rearranging, gives

$$D_1 = F\,(Z_F - x_{B1})(x_{B2} - x_{D2})/(x_{D1} - x_{D2})(x_{B2} - x_{B1}) \tag{4-9}$$

For very pure bottom products, i.e., $x_{B1} \simeq 0$, $x_{B2} \simeq 1.0$

Equation (4-9) reduces to

$$D_1 = F \cdot Z_F (1-x_{D2})/(x_{D1}-x_{D2}) \qquad (4\text{-}10)$$

and equation (4-8) becomes

$$D_2 = F \cdot Z_F (1-x_{D1})/(x_{D1}-x_{D2}) \qquad (4\text{-}11)$$

B_1 and B_2 can be calculated from Equations (4-4) and (4-6), respectively.

Equations (4-10) and (4-11) are key equations in the design of the two-columns system. Notice that if x_{D2} approaches x_{D1}, in the denominator of those equations, the quantities D_1 and D_2 become infinite and separation will be impossible. Thus, we should keep the denominator of those equations at its highest value, for example, by increasing x_{D1} and/or decreasing x_{D2}. This can be accomplished, as will be shown later, by the reduction of column 1 pressure and/or increase of column 2 pressure. On the other hand, as we increase x_{D1} at fixed x_{D2} (or decrease x_{D2} at fixed x_{D1}), the values of D_1 and D_2 as well as the load on both columns should decrease.

4.5 Minimum Reflux Calculation

The minimum reflux ratio is defined as the ratio which requires an infinite number of trays for the separation desired. It corresponds to the minimum reboiler heat load and condenser cooling load

for the separation [43]. The reflux ratio is at its minimum value when an energy balance operating line coincides with a VLE tie line on a Hxy diagram [35].

For a non-equimolar overflow system, the minimum reflux ratio is given by

$$RR_{min} = \frac{R_{min}}{D} = \frac{h_I - H_{NT}}{H_{NT} - h_D} \tag{4-12}$$

where

h_D = distillate enthalpy, cal/gmol

H_{NT} = overhead vapor enthalpy, cal/gmol

The unknown value of h_I should be located at the intersection of the tie-line that passes through the feed point on the Ponchon-Savarit diagram and the vertical line at $x = x_D$. This is true for an equilibrium curve that is concave everywhere downward [35,43] or upward, as it is the case for the high pressure column of this study. Solving the equations of these two lines gives

$$h_I = \frac{(H-h) \cdot x_D - y \cdot h - x \cdot H}{(y-x)} \tag{4-13}$$

where the points (x,h) and (y,H) are the two ends of the VLE tie-line passing through the feed, as shown in Figure (4-2). These are searched by the MINREF subroutine until the energy balance operating line passes through the feed isotherm, i.e.,

$$\frac{H - h_F}{y - Z_F} = \frac{H - h}{y - x} \tag{4-14}$$

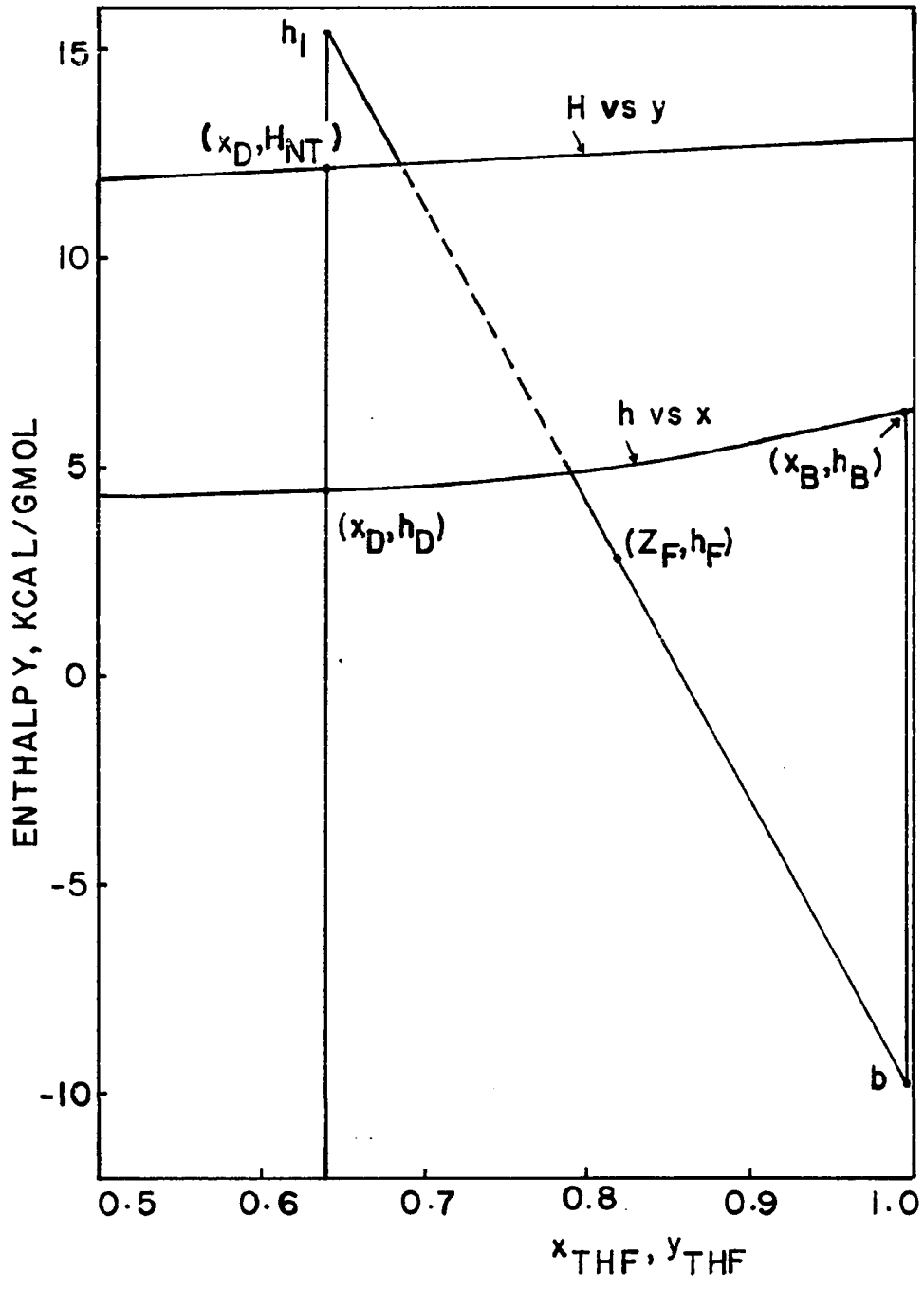

Figure (4-2) - Schematic Representation of Minimum Reflux Ratio for the High Pressure Column (Subcooled-Liquid Feed)

where (Z_F, h_F) is the feed point on the enthalpy-concentration diagram. Substitution for h_I from Equation (4-13) into (4-12) gives the minimum reflux ratio

$$RR_{min} = \frac{(H-h)(x_D-x) - (H_{NT}-h)(y-x)}{(H_{NT}-h_D)(y-x)} \qquad (4\text{-}15)$$

For negatively deviating mixtures with a tendency to form azeotropes, a stripping-section tie-line other than the one through the feed will give the lowest intersection on the vertical line, $x = x_B$ at b. Similarly, for some positively deviating mixtures, as it is the case of the low pressure column of this study; an enriching-section tie-line will give the highest intersection on the vertical line $x = x_D$. These then will govern the location of h_I [40,43]. In either case, h_I, b and feed point should fall on the same straight line and h_I is at the highest position in a pinch. For the last case, an initial guess is made for h_I, and the tie-lines that intersect the vertical line $x = x_D$ are searched by subroutine MINREF. h_I is then calculated using Equation (4-13) and compared to the previous value until the difference between two successive values is less than a specified relative error ($\varepsilon < 10^{-6}$). The minimum reflux ratio is then calculated using Equation (4-15). Reflux ratio, RR, is then set 1.2 times the minimum and reflux, R, is calculated as RR times distillate flow rate.

The reboiler duty is calculated from an overall energy balance on the column

$$Q_R = D \cdot h_D + B \cdot h_B + (R+D)(H_{NT}-h_D) - \sum_{i=1}^{2} F_i \cdot h_{Fi} \qquad (4\text{-}16)$$

and the condenser duty is given by

$$Q_c = (R+D)(H_{NT} - h_D) \qquad (4\text{-}17)$$

4.6 Design Program for Tray-to-Tray Calculations

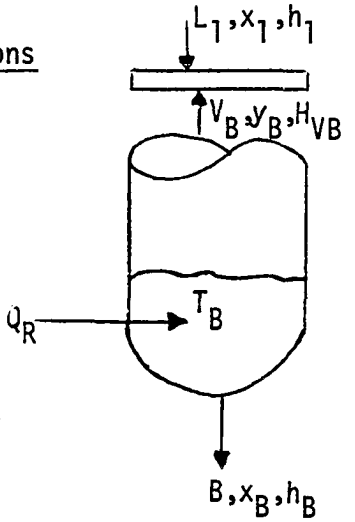

At the base of the column L_1, x_1 and V_B are unknowns. Q_R is known from total energy balance. Given x_B and P, calculate (y_B, T_B) and (h_B, H_{VB}) from equilibrium and enthalpy relationships, respectively.

Total material balance

$$L_1 = B + V_B \qquad (4\text{-}18)$$

Component material balance

$$L_1 \cdot x_1 = B \cdot x_B + V_B \cdot y_B \qquad (4\text{-}19)$$

Energy balance for bottom of the column

$$L_1 \cdot h_1 + Q_R = B \cdot h_B + V_B \cdot H_{VB} \qquad (4\text{-}20)$$

Trial and error solution:

1. Guess x_1
2. Calculate T_1 and y_1 from BUB subroutine
3. Calculate h_1 from ENTH subroutine
4. Substitute Equation (4-18) in (4-20) and calculate V_B

$$V_B = \frac{Q_R - B(h_B - h_1)}{H_{VB} - h_1} \qquad (4\text{-}21)$$

5. Calculate L_1 from Equation (4-18)

6. Calculate new value of x_1

$$x_1^{calc} = \frac{V_B \cdot y_B + B \cdot x_B}{L_1} \qquad (4\text{-}22)$$

7. Test

IF(ABS($x_1^{calc} - x_1$) · LT · ε) GO to 1

where ε is a convergence-tolerance error ($\varepsilon \leq 1 \cdot E\text{-}6$). These steps can be repeated for the second tray and so on up to the feed tray. At the feed tray and above, other terms should be added to the material and energy balance equations to account for the feed stream.

4.7 Adiabatic Flash Calculations

Flash calculations might be necessary to determine the flash temperature, liquid and vapor composition as well as the quality of the feed stream. These calculations are performed using AFLASH subroutine which consists of two loops, one inside the other.

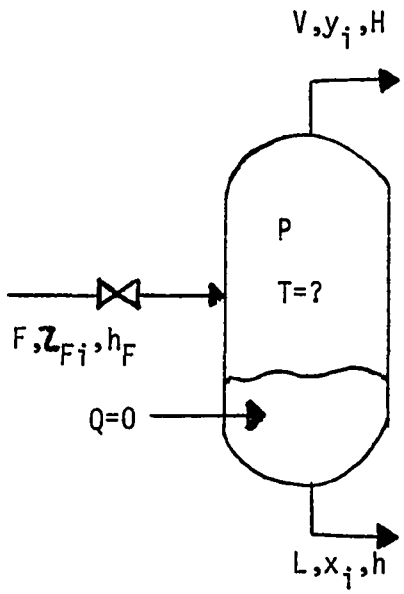

The main equations required are the energy and the material balance equations;

$$\frac{V}{F} = \frac{h_F - h}{H - h} \qquad (4\text{-}23)$$

$$y_i = Z_{Fi}K_i/[1+\frac{V}{F}(K_i-1)] \qquad (4\text{-}24)$$

where

Z_{Fi} = feed composition, mole fraction

h_F = feed enthalpy, cal/gmol

$K_i = y_i/x_i = \frac{\gamma_i p_i^s}{P}$ = K value for component i

h = enthalpy of liquid stream, cal/gmol

H = enthalpy of vapor stream, cal/gmol

For relatively close-boiling-range mixtures, such as THF-water system, King [12] suggests to converge the inner loop on the sum of mole fractions by changing temperature T, and the outer loop on the energy balance by changing the degree of vaporization V/F. This is because T, which must be between the bubble point and dew point that are close to one another, is less sensitive to the value of V/F.

The Newton-Raphson method was used for the convergence of the inner loop by changing T. The convergence was checked on

$$G = \sum_{i=1}^{2}(y_i-1.0) \leq \varepsilon \quad . \qquad (4\text{-}25)$$

The derivative of G with respect to temperature is given by

$$\frac{\partial G}{\partial T} = 2.303 \sum_{i=1}^{2} \frac{1 - V/F}{1 + \frac{V}{F}(K_i-1)} \cdot \frac{B_i}{(T-273.15+C_i)^2} \qquad (4\text{-}26)$$

where y_i is given by Equation (4-24). B_i and C_i are the second and third constants of the Antoine equation. The outer loop was

converged using the interval halving technique by changing $\frac{V}{F}$.

4.8 Feed Tray Location

The criteria used to locate feed tray for any feed, subcooled, saturated or flashed, is to calculate tray-liquid composition first without including the feed stream and then by including the feed stream in the material and energy balance equations. The two liquid compositions are compared. If the liquid composition at the tray including the feed stream, is greater than that not including it, this means that the later tray should be the optimum feed tray. A similar procedure can be used to locate the recycle-stream feed tray. This is true for column 1 where the composition of the more volatile component increases up the column.

For column 2, where the composition of the more volatile component decreases as we move up the column the feed tray is located when the liquid composition at the tray including feed stream is less than the composition at the tray not including feed stream. Again, the later should be the optimum feed tray.

4.9 Top Tray Location

The vapor composition from each tray in the rectifying section is compared with the desired distillate composition. When the former is greater than the latter, (it should be less for column 2) this means that this tray is the top tray.

4.10 Body of the Design Program

The steady-state design program consists of the main program where input data are read; azeotropic composition and temperature are calculated by calling subroutine AZEO; the required distillate purities are set and the distillate flow rates are calculated. This also calls subroutines COLMN1 and COLMN2 for design calculations. Other subroutines are:

a. COLMN1 and COLMN2: These calculate the bottoms flow rates, total number of trays, reboiler and overhead condenser heat duties, and the location of the feed tray(s) for column 1 and 2, respectively. These programs also call for other subroutines to get feed quality, minimum reflux ratio, and print the results.

b. GAMA: This calculates pure component vapor pressures, liquid molar volumes, as well as the interaction energy parameters and the constants required to calculate the activity coefficients using Wilson's equations. The K-values are also calculated in this subroutine.

c. BUB: For a given liquid composition and pressure, this subroutine calculates the corresponding vapor composition and bubble point temperature using the Newton-Raphson method. The activity coefficients are called from subroutine GAMA.

d. ENTH: This calculates the liquid and vapor enthalpies for a given temperature and composition of the mixture.

e. AZEO: For a given column pressure, the azeotropic temperature and composition can be calculated by this subroutine.

f. MINREF:: This calculates the minimum reflux ratio for either column as discussed earlier.

g. AFLASH: Checks the quality of the feed(s) and calculates the liquid and vapor compositions of the flashed feed, as well as their enthalpies and the degree of vaporization.

h. OUTPUT: Prints out results for either column.

It should be mentioned here that all the programs used in this study are our own programs.

4.11 Presentation of the Design Program Results

4.11.1 Basis of Calculations

In reference to the nomenclature used in Figure (4-1), the feed F to column 1 will be preheated by its bottom product. The following specifications are used in all runs unless otherwise mentioned:

Column 1

P_1 = 760 mmHg

F = 1000 gmol/hr

Z_F = .06 THF

T_F = 35°C (before preheater)

$x_{D1} = x_{AZ1} - .01$

$x_{B1} = 1 \times 10^{-6}$

Column 2

P_2 = 100 psig

$x_{D2} = x_{AZ2} + .01$

$1-x_{B2} = 1 \times 10^{-5}$

where x_{AZi} refers to the azeotropic composition of column i. A reflux ratio of 1.2 times the minimum is used in both columns. Again, all compositions are in mole fractions THF, flow rates in gmol/hr and heat duties in cal/hr.

The effects of various design parameters, such as feed composition, feed rate, preheat temperature of the feed, T_{FP}, products purities, distillate compositions and pressures of the columns, were explored. Tables (4-1) through (4-7) show the effect of these changes on the design of the two-column system, i.e., feed-tray location, N_F, total number of trays, N_T, and heat load of the reboilers, Q_R, and overhead condensers, Q_c.

4.11.2 Feed Composition Effect

When the composition of column 1 feed is increased, as shown in Table (4-1), the flow rate of the bottom product of column 1 decreases and that of column 2 increases. Thus, the preheat given to the feed by column 1 decreases and the condition of the feed changes from subcooled feed at very low feed compositions $Z_F \leq .035$ THF, to a flashed feed at intermediate compositions

TABLE (4-1): Effect of Feed Composition Change on the Design of the Two-Column System

	Column 1						Column 2		
Z_F	T_{FP},°C	% Flash	N_{F1}	N_{F2}	N_T	$Q_{R1} \times 10^{-6}$	N_F	N_T	$Q_{R2} \times 10^{-6}$
.03	86.3	0.00	3	5	15	0.757	12	18	0.600
.04	85.1	3.81	3	5	15	0.949	12	18	0.800
.04	82.8	4.11	3	4	15	1.333	12	18	1.120
.06	79.6	3.68	3	4	15	1.908	12	18	1.680
.12	76.6	3.08	3	4	14	2.483	12	18	2.240
.18	71.3	1.80	2	4	14	3.634	12	18	3.360
.24	66.6	0.50	2	4	14	4.784	12	18	4.481
.30	62.5	0.00	2	3	14	5.934	12	18	5.600

$.035 < Z_F \leq .265$, and subcooled again at $Z_F > .265$, depending on the bubble point temperature of the feed and the heat content of the bottom product. The distillate and reflux flow rates as well as the reboilers and condensers heat duties increase as the feed composition is increased.

4.11.3 Reflux Ratio Effect

The total number of trays required for the separation of a mixture increases and the heat loads decrease when reflux ratio is decreased. But, as shown in Table (4-2) column 1 is more sensitive, in terms of the total number of trays required, than column 2. This is due to the presence of a pinch in the vapor-liquid equilibrium curve of column 1 at its operating pressure.

TABLE (4-2): Effect of Reflux Ratio Change on the Design of Both Columns ($\beta_i = RR_i/RR_{i,min}$)

a - Column 1 : $RR_{1,min} = .2273$, $T_{FP} = 82.8°C$

β_1	RR_1	N_{F1}	N_{F2}	N_T	$Q_{R1} \times 10^{-6}$	$Q_{C1} \times 10^{-6}$
2.5	.568	3	3	7	1.627	-1.561
2.0	.455	3	4	8	1.514	-1.448
1.5	.341	3	4	10	1.401	-1.335
1.25	.284	3	4	13	1.344	-1.278
1.20	.273	3	4	15	1.333	-1.267
1.15	.261	3	4	17	1.322	-1.255
1.10	.250	3	4	21	1.310	-1.244
1.05	.239	3	5	29	1.299	-1.233

b - Column 2 : $RR_{2,min} = .3854$, $1-x_{B2} = 1 \times 10^{-4}$

β_2	RR_2	N_F	N_T	$Q_{R2} \times 10^{-6}$	$Q_{C2} \times 10^{-6}$
2.5	.964	8	11	1.365	-0.963
2.0	.771	9	12	1.270	-0.868
1.5	.578	9	13	1.176	-0.773
1.25	.482	10	15	1.129	-0.727
1.20	.463	10	15	1.120	-0.717
1.15	.443	10	16	1.110	-0.708
1.10	.424	11	17	1.101	-0.698
1.05	.405	11	19	1.091	-0.689

4.11.4 Distillate Composition Effect

When the distillate purity of one column is increased (i.e., its composition becomes closer to the azeotropic composition of that column) more trays are required and the reboiler and condenser heat duties increase. The effect on the other column is mainly a decrease in its heat duties. See Tables (4-3) and (4-4). But it should be noticed that, for a given change in the other column distillate composition, column 1 is more sensitive, in terms of the total number of trays than column 2. This is again attributed to the presence of the pinch in the VLE curve of that column.

4.11.5 Bottom-Product Purity Effect

As bottom product purities are increased, more trays are required but there is little increase in reboiler heat duties. See Table (4-5).

TABLE (4-3): Effect of Column 1 Distillate-Composition Change on the Design of Both Columns at $\beta_1 = \beta_2 = 1.2$

	Column 1				Column 2		
$\lvert x_{D1}-x_{AZ1}\rvert$,%	N_{F1}	N_{F2}	N_T	$Q_{R1}\times10^{-6}$	N_F	N_T	$Q_{R2}\times10^{-6}$
3.0	3	5	8	1.287	12	17	1.323
2.0	3	5	11	1.288	12	17	1.215
1.0	3	4	15	1.333	12	18	1.120
0.8	3	4	16	1.348	12	18	1.102
0.6	3	4	20	1.362	12	18	1.085
0.4	3	4	29	1.376	12	18	1.068

TABLE (4-4): Effect of Column 2 Distillate-Composition Change on the Design of Both Columns at $\beta_1 = \beta_2 = 1.2$

	Column 1				Column 2		
$x_{D2}-x_{AZ2}$,%	N_{F1}	N_{F2}	N_T	$Q_{R1}x10^{-6}$	N_F	N_T	$Q_{R2}x10^{-6}$
3.0	3	4	15	1.400	13	16	1.102
2.0	3	4	15	1.364	13	16	1.112
1.0	3	4	15	1.333	12	18	1.120
0.8	3	4	15	1.327	12	18	1.122
0.6	3	4	15	1.321	12	19	1.123
0.4	3	4	15	1.316	12	20	1.125
0.2	3	4	15	1.310	12	21	1.126

TABLE (4-5): Effect of Bottom Product Purity on the Design of the Two-Column System at $\beta_1 = \beta_2 = 1.2$

a - Column 1 (at $1-x_{B2} = 1x10^{-5}$)

x_{B1}	N_{F1}	N_{F2}	N_T	$Q_{R1}x10^{-6}$
$1x10^{-4}$	2	3	14	1.3310
$1x10^{-6}$	3	4	15	1.3328
$1x10^{-8}$	4	6	16	1.3328

b - Column 2 (at $x_{B1} = 1x10^{-6}$)

$(1-x_{B2})$	N_F	N_T	$Q_{R2}x10^{-6}$
$1x10^{-3}$	8	13	1.1195
$1x10^{-4}$	10	15	1.1201
$1x10^{-5}$	12	18	1.1201

4.11.6 Column Pressure Effect

The reduction of column 1 pressure and the increase of column 2 pressure have very significant effects on the design of the system.

a. When the pressure of column 1 was reduced from 760 to 350 mmHg, at P_2 = 100 psig, total number of trays increased while the heat duties for both columns decreased, as shown in Table (4-6). The percent of vapor in the feed and recycle stream to column 1 are also increased as P_1 is reduced, as also shown in Table (4-6).

TABLE (4-6): Effect of the Reduction of Column 1 Pressure on the Design of the System at P_2 = 100 psig. (Column 1 Feed and Recycle Trays are 3 and 4)

	P_1, mmHg	
Column 1:	760	350
Feed preheat temp., T_{FP}, °C	82.8	65.1
% Vapor in Feed F	4.11	4.89
% Vapor in Recycle D_2	32.75	41.72
N_T	15	22
$Q_{R1} \times 10^{-6}$	1.333	1.028
Column 2:		
N_F	12	13
N_T	18	19
$Q_{R2} \times 10^{-6}$	1.120	0.856

b. Increasing column 2 pressure (with P_1 fixed at 760 mmHg or 350 mmHg) results in a slight increase in the total number of trays of column 1 and a significant decrease in its heat duty. See Table (4-7.a,b). The effect on column 2 has a significant decrease in both the total number of trays and the heat duty. The last column in Table (4-7.a,b) shows the total heat required by the system as a

TABLE (4-7): Effect of Column 2 Pressure on the Design of the System. $\beta_1 = \beta_2 = 1.2$

a. P_1 = 760 mmHg

	Column 1				Column 2			
P_2,psig	N_{F1}	N_{F2}	N_T	$Q_{R1}x10^{-6}$	N_F	N_T	$Q_{R2}x10^{-6}$	$Q_T x10^{-6}$
50	3	5	13	1.691	14	19	1.522	3.213
100	3	4	15	1.333	12	18	1.120	2.453
150	3	4	15	1.213	11	16	0.993	2.206
200	3	4	15	1.150	10	15	0.937	2.087
250	3	4	16	1.112	10	14	0.911	2.023
300	3	4	16	1.085	9	14	0.905	1.990

b. P_1 = 350 mmHg

	Column 1				Column 2			
P_2,psig	N_{F1}	N_{F2}	N_T	$Q_{R1}x10^{-6}$	N_F	N_T	$Q_{R2}x10^{-6}$	$Q_T x10^{-6}$
50	3	4	22	1.166	14	20	1.024	2.190
100	3	4	22	1.028	13	19	0.856	1.884
150	3	4	22	0.973	12	17	0.805	1.778
200	3	4	22	0.943	11	16	0.788	1.731
250	3	4	22	0.923	10	15	0.786	1.709
300	3	3	22	0.909	9	14	0.791	1.700

function of column 2 pressure at P_1 = 350 and 760 mmHg, respectively. The percent in energy saving for running column 2 at, for example, 300 psig instead of 100 psig will be 10.0 and 18.9% at P_1 = 350 and 760 mmHg, respectively. Further discussion of this subject is presented in Chapter 5.

To conclude this chapter, we found that column 1 is more sensitive to changes in reflux ratio and distillate composition than column 2. Energy can be saved by increasing feed preheat temperature, recycle stream heat content or using lower reflux ratios. More energy saving can be achieved by reducing column 1 pressure and increasing that of column 2.

Further exploration of these effects and more will be made using the rating program described in the next chapter.

CHAPTER 5

STEADY-STATE RATING PROGRAM FOR NON-EQUIMOLAR OVERFLOW, NON-IDEAL BINARY SYSTEMS

5.1 Introduction

As mentioned earlier, the design program gives only a general idea about energy requirements for the system. In order to get exact values of reflux and energy loads, as well as to find the optimum distillate purities that require minimum energy consumption at various feed compositions and separation pressures, a rating program should be used.

5.2 Body of the Rating Program

The rating program, we developed, consists of the following:

a. Main Program: This has similar features as that of the steady-state design main program but calls the rating subroutine instead of the design subroutine.

b. Subroutine RATNG: This performs the rating problem calculations, as will be discussed later, and prints out the results for both columns.

c. Subroutines GAMA, BUB, AZEO, ENTH, MINREF: These have the same structure and purpose as discussed in Chapter 4.

5.3 Description of the Rating Program

The rating program starts by reading input data, calculates the azeotropic composition and temperature, sets the required distillate purities and calculates the distillate flow rates for both columns. The RATNG subroutine is then called. This subroutine should be fed with the feed rate, composition and temperature, location of feed trays, total number of trays and the required bottom and distillate purities.

Bottom products flow rates are calculated from total material balance. Enthalpies of input and output streams are calculated. The liquid composition and temperature of each tray are initialized and the corresponding vapor composition and enthalpies are calculated. The minimum reflux ratio is calculated and the reflux ratio is set 1.5 times the minimum as a starting value.

Calculations start from the bottom of the column and proceed upward tray-to-tray. The reboiler duty is calculated for each iteration to account for the change in reflux flow rate. Vapor and liquid molar flow rates are then calculated from energy and material balance equations. New liquid compositions are calculated from component material balance around the stripping section for the trays at and below the feed tray, and around the rectifying section for the trays above the feed tray. This procedure continues until the difference between the vapor composition from

the top tray, y_{NT}, and the required distillate purity, x_D, is less than a tolerance value, $\varepsilon \leq 10^{-6}$.

During the iterations it might happen that the new value of the liquid composition is greater for column 1 (less for column 2) than the specified distillate composition. In either case, a decrease in the reflux flow rate will bring these to the appropriate values. On the other hand, if the liquid composition just above the feed tray is greater for column 1 (less for column 2) than the composition at the feed tray itself, it should be adjusted by increasing the reflux flow rate incrementally.

It is also interesting to note that the interval halving, used to increment the reflux flow rate, was modified to be $\Delta R = \Delta R/\sqrt{2}$, instead of dividing by 2. This required more iterations in some cases, but it permitted the program to converge in those cases where overlapping of the region of parameter search was required.

5.4 Presentation of the Rating Program Results

5.4.1 Basis of Calculations

The basis of calculations in this chapter will be as follows:

Column 1	Column 2
P_1 = 760 mmHg	P_2 = 100 psig
F = 1000 gmol/hr	$1 - x_{B2} = 1 \times 10^{-4}$
Z_F = 0.06	$x_{D2} = x_{AZ2} + \Delta x_2/100$
T_{FP} = 35°C (before preheater)	N_T = 15
$x_{B1} = 1 \times 10^{-6}$	N_F = 10
$x_{D1} = x_{AZ1} - \Delta x_1/100$	
N_T = 15	
N_{F1} = 3	
N_{F2} = 4	

where Δx_1 and Δx_2 are the absolute difference between the required distillate composition and the azeotrope composition for columns 1 and 2, respectively.

The total number of trays in each column as well as feed-tray location were chosen based on the steady-state design results [see, for example, Table (4-2) in Chapter 4] and the steady-state economic study that will be presented in Chapter 7.

5.4.2 Distillate Composition Effect

As the distillate composition of the first column becomes purer (i.e., closer to the azeotrope) more reflux is required and the reboiler duty of that column is increased. The distillate flow from column 1 to column 2 will, in this case, decrease and thus decrease the reboiler duty of the second column. This effect is shown in

Table (5-1). This effect is reversed when the second column distillate composition approaches its azeotrope, as shown in Table (5-2), because the recycle loop gets smaller.

The distillate composition of one column was fixed and that of the other column was varied. The energy required by both columns, Q_T, was found to be more sensitive to distillate composition changes of the first column than the other. The optimum distillate compositions are those that minimize the total energy required by the system. These values, as shown in Figure (5-1), are $\Delta x_1 = \Delta x_2 = 1.1\%$.

It should be noticed that the optimum in Figure (5-1) is flat for both columns-distillate composition, for example, increasing Δx_1 from .8 to 1.1%, at fixed Δx_2, resulted in less than 0.5% saving in the total energy required by the system. As mentioned in Chapter 4, columns pressure have more effect on the system total energy requirement. This will be discussed in more detail later in this chapter.

The system specified above with $\Delta x_1 = \Delta x_2 = 1.1\%$ will be called the "Base" case, and its schematic flow diagram is shown in Figure (5-2). In the rest of this section we will show the effect of changes in feed composition, distillate composition and column pressure system flow rates and total energy requirement.

TABLE (5-1): Effect of Distillate Composition of Column 1 on the System Flow Rates and Reboilers Heat Duties at Δx_2 = 1.1%

	Column 1			Column 2			
Δx_1,%	R_1	D_1	$Q_{R1} \times 10^{-6}$	R_2	D_2	$Q_{R2} \times 10^{-6}$	$Q_T \times 10^{-6}$
.8	39.6	128.8	1.3571	30.9	68.8	1.0981	2.4552
.9	37.2	129.6	1.3433	31.0	69.6	1.1066	2.4499
1.0	35.1	130.4	1.3317	31.2	70.4	1.1152	2.4469
1.1	33.2	131.2	1.3217	31.3	71.2	1.1239	2.4456*
1.2	31.4	132.1	1.3131	31.4	72.1	1.1327	2.4458
1.3	29.8	132.9	1.3057	31.6	72.9	1.1416	2.4483
1.4	28.4	133.8	1.2993	31.7	73.7	1.1507	2.4500
1.5	27.0	134.6	1.2938	31.8	74.6	1.1598	2.4536

TABLE (5-2): Effect of Distillate Composition of Column 2 on the System Flow Rates and Reboilers Heat Duties at Δx_1 = 1.1%

	Column 1			Column 2			
Δx_2,%	R_1	D_1	$Q_{R1} \times 10^{-6}$	R_2	D_2	$Q_{R2} \times 10^{-6}$	$Q_T \times 10^{-6}$
.8	32.85	129.93	1.3130	34.85	69.93	1.1368	2.4498
.9	32.95	130.36	1.3159	33.54	70.36	1.1316	2.4475
1.0	33.05	130.80	1.3188	32.37	70.80	1.1274	2.4462
1.1	33.15	131.24	1.3217	31.29	71.24	1.1239	2.4456*
1.2	33.26	131.69	1.3246	30.30	71.68	1.1211	2.4457
1.3	33.37	132.14	1.3276	29.37	72.14	1.1187	2.4463
1.4	33.47	132.60	1.3306	28.49	72.60	1.1168	2.4474
1.5	33.58	133.07	1.3337	27.65	73.06	1.1152	2.4489

*Minimum total energy required.

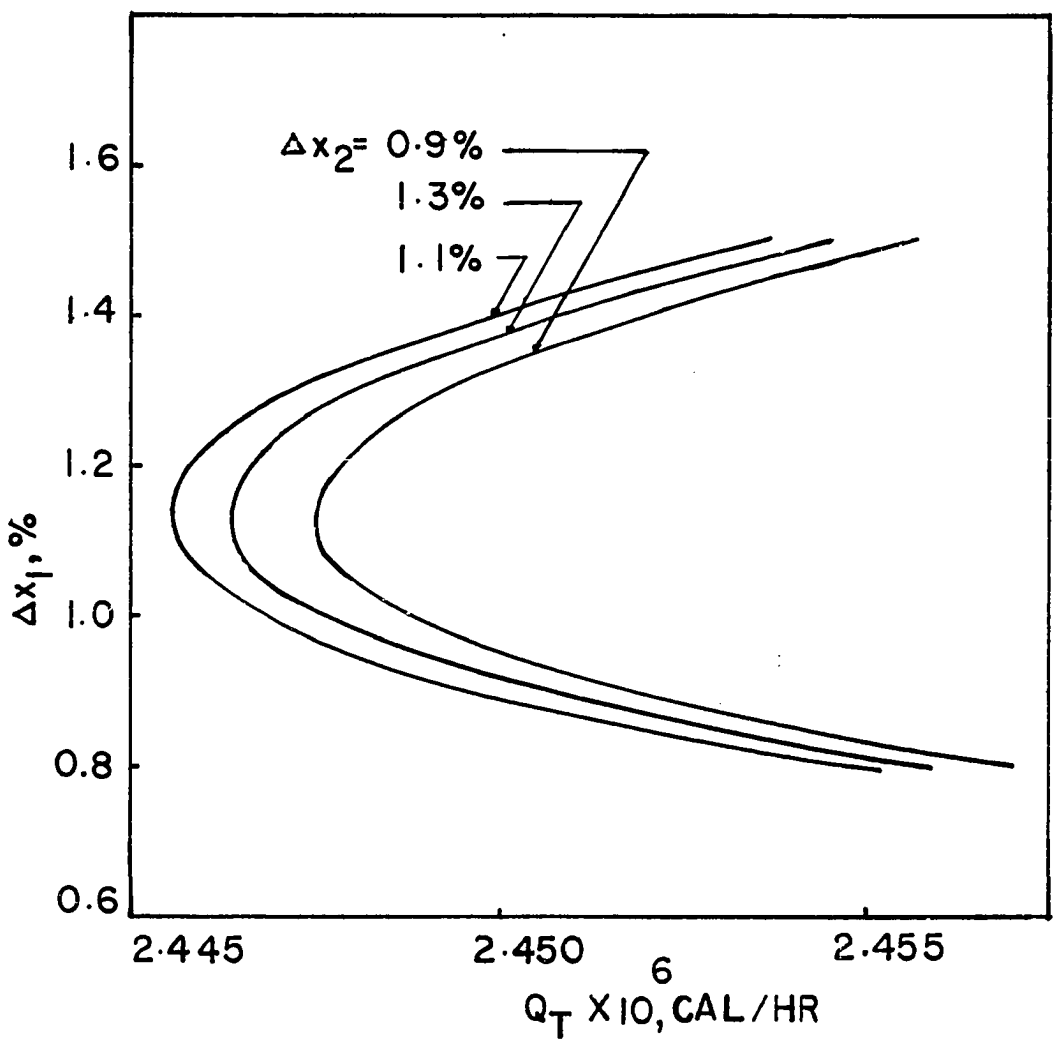

Figure (5-1) - Variation of Total Energy Required With Distillate Composition of Both Columns

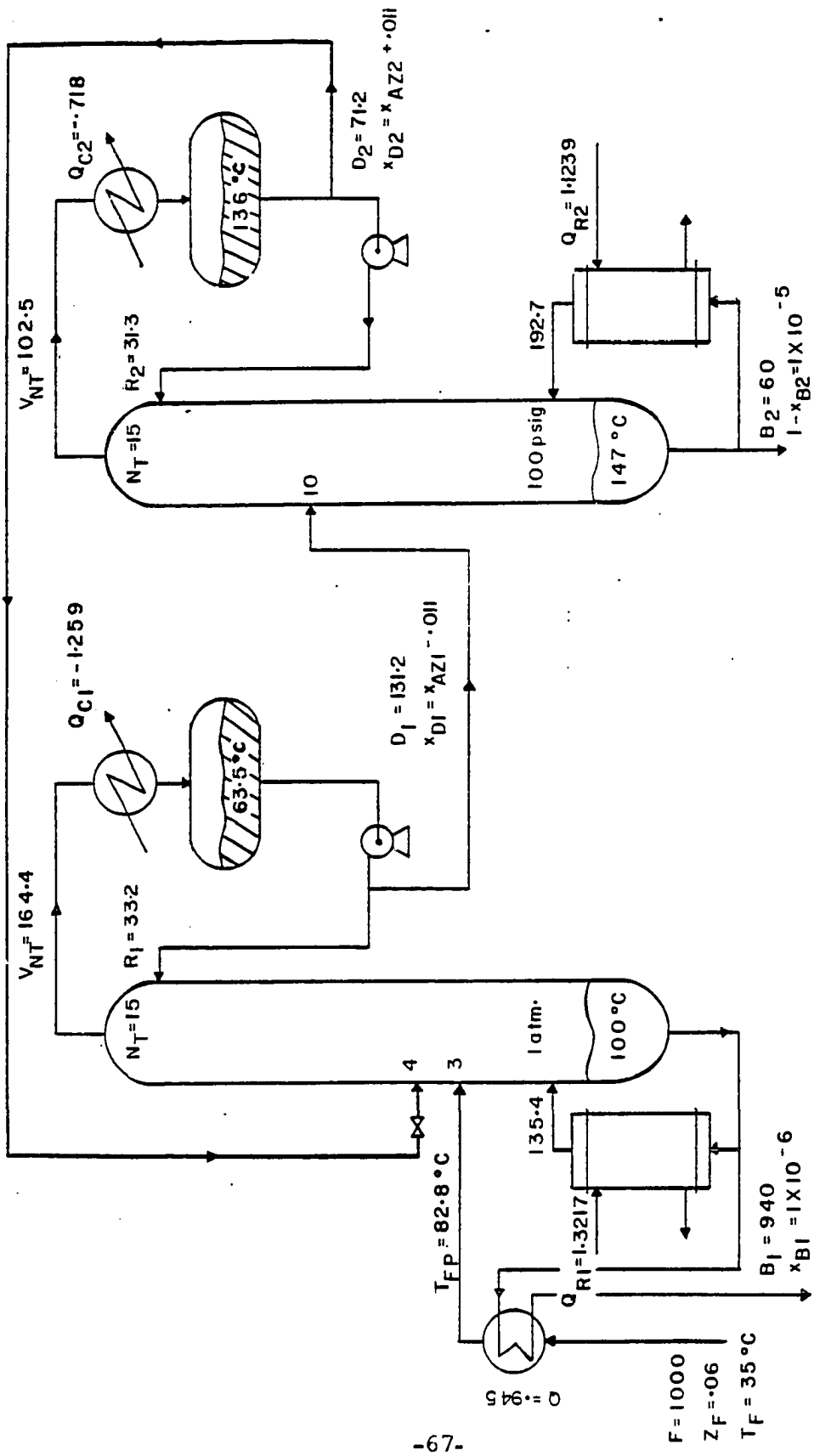

Figure (5-2) - Flowsheet for the Base Case [Case I.1]

Q_T = 2.446; Q's, Mcal/hr

5.4.3 Feed Composition Effect

As the feed composition was increased, all flow rates, except B_1, increased by almost the same ratio, as shown in Table (5-3). In this case, the flow rate of column 1 bottom product, B_1, decreases. This resulted, as shown in Table (5-3), in a decrease in the feed preheat temperature and contributed to the increase in the reboiler duty of column 1. The total energy required by the system was also increased by a factor little less than that of feed composition increase. On the other hand, the energy required per mole THF product, Q_T/B_2, gets smaller as the feed composition is increased.

TABLE (5-3): Effect of Feed-Composition Change on Total Energy REquirement, Feed Preheat Temperature and Flow Rates of the System

Z_F	.06	.15	.30
$Q_{R1} \times 10^{-6}$	1.322	3.024	5.862
$Q_{R2} \times 10^{-6}$	1.124	2.810	5.620
$Q_T \times 10^{-6}$	2.446	5.834	11.482
Q_T/B_2	0.0408	0.0389	0.0383
T_{FP} , °C	82.8	73.8	62.4
B_1	940.0	850.0	700.0
R_1	33.2	82.1	163.6
D_1	131.2	328.1	656.2
B_2	60.0	150.0	300.0
R_2	31.3	78.2	156.5
D_2	71.2	178.1	356.2

5.4.4 Column Pressure Effect

As mentioned in Chapter 4, the reduction of column 1 pressure and the increase of column 2 pressure has a significant effect on the total energy consumption of the system. The pressure of the first column can be reduced as long as it is possible to use cooling water efficiently in the overhead condenser. The pressure of column 2 can be increased as long as high pressure steam required for the reboiler is economically available. No high temperature sensitivity of THF has been reported.

a. When the pressure of column 1 is reduced from 760 to, say, 350 mmHg, (which corresponds to 43.5°C at the top of the column); the azeotrope at this pressure becomes richer in THF. This will result in a lower reflux flow rate and a lower reboiler duty of that column. At the same time, column 1 distillate fed to the second column is now richer in THF and has lower flow rate. This will result also in a reduction of the reboiler duty of the second column. These results are shown in Table (5-4).

TABLE (5-4): Effect of Reduction of Column 1 Pressure on the Flow Rates and Total Energy Requirement, at P_2 = 100 psig, $\Delta x_1 = \Delta x_2$ = 1.1%

P_1,mmHg	x_{D1}	R_1	D_1	$Q_{R1} \times 10^{-6}$	R_2	D_2	$Q_{R2} \times 10^{-6}$	$Q_T \times 10^{-6}$
760	.8097	33.2	131.2	1.322	31.3	71.2	1.124	2.446
350	.8570	26.1	101.4	1.036	23.3	41.4	0.867	1.903

b. Increasing the pressure of column 2 makes the azeotrope of the THF-water system become richer in water, i.e., less THF in it. Thus, less THF will be taken overhead in the second column. This means less reboiler heat duty is needed. See Table (5-5). Column 2 distillate product, which is recycled to column 1, is now richer in water and reduced in quantity. Thus the load on column 1 is also reduced, as shown in Table (5-5). Also, as the pressure of column 2

TABLE (5-5): Effect of Increase of Column 2 Pressure On the System at P_1 = 760 mmHg, $\Delta x_1 = \Delta x_2$ = 1.1%

P2,psig	R_1	D_1	$Q_{R1} \times 10^{-6}$	R_2	D_2	$Q_{R2} \times 10^{-6}$	$Q_T \times 10^{-6}$
50	42.1	171.2	1.6772	57.1	111.2	1.5687	3.2459
100	33.2	131.2	1.3217	31.3	71.2	1.1239	2.4456
150	30.1	118.0	1.2027	20.6	58.0	0.9882	2.1909
200	28.5	111.3	1.1411	14.7	51.3	0.9315	2.0726
250	27.5	107.2	1.1026	10.9	47.3	0.9059	2.0085
300	26.9	104.4	1.0759	8.3	44.4	0.8954	1.9713

is increased, the temperature and enthalpy of the recycled distillate will increase. This means, more energy is fed to column 1 in the recycle stream, which will result in more reduction in the reboiler duty of that column.

c. Lastly, Table (5-6.a,b) shows the optimum distillate compositions and the percent away from the azeotrope, Δx, that require

TABLE (5-6): Optimum Value of Δx_1 and Minimum Total Energy, Q_{Tm}, as a Function of Column 2 Pressure

a - P_1 = 350 mmHg, $\Delta x_2^{opt.}$ = 1.5%

P_2,psig	x_{D1}	x_{D2}	$\Delta x_1^{opt.}$	$Q_{R1} \times 10^{-6}$	$Q_{R2} \times 10^{-6}$	$Q_{Tm} \times 10^{-6}$
50	.856	.681	1.2	1.1768	1.0801	2.2569
100	.852	.624	1.6	1.0008	0.8898	1.8906
150	.850	.587	1.8	0.9321	0.8339	1.7660
200	.846	.542	2.0	0.8907	0.8204	1.7111
250	.845	.527	2.1	0.8657	0.8192	1.6849

b - P_1 = 760 mmHg, $\Delta x_2^{opt.}$ = 1.1%

P_2,psig	x_{D1}	x_{D2}	$\Delta x_1^{opt.}$	$Q_{R1} \times 10^{-6}$	$Q_{R2} \times 10^{-6}$	$Q_{Tm} \times 10^{-6}$
50	.814	.685	0.7	1.7228	1.5039	3.2267
100	.810	.628	1.1	1.3217	1.1239	2.4456
150	.807	.591	1.4	1.1788	1.0081	2.1869
200	.805	.565	1.6	1.1044	0.9594	2.0638
250	.804	.546	1.7	1.0600	0.9355	1.9955
300	.803	.531	1.8	1.0279	0.9269	1.9548

minimum total energy, Q_{Tm}, for a given column 2 pressure at P_1 = 350 and 760 mmHg, respectively. The optimum value of Δx_2 stays almost constant at 1.5 and 1.1 % at P_1 = 350 and 760 mmHg, respectively, regardless of column 2 pressure. For column 1, the optimum value of Δx_1 increases as P_2 is increased. See Table (5-6.a,b).

In summary, we have seen that there is an optimum value of Δx_1 and Δx_2 where the total energy required by the system is minimized. Reduction of column 1 pressure and increasing column 2 pressure have major effect on minimizing total energy required. In the next chapter we are going to find the optimum combination of these pressures that requires the least total energy when energy conservation schemes are used. In this case, the optimum values of Δx_1 and Δx_2 are used.

CHAPTER 6

ENERGY CONSERVATION AND HEAT ECONOMY

6.1 Introduction

This chapter deals with the possible options of conserving the total energy required by the system, Q_T, by using energy integration, heat economizers and/or vapor recompression. The calculations have the same basis as in Chapter 5 and at the optimum distillate compositions.

6.2 Energy Integration

Operating the second column at an elevated pressure (and temperature) presents an option of using its condensor to reboil the first column. This uses the energy fed to the second column twice and reduces energy consumption in the first column. Energy integration was investigated at P_1 = 350 and 760 mmHg and various pressures of the second column. The results given in Table (6-1) are based on those given in Table (5-6.a,b) and the calculated overhead condenser duty of column 2 at various pressures. The total heat consumption, Q_T, was calculated by subtracting Q_{c2} given in Table (6-1.a,b) from Q_{Tm} given in Table (5-6.a,b). It is clear from these results that:

a. The energy available from the overhead vapor of column 2, Q_{c2}, is always less than the energy required to reboil the first

TABLE (6-1): Total Heat Consumption of the Energy Integrated System as a Function of Column 2 Pressure

(a) P_1 = 350 mmHg, Δx_2 = 1.5%

P_2,psig	$Q_{R1} \times 10^{-6}$	$Q_{c2} \times 10^{-6}$	Q_{c2}/Q_{R1}	$Q_T \times 10^{-6}$
50	1.1768	-0.7216	0.6132	1.5353
100	1.0008	-0.4642	0.4638	1.4263
150	0.9321	-0.3572	0.3832	1.4088*
200	0.8907	-0.3001	0.3369	1.4110
250	0.8657	-0.2615	0.3021	1.4234

(b) P_1 = 760 mmHg, Δx_2 = 1.1%

P_2,psig	$Q_{R1} \times 10^{-6}$	$Q_{c2} \times 10^{-6}$	Q_{c2}/Q_{R1}	$Q_T \times 10^{-6}$
50	1.7228	-1.1636	0.6754	2.0631
100	1.3217	-0.7179	0.5432	1.7277
150	1.1788	-0.5493	0.4660	1.6376
200	1.1044	-0.4563	0.4132	1.6075
250	1.0600	-0.3945	0.3722	1.6010*
300	1.0279	-0.3512	0.3417	1.6036

*Minimum total energy required with heat integration.

column, Q_{R1}. The insufficient boilup for the latter column can be made up using another low-pressure steam reboiler.

b. Although the temperature of the overhead vapor from column 2 increases as P_2 is increased, the ratio of the energy available from that vapor to that required to reboil column 1, Q_{c2}/Q_{R1}, decreases as P_2 is increased or P_1 reduced. This is due to the sharp reduction of the overhead-vapor flow rates of both columns due to less volatile material (THF) in the overhead streams as P_2 is increased or P_1 reduced. This means that the energy available from column 2 overhead to reboil column 1 decreases as P_2 is increased or P_1 decreased. This works in opposite direction to that of pressure, i.e., for example, as column 2 pressure is increased, at fixed P_1; the total energy required decreases but the energy available to reboil column 1 from column 2 overhead decreases. Thus, there should be an optimum P_2 where the total energy required is minimum.

c. The optimum pressure for column 2, as shown in Table (6-1.a,b) and Figure (6-1), occurs at P_2 = 150 psig when P_1 = 350 mmHg, and at P_2 = 250 psig when P_1 = 760 mmH_g. But the former combination, i.e., P_1 = 350 mmHg and P_2 = 150 psig, requires less energy than the latter, and thus it will be called the "Optimum Pressure" case. The optimum Δx_1 and Δx_2 in this case as shown in Table (5-6.a), are 1.8 and 1.5%, respectively, and the feed to column 1 is preheated by the bottom product of that column.

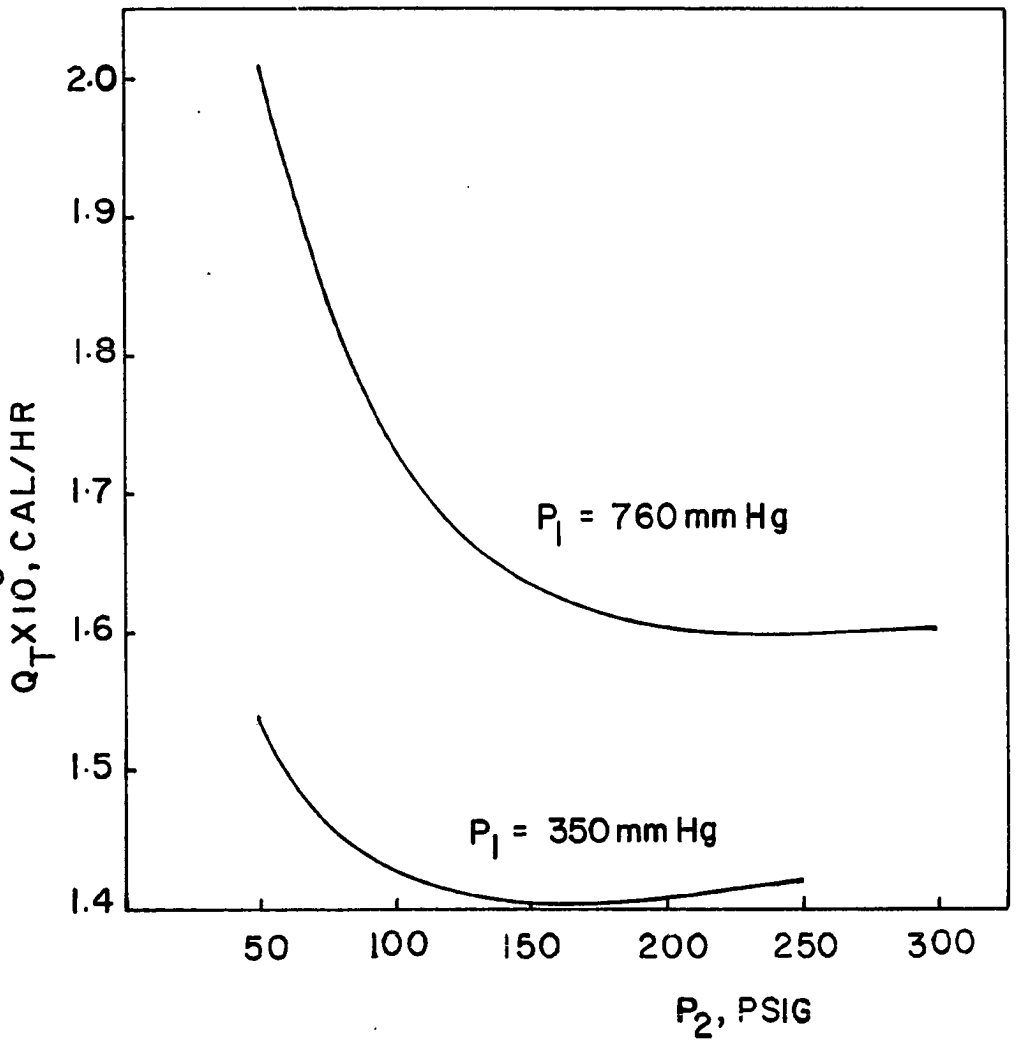

Figure (6-1) - Total Energy Required With Heat Integration as a Function of Pressure

6.3 Heat Economizers

The standard configuration for the base case and the optimum-pressure case assumes that the feed to column 1 is preheated by the bottom product of that column. More energy can be saved if the feed is also preheated by the overhead vapor of the first column; provided that the vapor temperature is high enough to transfer heat to the feed. It is assumed that a difference of at least 10°C (18°F) is required between the entering cold stream (feed) and the leaving hot stream (vapor) in order to have an efficient feed preheater. The distillate product from column 1 can also be preheated by the bottom product of column 2 before entering that column.

Using the notation given in Table (6-2), Table (6-3) shows the feed-preheat temperatures, reboiler duties and total energy required for the various energy conservation schemes listed in Table (6-2). It is clear from Table (6-3) that the system total energy requirement becomes minimum when both heat economizers and energy integration are used (Cases I.4 and II.4). For Case I.4, the overhead vapor and bottom product of column 1 are both used to preheat the feed while the second column bottom is used to preheat the feed of that column. Column 2 overhead vapor is used to reboil column 1. The flowsheet of this scheme is shown in Figure (6-2). It should be mentioned here that not all the overhead vapor of column 1 is condensed in the feed preheater (limited ΔT) and another condenser is required.

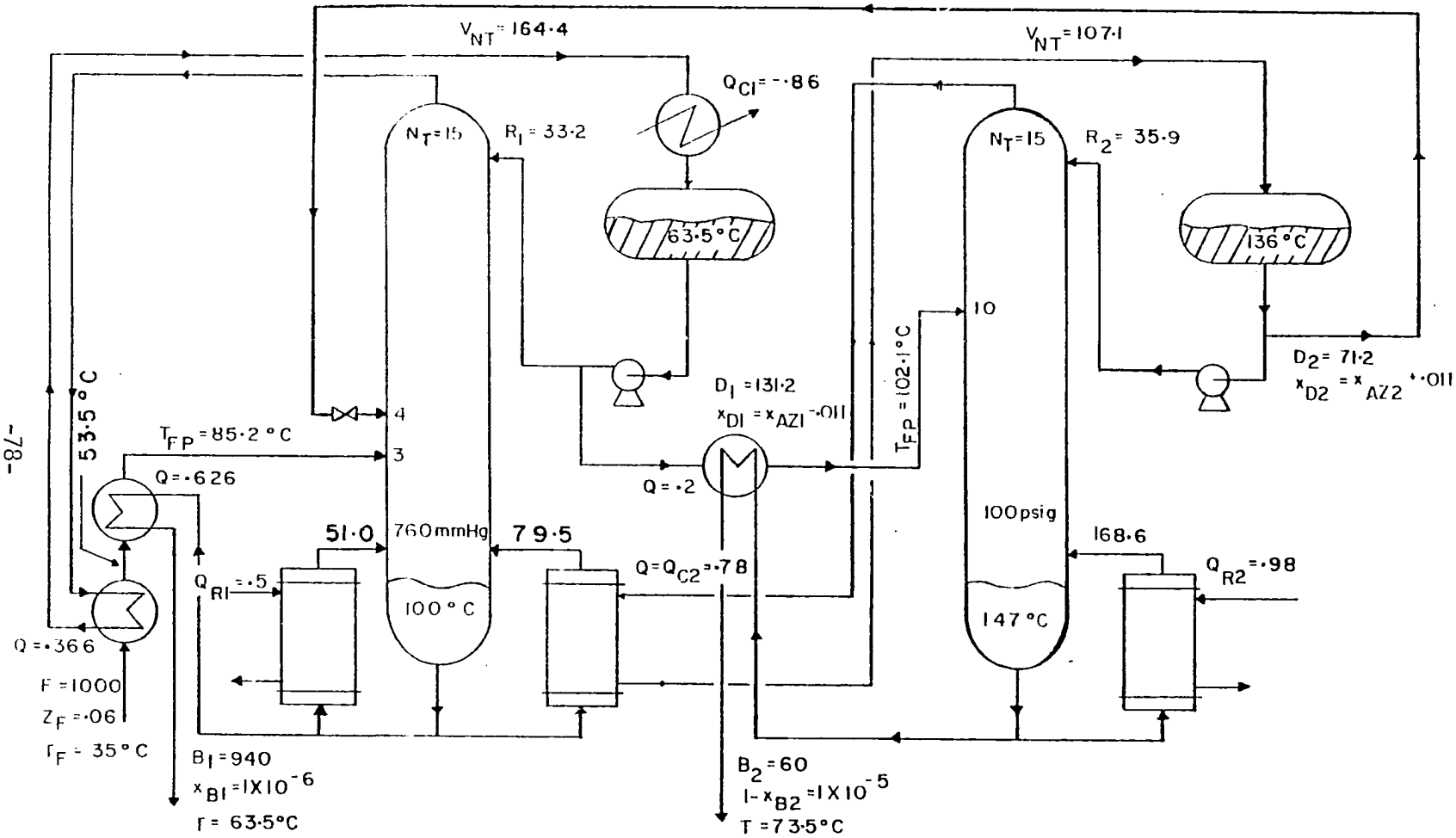

Figure (6-2) - Flowsheet and Energy Requirement for Case I.4 (P_1 = 760 mmHg, P_2 = 100 psig, Using Both Energy Integration and Heat Economizers, Q_T = 1.480; Q's, Mcal/hr

TABLE (6-2): Notation Used for Various Energy Conservation Schemes

Case	Notation
Base Case	Case I.1
With heat economizers	Case I.2
With energy integration	Case I.3
With both heat economizers and energy integration	Case I.4
With heat economizers and vapor recompression	Case I.5
Optimum-Pressure Case	Case II.1
With heat economizers	Case II.2
With energy integration	Case II.3
With both heat economizers and energy integration	Case II.4

TABLE (6-3): Feed-Preheat Temperature and Energy Requirement for Various Energy Saving Schemes [See Table (6-2]

Case	$T_{FP,1}$ °C	$T_{FP,2}$, °C	$Q_{C2} \times 10^{-6}$	$Q_{R1} \times 10^{-6}$	$Q_{R2} \times 10^{-6}$	$Q_T \times 10^{-6}$
I.1	82.8	63.5	-0.7179	1.3217	1.1239	2.4456
I.2	85.2	102.1	-0.7406	1.2745	0.9883	2.2628
I.3	82.8	63.5	-0.7179	1.3217	1.1239	1.7277
I.4	85.2	102.1	-0.7406	1.2745	0.9883	1.4828
II.1	65.1	42.6	-0.3572	0.9399	0.8339	1.7738
II.2	65.1	120.1	-0.4187	0.9399	0.5895	1.5294
II.3	65.1	42.6	-0.3572	0.9399	0.8339	1.4088
II.4	65.1	120.1	-0.4187	0.9399	0.5895	1.1107

For Case II.4, where the pressure is optimum, we did the same as in Case I.4 except that the overhead vapor of column 1 cannot be used to preheat the feed of that column ($\Delta T < 10°C$). The flowsheet of this case is shown in Figure (6-3).

6.4 Vapor Recompression

Vapor recompression represents another alternative for the use of the heat of condensation of the overhead vapor of a column to reboil its bottoms, provided that the temperature difference between the top and the bottom of the column is low. In this case, a compressor that draws suction on the overhead vapor, compressing it nearly isentropically and raising both pressure and temperature, is needed. If the vapor is saturated at suction conditions, it will become superheated at discharge. The condensing temperature of the overhead vapor, after recompression, must be above the boiling point of the bottom of the column by whatever temperature difference is needed to transfer heat through the reboiler [37]. Since the temperature difference between the top and base of column 2 is low ($< 20°C$), we are trying to evaluate the use of vapor recompression for this system. Figure (6-4) shows the flowsheet for this case.

The calculation of the theoretically required work by the compressor is based on Equation (6-1), which is valid for the polytropic flow compression of an ideal gas [41]:

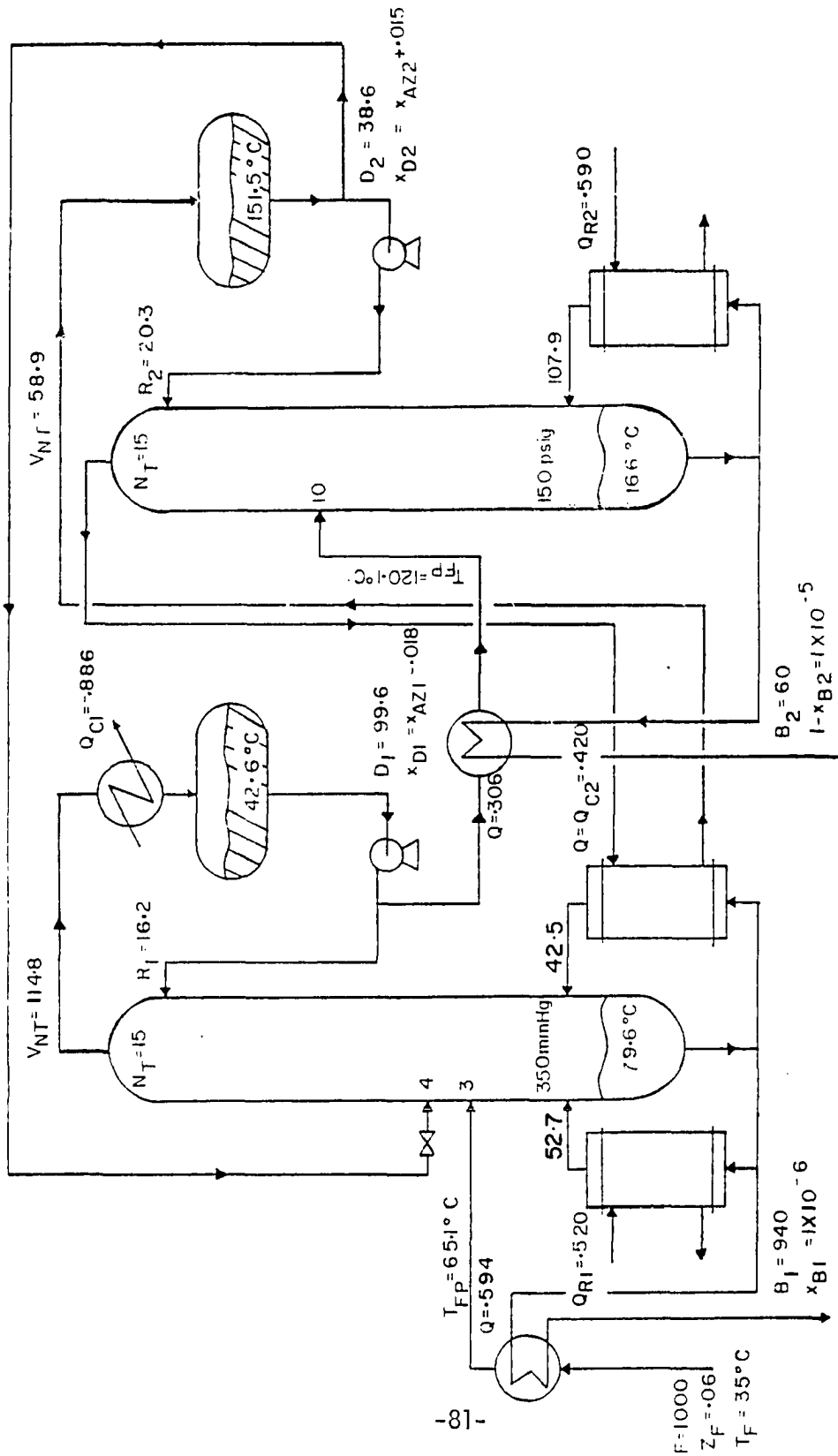

Figure (6-3) - Flowsheet and Energy Requirement for Case II.4 (P_1 = 350 mmHg, P_2 = 150 psig, Using Both Energy Integration and Heat Economizers), Q_T = 1.110; Q's, Mcal/hr

$$W = V\ RT_s\left(\frac{\kappa}{\kappa-1}\right)\left[\left(\frac{P_d}{P_s}\right)^{\frac{\kappa-1}{\kappa}} - 1\right] \qquad (6\text{-}1)$$

where

V = vapor flow rate, gmol/hr

$\kappa = c_p/c_v$

R = gas constant, 1.9872 cal/gmol°K.

T_s = temperature at compressor suction, °K

P_s, P_d = pressure at suction and discharge of the compressor, respectively, atm.

C_p, C_v = specific heats at constant pressure and volume respectively, cal/gmol°K

On the other hand, the temperature of the recompressed vapor at the compressor discharge was calculated using the relation

$$T_d = T_s\left(\frac{P_d}{P_s}\right)^{\frac{\kappa-1}{\kappa}} \qquad (6\text{-}2)$$

Assuming that the recompressed vapor is to be condensed at a temperature 15°C above that of the bottom of the column; the saturation pressure of the vapor, P_d, was calculated and substituted in Equations (6-1) and (6-2) to get the work required and temperature at the discharge of the compressor. The results of this investigation for Case I.5 (Base case with heat economizers and vapor recompression) are summarized in Table (6-4). When vapor recompression was applied on the separation of the THF-water system, we noticed the following:

TABLE (6-4): Summary of Vapor Recompression Results For Case I.5 [See Table (6-2)].

Column 2 pressure, P_s, atm.	7.8
Column 2 top temperature, T_s,°K	409.0
Column 2 base temperature, °K	420.0
Column 2 overhead-vapor flow rate, gmol/hr	107.13
Vapor from flashed reflux, gmol/hr	3.83
Required condensation temperature, T_c,°K	435.0
Calculated saturation pressure at T_c, P_d,atm.	13.78
Average heat, capacity at T_s, cal/gmol°K	22.28
Heat capacity ratio, κ	1.01
Calculated temperature at compressor discharge, T_d,°K	430.3
Work required by compressor, $Wx10^{-6}$ at η = 50%,cal/hr	0.1053
Column 1 reboiler duty, $Q_{R1}x10^{-6}$, cal/hr	1.2204
Column 2 reboiler duty, $Q_{R2}x10^{-6}$, cal/hr	0.9833
Heat available from vapor recompression $x10^{-6}$,cal/hr	0.7577
Total heat required, $Q_T x10^{-6}$, cal/hr	1.5513

a. The heat available from the recompressed vapor is not sufficient to reboil column 2. Thus another high-pressure steam reboiler is needed. This is because the vapor cannot be superheated at the above calculated saturation pressure (κ is very close to 1.0). No trim coolers will be needed in this case. The additional steam reboiler, in this case, has a heat load of $0.2256x10^6$ cal/hr.

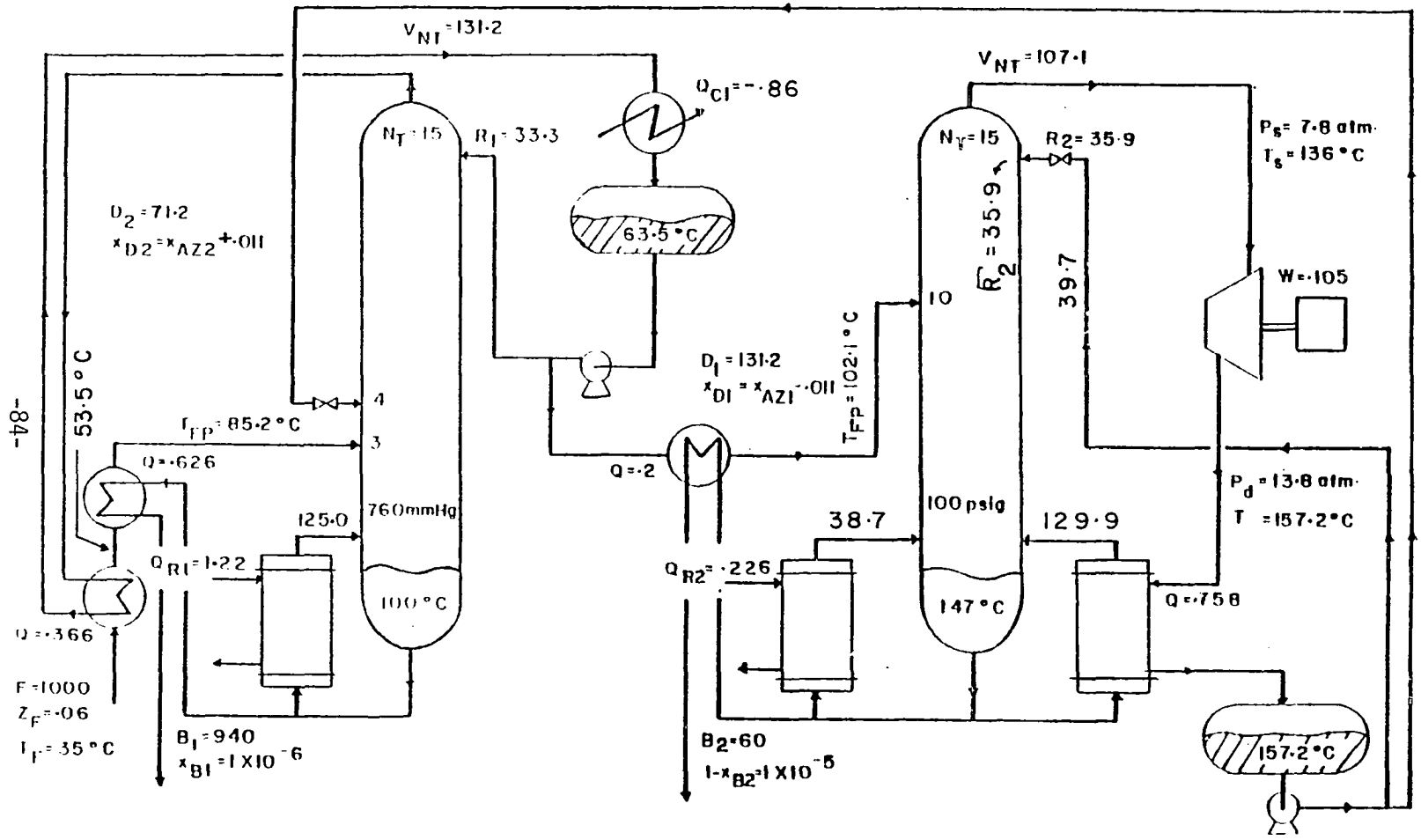

Figure (6-4) - Flowsheet and Energy Requirement for Case I.5 (P_1 = 760 mmHg, P_2 = 100 psig, Using Both Heat Economizers and Vapor Recompression), Q_T = 1.551; Q's, Mcal/hr

b. Both reflux and distillate of the second column are now at higher temperature and pressure than they were without vapor recompression. The external reflux returned to the column should be equal to the sum of the internal reflux and the amount of vapor produced from flashing that stream at the top of the column. See Figure (6.4). This will increase the load on the compressor and more work will be required. On the other hand, the distillate recycled to the first column has now more energy which results in a decrease in that column heat load.

c. In terms of energy consumption, Case I.5 requires 4.6% more energy than Case I.4. In addition, compressors usually need a fairly high maintenance cost.

In conclusion, we see that using both heat economizers and energy integration scheme, for either the Base Case or Optimum Pressure Case, is the best in terms of saving energy. In the next chapter, we are going to compare, in terms of dollars, the best energy saving scheme (Case I.4) with the Base Case (Case I.1), at P_1 = 760 mmHg and P_2 = 100 psig.

CHAPTER 7

STEADY-STATE ECONOMIC EVALUATION OF THE TWO COLUMN SYSTEM

7.1 Introduction

In this chapter, the heat exchangers used as feed preheaters, reboilers or condensers, were designed. The cost of heat exchangers and utilities (steam and cooling water) were evaluated for various energy conservation schemes. The column's size and installed cost were calculated. Then the optimum reflux ratio for the base case (I.1) and optimum pressure case (II.1) were evaluated.

These calculations were based on a feed rate of 2×10^6 gmol/hr, containing 6 mole % THF, and on a system operation of 350 days/year.

7.2 Heat Exchangers Design and Cost

The heat transfer area (A, m^2) of a heat exchanger was calculated from

$$A = \frac{Q \times 10^{-4}}{U \cdot \Delta t_m} \qquad (7\text{-}1)$$

where

Q = heat load of the exchanger, cal/hr

U = overall heat transfer coefficient, cal/hr cm^2 °C

Δt_m = logarithmic-mean temperature difference, °C

The values of U were taken as 50 and 75 cal/hr cm^2 °C for liquid-liquid and vapor-liquid heat exchanging fluids, respectively. Counter-

current flow was assumed in all heat exchangers. A temperature difference of about 10°C was assumed between the hot stream entering and the cold stream leaving the exchanger, unless otherwise mentioned.

The cost of the exchanger was based on a 3/4" outer diameter tube, 1" square pitch, 16 ft. long bundles of carbon steel construction. The rating design pressure was taken as 150 psia for all exchangers, except second-column reboiler and the condenser/reboiler used to reboil column 1, which were taken as 300 psia. The cost was then taken from Figure (14-13), Reference [31]. These calculations were done for cases I.1 - I.4 [See Table (6-2)]. Results of this investigation are summarized in Tables (7-1) - (7-3), for feed preheaters, overhead condensers and reboilers, respectively. The calculations in Table (7-2) were based on a cooling-water input tempera-

TABLE (7-1): Feed Preheaters Design and Cost for Cases I.1 and I.2.

	Case I.1	Case I.2		
	Column 1	Column 1		Column 2
Feed preheat source	Bottoms	O/H	Bottoms after O/H	Bottoms
Feed input temp., °C	35.0	35.0	53.5	63.5
Feed output temp., °C	82.8	53.5	85.2	102.1
Hot stream input temp., °C	100.0	63.5	100.0	147.0
Hot stream output temp., °C	45.0	63.5	63.5	73.5
$Qx10^{-9}$, cal/hr	1.89	0.6	1.25	0.4
A, m^2	284.6	45.3	204.3	34.4
Preheater cost, $	30,000	9,500	23,000	8,000
Total Cost, $	30,000		40,500	

TABLE (7-2): Overhead Condensers Design and Cost For Cases I.1 and I.2

	Case I.1		Case I.2	
	Column 1	Column 2	Column 1	Column 2
Condensation temp., °C	63.5	136.0	63.5	136.0
$Q_C \times 10^{-9}$, cal/hr	2.52	1.48	1.85	1.55
A, m^2	186.2	21.3	142.5	22.3
Condenser cost, $	23,000	6,000	19,000	6,500
Total cost, $	29,000		25,500	

TABLE (7-3): Reboilers Design and Cost Without and With Heat Integration

a. Without heat integration:

	Case I.1		Case I.2	
	Column 1	Column 2	Column 1	Column 2
Base temp., °C	100.0	147.0	100.0	147.0
$Q_R \times 10^{-9}$, cal/hr	2.64	2.29	2.55	1.89
A, m^2	179.7	155.6	173.3	133.2
Reboiler cost, $	23,000	23,000	22,000	22,000
Total cost, $	46,000		44,000	

b. With heat integration:

	Column 1		Column 2
	Condenser/Reboiler	L.P. Steam Reboiler	Reboiler
Base temp., °C	100.0	100.0	147.0
$Q \times 10^{-9}$, cal/hr	1.53*	1.01**	1.89
A, m^2	56.7	67.4	133.2
Reboiler cost, $	13,000	15,000	22,000
Total cost, $	50,000		

* $Q = Q_{C2}$ ** $Q = Q_{R1} - Q_{C2}$

ture of 90°F (32.2°C) and output temperature of 130°F (54.4°C). The cooling-water output temperature for vacuum column at 350 mmHg was taken as 104°F (40°C). The temperature of the steam used to reboil the columns was assumed to be 20°C above the base temperature of the columns shown in Table (7-3). Table (7-4) shows the total heat exchangers cost for the above three cases.

TABLE (7-4): Total Cost of Heat Exchangers for Various Energy Conservation Schemes [See Table (6-2)]

	Case I.1	Case I.2	Case I.3	Case I.4
Feed preheaters cost, $	30,000	40,500	30,000	40,500
Condensers cost, $	29,000	25,500	23,000	19,000*
Reboilers cost, $	46,000	44,000	55,000	50,000
Total cost, $	105,000	110,000	108,000	109,500

*The overhead vapor of column 2 is used to reboil column 1, i.e., no condenser is used for column 2.

It is clear that using heat economizers (Case I.2) and/or energy integration (Cases I.4 and I.3, respectively) require higher capital investment than the Base Case (Case I.1). In the next section we will show the saving in energy cost for all of these cases.

7.3 Utilities Cost

Assuming a temperature difference of 20°C between the column base and the stream temperatures, the annual cost of steam (C_{st},$) was calculated as

$$C_{st} = \frac{C_s \cdot Q_R \cdot H_y}{252\lambda} \qquad (7\text{-}2)$$

where

C_s = cost of steam, \$/1000 lbs

Q_R = reboiler duty, cal/hr

H_y = operation hours per year, hr/year

λ = latent heat of steam Btu/lb

The values of C_s were taken as 6.0 \$/1000 lbs for low pressure steam and 8.0 \$/1000 lbs for high pressure steam from Reference [33] updated to the 1982 prices.

Annual cooling water cost was calculated from

$$C_{cw} = \frac{C_C \cdot H_y \cdot Q_C}{3785\ C_p(t_2-t_1)} \qquad (7\text{-}3)$$

where

C_c = cost of cooling water, \$/1000 gal

Q_c = condenser duty, cal/hr

C_p = heat capacity of water = 1 cal/g °C

t_1, t_2 = cooling water input and output temperatures, °C

The values of t_1 and t_2 were taken as 32.2 and 54.2°C. C_c = 0.12 \$/1000 gal. Results of this investigation are summarized in Table (7-5). These results are based on H_y = 8,400 hr/year; λ = 946.8 Btu/lb for low pressure steam (28.8 psia) and 885.3 Btu/lb for high pressure steam (105 psia).

TABLE (7-5): Annual Cost of Steam and Cooling Water for Various Energy Conservation Schemes [See Table (6-2)]

	Case I.1		Case I.2		Case I.3		Case I.4	
	C-1	C-2	C-1	C-2	C-1	C-2	C-1	C-2
a - Steam								
Reboiler duty, $Q_R \times 10^{-9}$, cal/hr	2.64	2.29	2.55	1.89	1.23	2.29	1.01	1.89
Annual cost of steam, $1000	557.7	689.8	538.7	593.4	260.1	689.8	211.0	593.4
Total steam cost, $1000	1,247.5		1,132.1		959.9		804.4	
Saving in steam cost, %	0.0		9.25		23.05		35.52	
b - Cooling water								
Condenser duty, $Q_C \times 10^{-9}$, cal/hr	2.52	1.48	1.85	1.55	2.52	1.48	1.85	0.0
Annual cost of C.W., $1000	30.5	17.9	22.4	18.8	30.5	17.9	22.4	0.0
Total C.W. cost, $1000	48.4		41.2		48.4		22.4	
Saving in C.W. cost, %	0.0		14.88		0.0		53.72	

Note: C-1 refers to Column 1 , C-2 refers to Column 2

The percentage of the annual saving in utilities cost, compared with the Base Case (Case I.1) is also shown in Table (7-5) for the various cases described above. It is clear from these results that Case I.4 is much better, in terms of energy conservation, than the others.

7.4 Column Size and Cost

The diameter of the column was calculated using the formula

$$D_c = 0.01881 \left(V_{max} \cdot \overline{M}_W / \overline{\rho}_V \, U_{VN}\right)^{1/2} \qquad (7\text{-}4)$$

where

V_{max} = maximum vapor flow rate in the column, gmol/hr

$\overline{M}_W$ = average molecular weight, g/gmol

$\overline{\rho}_V$ = average density of the vapor mixture, g/cc

U_{VN} = net vapor velocity, cm/sec

D_c = column diameter, cm.

The vapor density was calculated using the ideal gas law. The net vapor velocity was then found from Figure (13.21), Reference [45], for a tray spacing of 18".

The height of the column was calculated assuming tray spacings of 24" and skirt height of 15 ft. at the bottom of the column. The thickness of the column's shell for pressure vessels was calculated using the relation

$$t_s = \frac{P \cdot r_i}{S \cdot E_j - 0.6P} + t_c \qquad (7\text{-}5)$$

where

P = maximum allowable internal pressure, psig

r_i = column radius, in.

S = maximum allowable working stress, psi

E_j = efficiency of joints, fraction

t_s = minimum wall thickness, in.

t_c = allowance for corrosion, in.

The values of S and E_j were taken from Table 4, Reference [30]. The corrosion allowance was taken as 1/8" per 10 years of vessel life. For vacuum vessels, the thickness was found from Figure (3), Reference [25]. Results of these calculations along with columns operating conditions are listed in Table (7-6) for Case I.1.

On the other hand, the cost of the installed column (No tanks, pumps or heat exchangers) was calculated using the procedure used by Millers and Kapeila [24], using a wage rate of $16/hour. These costs along with the cost of heat exchangers, calculated in section 7.2, were updated to the 1982 prices by multiplying by a factor of 1.2. Results of these calculations will be presented in the next section.

TABLE (7-6): Operating Conditions and Size of the Columns for the Base Case [Case I.1].

	Column 1	Column 2
Level of max. vapor flow rate	Top of column	Base of column
Temperature, °C	63.5	420.0
Pressure, mmHg	760.0	5930.1
Composition, X_{THF}	0.8074	0.9999
$\overline{M}_W$, g/gmol	62.2	72.1
$\overline{\rho}_\ell$, g/cc	0.8663	0.7649
$\overline{\rho}_V$, g/cc	$2x10^{-3}$	0.01598
U_{VN}, cm/sec	121.92	39.62
V_{max}, $x10^3$ gmol/hr	331.51	419.81
Column diameter, cm	163.58	113.69
Shell thickness, cm	1.27	2.22
Column height, m	14.48	15.85

7.5 Optimum Reflux Ratio

Using the above procedures, the cost of the installed columns, heat exchangers and utilities were calculated at various values of $\beta(= RR/RR_{min})$. The results of this investigation are shown in Tables (7-7) and (7-8) for the base case at P_1 = 760 mmHg, P_2 = 100 psig, and the optimum pressure case at P_1 = 350 mmHg, P_2 = 150 psig. $X_{B1} = 1x10^{-6}$ and $1-x_{B2} = 1x10^{-4}$. The total capital cost was assumed to be depreciated in 5 years. From these results, one can notice the following:

TABLE (7-7): Estimated Cost of the Installed Columns, Heat Exchangers and Utilities for the Base Case (I.1) as a function of of $\beta(RR_{min_1} = .2273, RR_{min_2} = .3854)$

	Total Capital Cost, $		Annual Capital Cost, $			
β	Column	H.E.	Column and H.E.	Steam	C.W.	Total, $
Column 1						
1.10	732,086	90,240	164,465	548,200	29,950	742,615
1.20	642,732	91,200	146,786	557,700	30,500	734,986*
1.25	623,762	91,680	143,088	562,500	30,800	736,388
1.50	549,986	94,080	128,813	586,100	32,100	747,013
Column 2						
1.05	643,080	33,360	135,288	677,080	17,200	829,568*
1.10	616,278	34,008	130,057	682,980	17,430	830,467
1.20	581,400	34,800	123,240	689,800	17,900	830,940
1.25	583,334	35,280	123,722	695,750	18,140	837,613
1.50	560,604	37,560	119,633	729,800	19,300	868,733

*Minimum annual cost.

(1) The total capital cost [second column in Tables (7-7) and (7-8)] for column 1 is much affected by changing β due to sharp increase in the total number of trays, while column 2 is less affected by changing β.

TABLE (7-8): Estimated Cost of the Installed Columns, Heat Exchangers and Utilities for the Optimum Pressure Case (II.1) as a Function of β (RR_{min_1} = .2103, RR_{min_2} = .3791)

	Total Capital Cost, $		Annual Capital Cost, $			
β	Column	H.E.	Column and H.E.	Steam	C.W.	Total, $
Column 1						
1.15	961,750	97,200	211,790	402,270	62,550	676,610
1.20	786,430	98,040	176,890	406,030	63,096	646,020
1.25	734,112	98,400	166,500	409,120	63,608	639,230
1.50	586,615	100,800	137,480	425,200	66,270	628,950*
2.0	513,260	103,200	123,290	457,150	68,000	648,440
Column 2						
1.15	485,560	46,200	106,152	509,030	8,200	623,382
1.20	469,128	46,800	103,186	511,890	8,300	623,375
1.25	453,312	47,400	100,142	514,750	8,410	623,302*
1.50	447,948	49,800	99,550	528,750	8,960	637,260

*Minimum annual cost.

(2) The optimum value for β varies with column pressure and it is increasing with either reducing the first column pressure or increasing the second column pressure. For example, the optimum value of β for column 1 was increased from 1.2 to 1.5 when P_1 was reduced from 760 to 350 mmHg, and from 1.05 to 1.25, for column 2, when P_2 was increased from 100 to 150 psig.

(3) Although reduction of column 1 pressure or increase of column 2 pressure increases the total capital cost, the total annual capital cost [last column in Tables(7-7) and (7-8)] decreases due to decrease in energy consumption, i.e., operating the two-columns system at 350 mmHg and 150 psig is about 20% cheaper than operating at 760 mmHg and 100 psig.

(4) Lastly, the value of β used throughout this study (at P_1 = 760 mmHg and P_2 = 100 psig) is now confirmed as 1.2 for column 1 and also for column 2 without much loss in the annual capital cost.

CHAPTER 8

MODELING AND SIMULATION

8.1 Introduction

The two-column system studied in this work has the main feature that both columns are highly interacting, in the sense that any disturbance that occurs in one column is directly transmitted into the other through the distillate flows. Thus these columns should be studied as one complete unit.

In this chapter we will describe the basic modeling of a distillation column and point out the simplifications that were made for the particular system in this study.

8.2 Basic Column Modeling

A distillation column can be modeled by a set of non-linear ordinary differential equations describing the conservation of material and energy around each tray [19]. For a binary system, three equations per tray follow from this approach.

A. Total material balance

$$\frac{dM_n}{dt} = L_{n+1} - L_n + V_{n-1} - V_n \qquad (8\text{-}1)$$

B. Component continuity

$$\frac{d(M_n x_n)}{dt} = L_{n+1}\, x_{n+1} - L_n x_n + V_{n-1}\, y_{n-1} - V_n y_n$$

C. Energy balance

$$\frac{d(M_n h_n)}{dt} = L_{n+1}\, h_{n+1} - L_n h_n + V_{n-1}\, H_{n-1} - V_n H_n \qquad (8\text{-}3)$$

In order to simplify the model, the derivative terms in Equations (8-2) and (8-3) were expanded into

$$\frac{d(M_n x_n)}{dt} = x_n \frac{dM_n}{dt} + M_n \frac{dx_n}{dt} \qquad (8\text{-}4)$$

and

$$\frac{d(M_n h_n)}{dt} = h_n \frac{dM_n}{dt} + M_n \frac{dh_n}{dt} \qquad (8\text{-}5)$$

The derivative of the enthalpy term was set equal to zero, because the enthalpy changes as a function of temperature are very fast. The total continuity equation was then used to eliminate $\frac{dM_n}{dt}$. With this approximation, Equations (8-2) and (8-3) reduce to

$$\frac{dx_n}{dt} = [\, L_{n+1}(x_{n+1} - x_n) + V_{n-1}(y_{n-1} - x_n) - V_n(y_n - x_n)]/M_n \qquad (8\text{-}6)$$

and

$$V_n = [\, L_{n+1}(h_{n+1} - h_n) + V_{n-1}(H_{n-1} - h_n) - V_n(H_n - h_n)]/(H_n - H_{n-1}) \qquad (8\text{-}7)$$

The ordinary differential Equations (8-1) and (8-6) and the algebraic Equation (8-7) that describe the dynamic changes on each tray were

solved simultaneously with the non-linear algebraic equation for vapor-liquid equilibrium described earlier, via digital simulation.

Because the molar tray-holdups vary with time, at each time and for each tray the liquid rates must be calculated. Therefore, a linearized form of the Francis Weir formula was employed to describe the relationship between liquid flow over the weir (L, gmol/hr) and the holdup on the tray (M, gmol)

$$L = 6.6\times10^{9}\, W_{\ell}\, \bar{\rho}_{\ell} \cdot \left(\frac{M_v}{A_t} - W_h\right)^{3/2} / \bar{M}_W \qquad (8\text{-}8)$$

where

M_v = volumetric tray holdup, m^3, given by

$$M_v = 1\times10^{-6}\, M \cdot \bar{M}_W / \bar{\rho}_{\ell} \qquad (8\text{-}9)$$

and

A_t = tray area, m^2

W_{ℓ} = weir length, m

W_h = weir height, m

$\bar{\rho}_{\ell}$ = average density of the mixture, g/cc

$\bar{M}_W$ = average molecular weight of the mixture, g/gmol.

A summary of the final dynamic model of the two columns is shown in Table (8-1).

8.3 Dynamic Model Assumptions

In designing the dynamic model, the following assumptions were made:

TABLE (8-1): Summary of Column Modeling

	Column 1	Column 2
No. of trays in the system	15	15
No. of differential equations per tray	2	2
No. of algebraic equations per tray	1	1
Total no. of tray equations plus reboiler and condenser equations	48	48
Functional relationships used by the model	Equilibrium, Enthalpy, Liquid hydraulic,Molar density	
Computation of vapor-liquid equilibrium	Pressure in each column is assumed constant. VLE are calculated as outlined earlier in Chapter 3.	
Additional assumptions	Linearized versions of Francis weir formula	

a. The dynamics of the reboilers and condensers were neglected since their response is usually much faster than the response of the column itself [19].

b. Constant pressure throughout each column and negligible pressure drop across the trays.

c. Perfect mixing of the liquid on each tray.

d. Negligible tray-heat losses.

e. Ideal trays, i.e., 100% efficiency. This assumption helps reduce the total number of trays, and therefore the total number of ordinary differential equations required to describe the system.

f. Reflux drum and column base contents are perfectly mixed.

g. Partial reboilers and total condensers.

h. Overhead vapor of column 1 is subcooled after being condensed to 30°C.

i. The heat integrated scheme with heat economizers shown in Figure (6-2) is used. The dynamics of the condenser/reboiler are also neglected.

j. A lag of 15 seconds was assumed in temperature measurement. Temperature transmitter spans of 50°C were assumed to get dimensionless gains and transfer functions of the temperature control loops discussed in next chapter.

k. Hold-up times of 5 minutes were assumed for the reflux drums and base of the columns.

TABLE (8-2): Columns and Tray Specifications at Steady State

	Column 1	Column 2
Column pressure, psig	0	100
Feed: Temperature, °C	85.20	86.30
Composition	0.06	0.8097
Recycle: Temperature, °C	135.85	-
Composition	0.6495	-
Column diameter, cm	161.74	118.24
Tray weir length, cm	117.17	85.13
Tray weir height, cm	5.08	5.08
Range of tray holdups, Kgmol	1.69 - 8.93	0.95 - 1.05
Holdup in reflux drum, Kgmol	26.60	17.55
Holdup in the column base, Kgmol	178.43	39.36

Table (8-2) summarizes columns and trays specifications and gives the range of the hold-ups on the trays, in the reflux drums and the base of the columns. As shown in Table (8-2), the ratio of holdups in the reflux drum or base of the columns to that on the trays are high (> 10). This was found to have no effect on the numerical stability of the integration.

Simple Euler integration algorithm with a constant integration step was used to numerically integrate the differential equations as follows:

a. Predict tray holdup, M, and liquid composition, x, at the next time interval for all trays

$$M_{tl} = M_{to} + \left(\frac{dM}{dt}\right)_{to} \cdot \Delta t \qquad (8\text{-}10)$$

$$x_{tl} = x_{to} + \left(\frac{dx}{dt}\right)_{to} \cdot \Delta t \qquad (8\text{-}11)$$

b. Calculate new vapor mole fractions and enthalpies from equilibrium and enthalpy relationships.

c. Calculate liquid flow rates from Francis formula knowing M_n.

d. Calculate V_B from energy balance around reboiler, knowing reboiler duty.

e. Calculate vapor rates from each tray, starting at the bottom, from tray energy balances.

The dynamic model was tested for numerical stability using various integration intervals. It was found that an integration interval of 4×10^{-4} hrs. (1.44 sec.) was the maximum value that could be used to run the two columns simultaneously without numerical stability problems. The model was tested for step changes in feed rate, feed composition, reflux rate or reboiler heat input.

All these tests were made while the reflux drum and base levels were controlled by proportional-only level controller using the distillate and bottom product flow rates, respectively. The computing time was about 0.02 and 0.03 seconds per iteration for columns 1 and 2, respectively on CYBER 720. About 75% of that time was used for vapor-liquid equilibrium and enthalpy calculations.

It should be mentioned here that we chose to study the dynamics and control of the base case (P_1 = 760 mmHg, P_2 = 100 psig) with heat economizers and energy integration for the following reasons:

(1) It is the state of the art case used in industry, where the results of this study could be applied.

(2) The certainity of the VLE data at these pressures.

(3) We expect little difference in dynamics and controllability from that of the optimum pressure case when both heat economizers and energy integration are used.

CHAPTER 9

CONTROL OF THE TWO-COLUMN SYSTEM

9.1 Introduction

A control system for the separation of the THF-water azeotrope using the two heat-integrated columns operating at two different pressures will be discussed in this chapter. The objective is to keep the composition of the two bottom products (water from column 1 and THF from column 2) near specification purities, while using as little energy as possible. The control scheme must give stable and efficient operation for this interacting system.

In this chapter, the dynamic model discussed in Chapter 8 will be used to test the performance of several control schemes in handling different disturbances.

9.2 Steady-State Considerations

The steady-state design of the system for the separation of 6% THF - 94% water mixture, is given in Figure (6-2). Column 1 operates at atmospheric pressure and column 2 at 100 psig. Other assumptions are mentioned earlier in Chapter 8.

Before different control schemes were tested on the dynamic model, some steady-state economic aspects on the control system design were explored. As discussed earlier in Chapter 5, for specified operating pressures of the two columns, there will be an optimum

distillate composition for each columns that requires minimum total energy to operate the system. For example, for the 1 atm - 100 psig system, the minimum energy required was at $|x_{D1} - x_{AZ1}| = 1.1\%$ and $x_{D2} - x_{AZ2} = 1.1\%$, as shown in Figure (5-1).

Luyben [20] discussed the control system design of a distillation column from steady-state energy conservation standpoint. Tolliver [42] discussed how energy and material balance programs can be used to select the best basic control scheme. Based on these studies, and at constant bottom and distillate product purities in each column, the ratios R/D, R/F and V/F were calculated as a function of feed composition of that column using the Rating Program. These results are shown in Figures (9-1) and (9-2) for columns 1 and 2, respectively. Whichever ratio is most constant or gives the lowest slope, i.e., lowest change of ratio with feed composition, could provide an alternative to dual composition control. As shown in Figures (9-1) and (9-2), it is clear that the R_1/D_1 curve for column 1 and R_2/D_1 curve for column 2 have the lowest slopes. Thus the distillate purity of the first column could be controlled by manipulating the R_1/D_1 ratio, and that of the second column by R_2/D_1 ratio.

The other manipulated variable in each column should hold the bottoms products near their specifications. These products are of very high purities (impurities < 100 ppm). Buckley [3], mentioned that adequate resolution of both measurement and manipulation may be difficult to achieve when the column is designed so that product

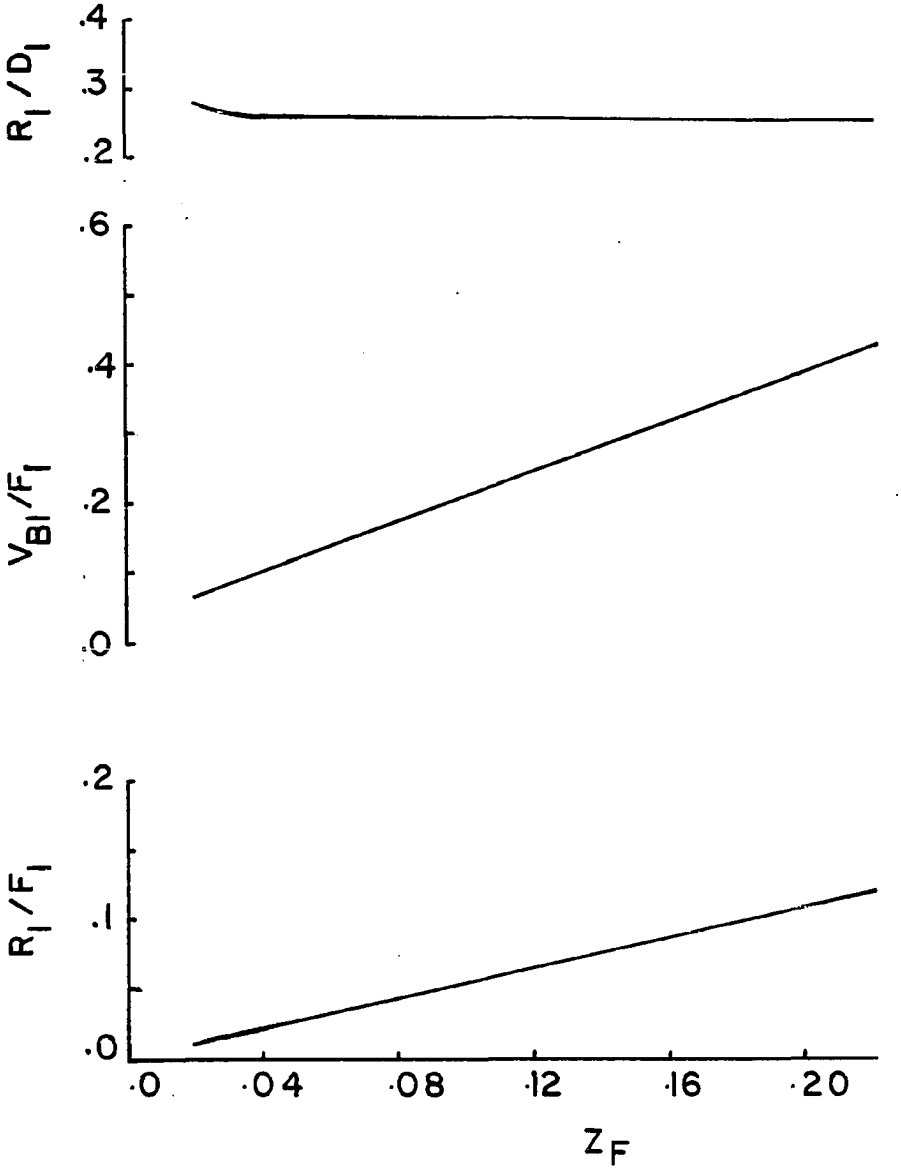

Figure (9-1) - Calculated R/F, V/F and R/D Ratios for Column 1 as a Function of its Feed Composition

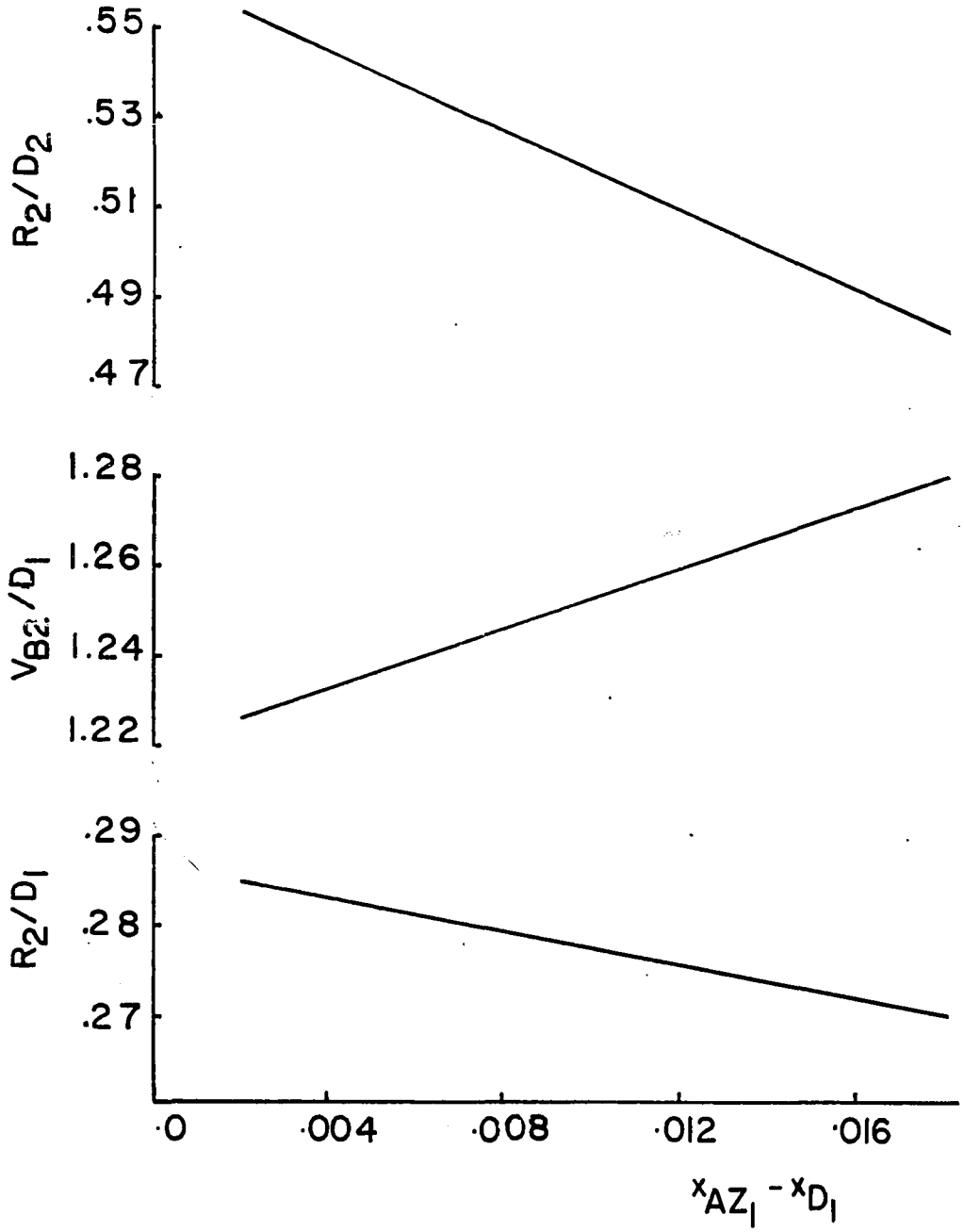

Figure (9-2) - Calculated R/F, V/F and R/D Ratios for Column 2 as a Function of its Feed Composition

specifications of impurities are less than 100 ppm. Fuentes [6] mentioned that systems with high relative volatility respond so quickly that large deviations in products purity occur before the analyzer can respond. Thus, we are going to use indirect composition control to keep these products within specifications. Inspecting Figures (9-3) and (9-4) which show the composition and temperature profiles of the trays along columns 1 and 2, respectively, indicates that column 1 has a sharp temperature profile [curve B in Figure (9-3)] between trays 1 and 3, and column 2 has a normal temperature profile [curve B in Figure (9.4)] between trays 4 and 8. We chose to control the temperature at a tray where significant change in temperature occurs, i.e., at tray number 2 for column 1 and 6 for column 2, by manipulating the steam flow to the corresponding reboilers of these columns.

9.3 Control Schemes for the Two-Column System

We have already established that from an energy point of view two compositions can be indirectly controlled by manipulating two other variables. These compositions will deviate from their steady-state values when the system is disturbed. The smaller the deviation the better the control scheme.

In the previous section we outlined the control scheme we intend to apply on our model. Namely, R_1/D_1 and reboiler duty for column 1, and R_2/D_1 and reboiler duty for column 2. Other control loops required in the system are:

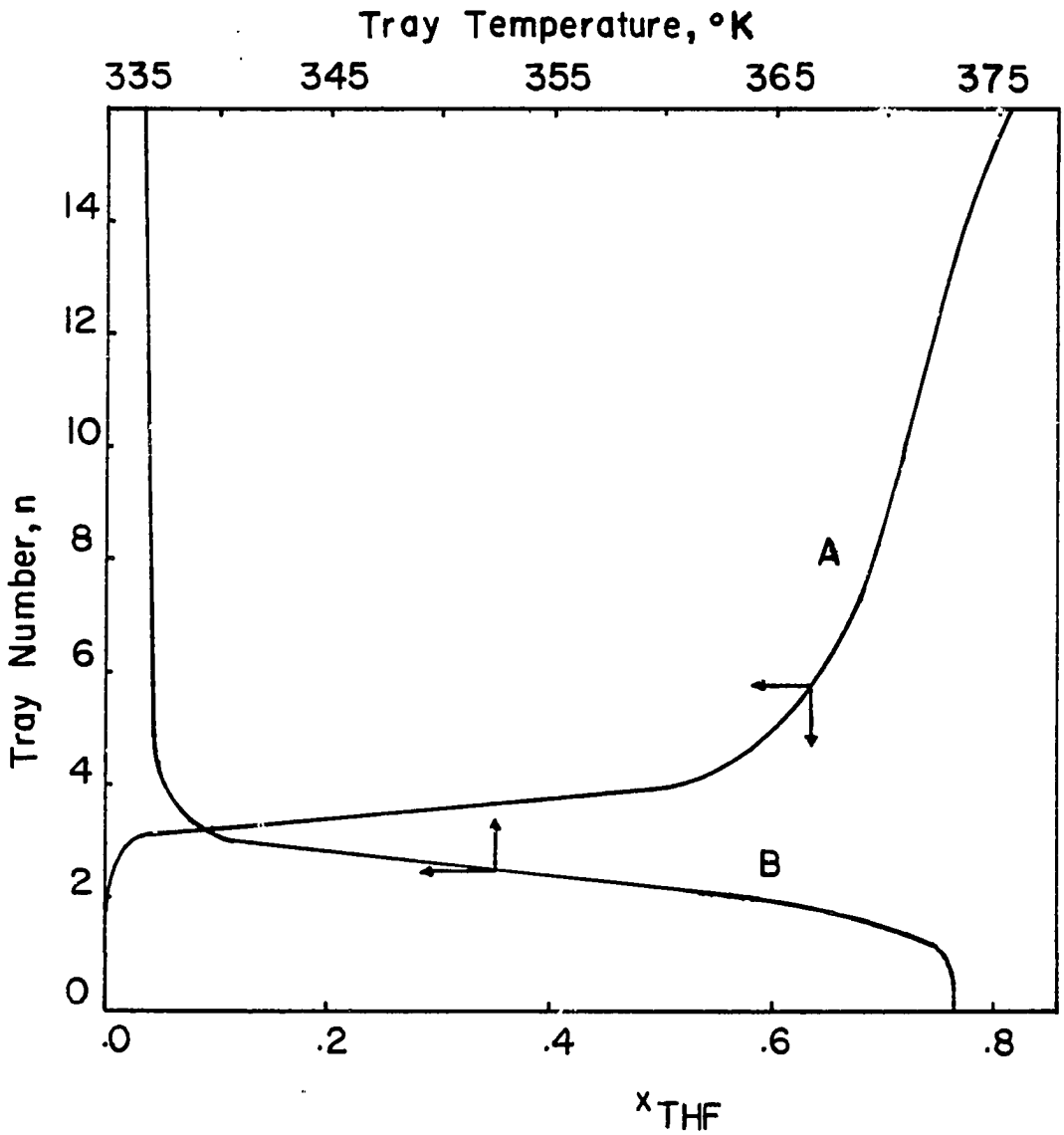

Figure (9-3) - Composition and Temperature Profiles for Column 1

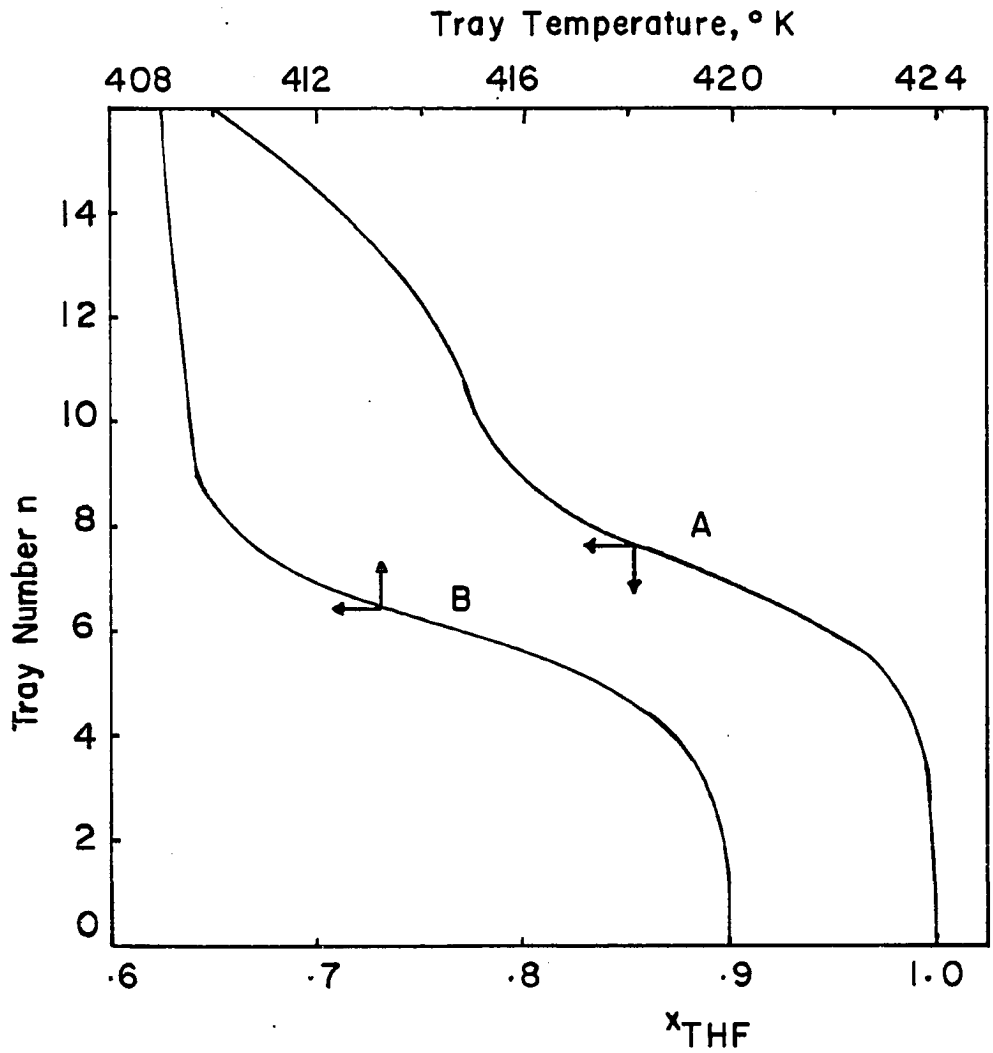

Figure (9-4) - Composition and Temperature Profiles for Column 2

(1) Reflux drum level is to be controlled by manipulating distillate flow rate by proportional-only level controller.

(2) Base level is to be controlled by manipulating bottoms flow rate by proportional-only level controller.

(3) As mentioned earlier, the overhead vapor of column 1 is first condensed to its bubble point then subcooled to 30°C. This will provide enough sensible heat in the overhead condensate in order to avoid losses of valuable material (THF) from the reflux drum of that column. The temperature of the subcooled liquid is to be controlled by manipulating the flow rate of cooling water to the overhead coolers. The pressure of the column is then controlled by venting non-condensibles to atmosphere. High pressure inert gas should be added to the reflux drum after the coolers. See Figure (9-5).

(4) Column 2 pressure is controlled by throttling the liquid leaving the condenser/reboiler [37].

The control scheme of the system described above is shown in Figure (9-5). This will be called Scheme 1. Two other schemes are also considered. These are:

(1) Constant reflux scheme (Scheme 2). Here, the same features of Scheme 1 are used except that the R_1/D_1 and R_2/D_1 ratios are replaced by constant R_1 and R_2 in columns 1 and 2, respectively. See Figure (9-6).

(2) Shinskey's material balance scheme (Scheme 3). This is shown in Figure (9-7). Here, distillate flow rate is used as the

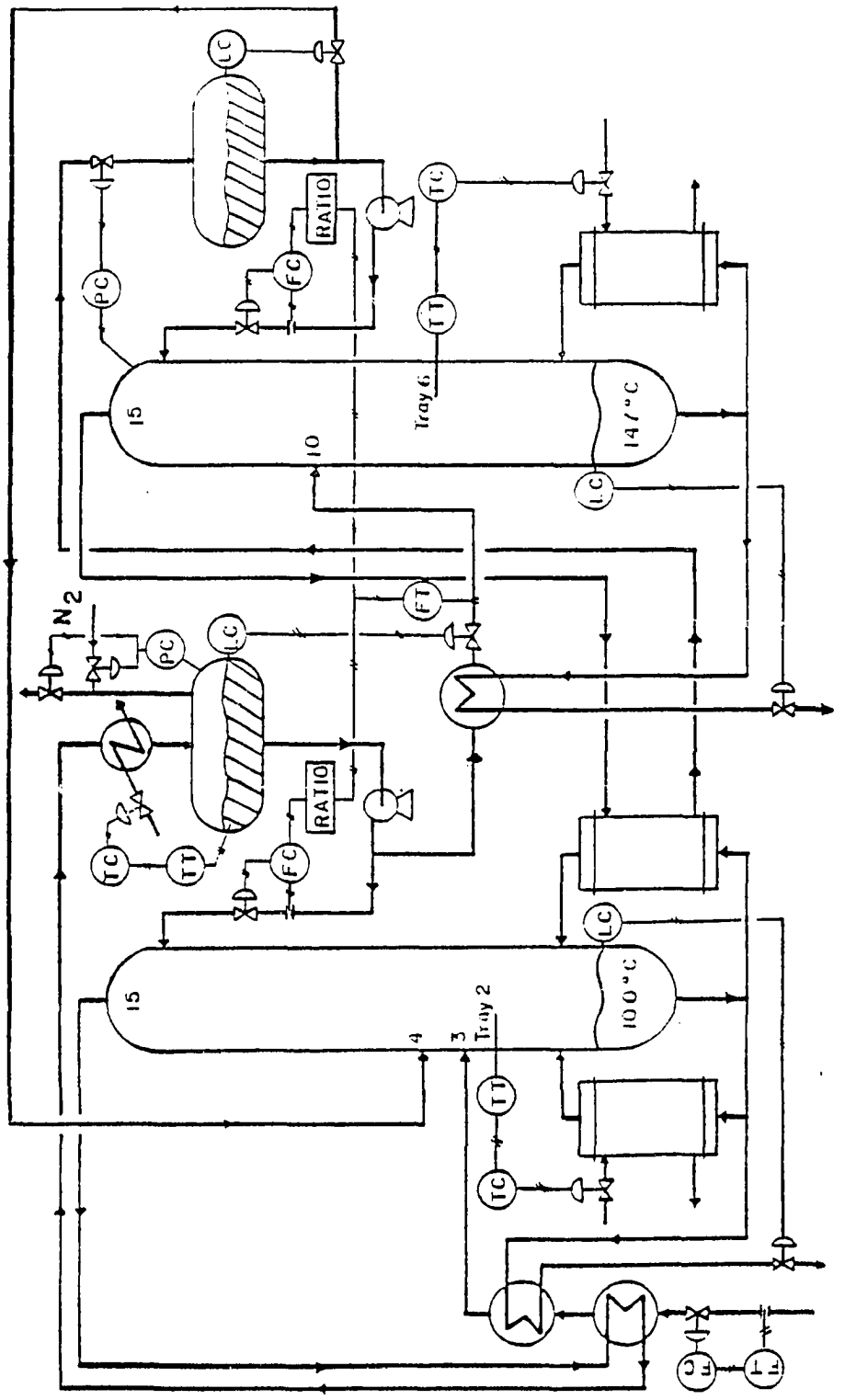

Figure (9-5) - Constant R_1/D_1 and R_2/D_1 Control Scheme, Scheme 1

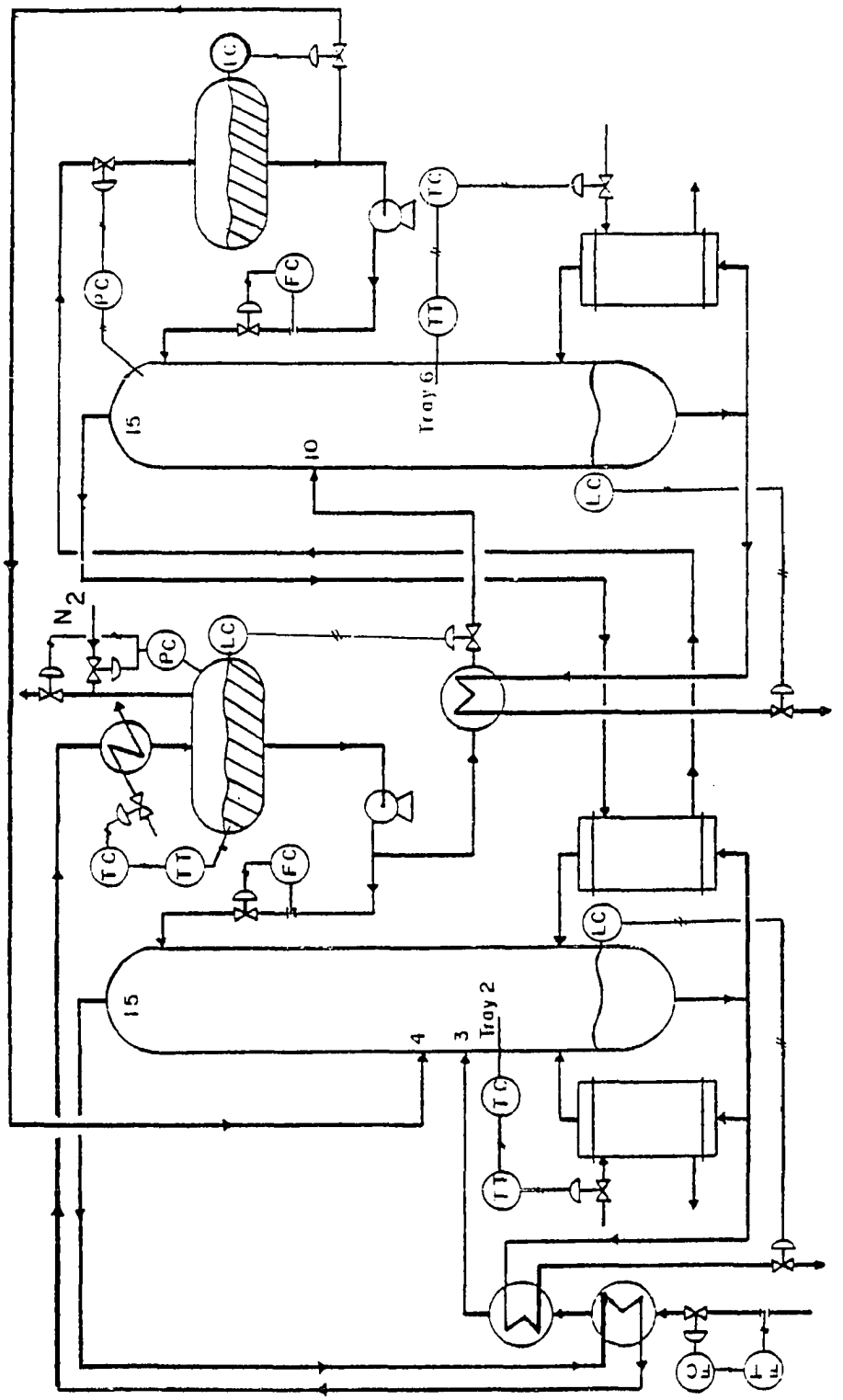

Figure (9-6) - Constant Reflux Control Scheme, Scheme 2

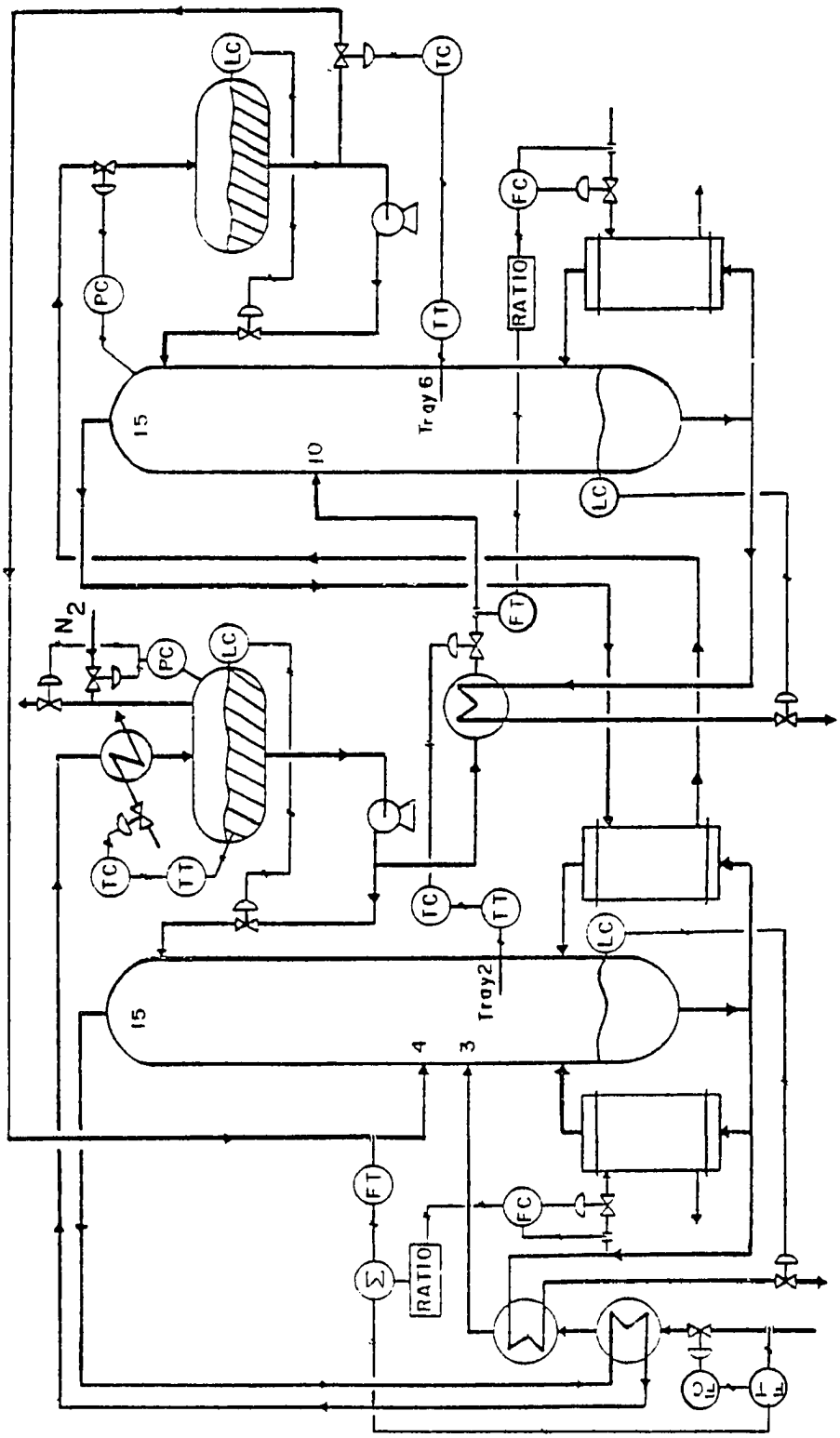

Figure (9-7) - Shinskey's Material-Balance Control Scheme, Scheme 3

manipulated variable to control the temperature of control tray in both columns. Steam flow rate is ratioed to the respective feed rates of the columns. Tight level control is used to keep constant level in reflux drums, by setting reflux flow rate as the difference between overhead vapor and distillate flow rate.

In the next section, we are going to find the transfer functions that relate the controlled variables and manipulated variables for Schemes 1 and 3.

9.4 Controller Design

Pulse tests of the mathematical model were used to find the transfer functions relating the controlled and manipulated variables. Approximate first order plus dead time transfer functions were fitted to the Bode plots calculated by Fourier transformation of the pulse data. The Bode plots for Scheme 1(or 2) are shown in Figures (9-8) and (9-9) for columns 1 and 2, respectively. These plots were obtained by changing the reboiler duties of the columns by + or -2% from the steady state values. The width of the pulses, in this case, were 0.6 and 1.5 minutes for columns 1 and 2, respectively. Summary of the results of the pulse test for Scheme 1 are shown in Table (9-1) along with the calculated controllers settings, using the Ziegler-Nichols method and the frequency-domain technique described by Luyben [19] for proportional-integral controllers.

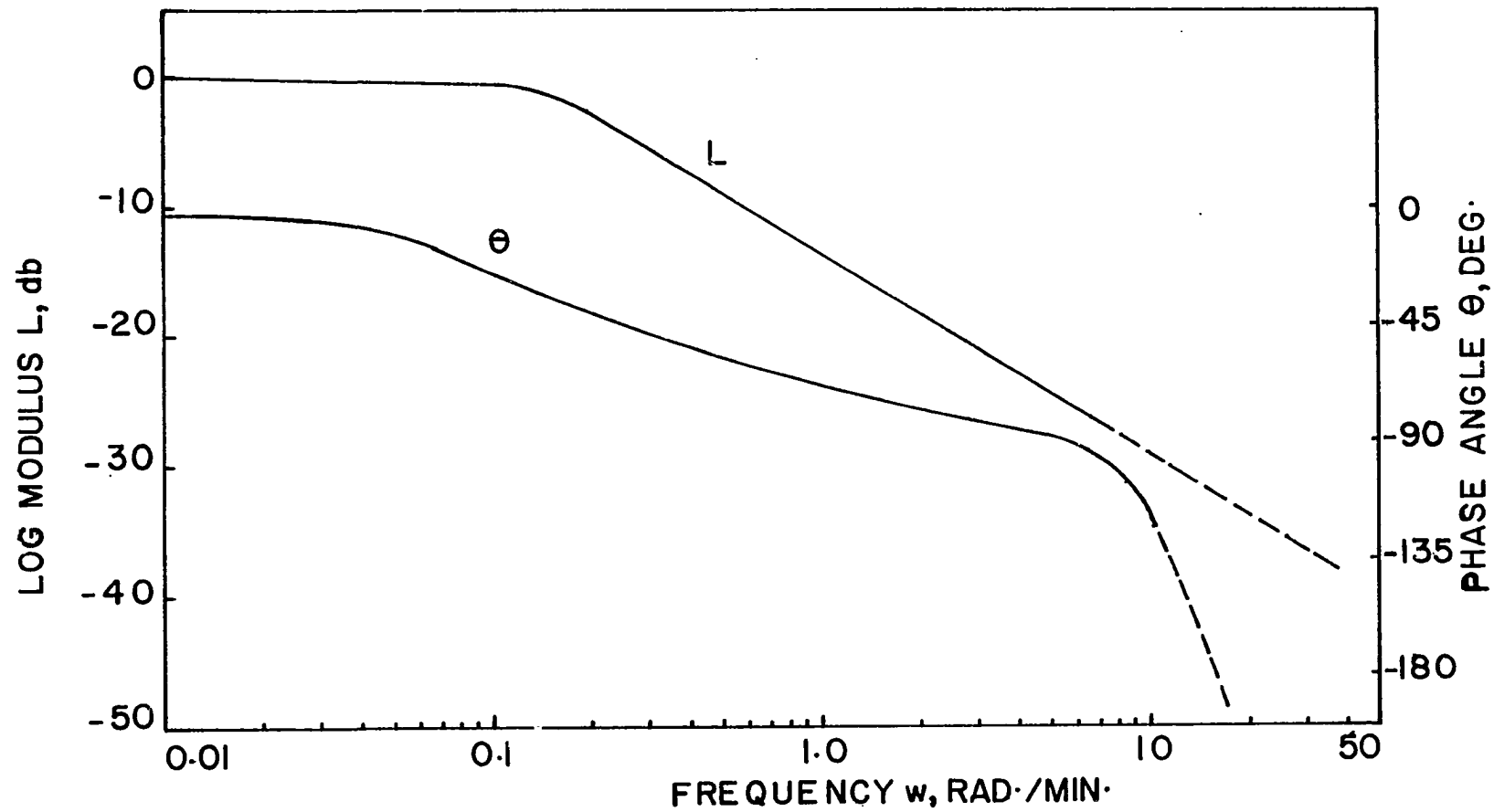

Figure (9-8) - Bode Plot of Control-Tray Temperature Transfer Function of Column 1 for a Pulse Change of +2% in Q_{R1}

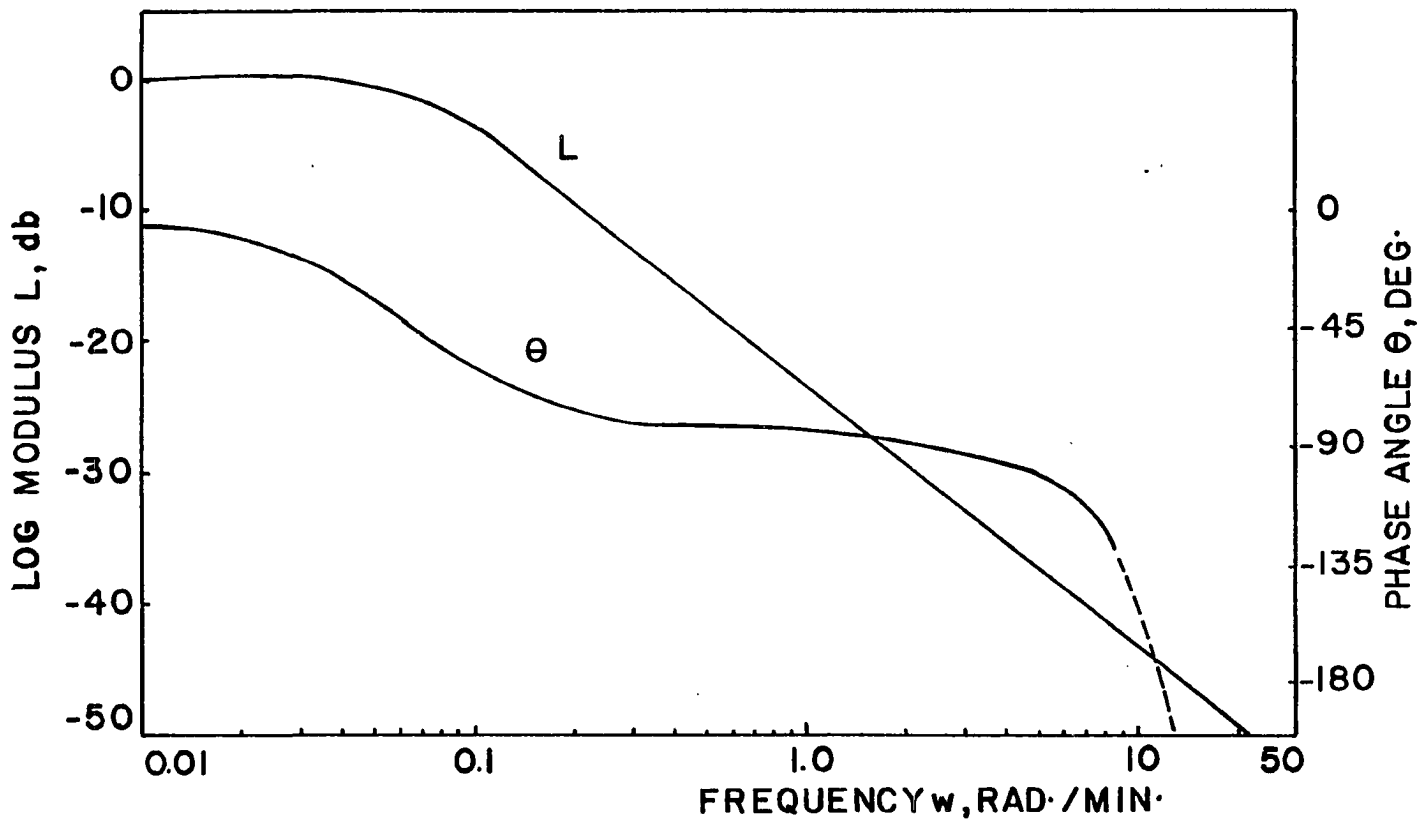

Figure (9-9) - Bode Plot of Control-Tray Temperature Transfer Function of Column 2 for a Pulse Change of -2% in Q_{R2}

TABLE (9-1): Summary of Pulse Test Results and Controllers Settings For Scheme 1

	Column 1	Column 2
Process gain, k_p, dimensionless	12.857	4.864
Process time constant, τ_p, min.	2.22	14.3
Process dead time, min.	0.1048	0.1495
Ultimate gain, k_u	3.096	30.76
Ultimate frequency, ω_u, rad/min	15.27	10.55
Ultimate period, P_u, min.	0.412	0.596

PI-Controller settings	k_c	$\tau_{I,min.}$	k_c	$\tau_{I,min.}$
Ziegler-Nichols	1.408	0.343	13.843	0.537
Design	1.189	0.103	13.482	0.163

All process and controller gains are dimensionless, assuming temperature transmitter gains of 12 psi/50°C and valve gains equal to the steady-state values of reboiler duties. It is clear from Table (9-1) that column 1 has higher process gain and lower process time constant than column 2. Thus, column 1 should respond faster than column 2, and its controller should have lower gain and time constant than column 2. See the controllers settings in Table (9-1). The transfer functions for this scheme are shown in Table (9-2.a).

For Scheme 3, the pulse test was done by making a 10% change in distillate flow rate, for each column, at a pulse width of 3 minutes, assuming perfect reflux drum level control. The Bode plots for this test are shown in Figures (9-10) and (9-11), for columns 1 and 2,

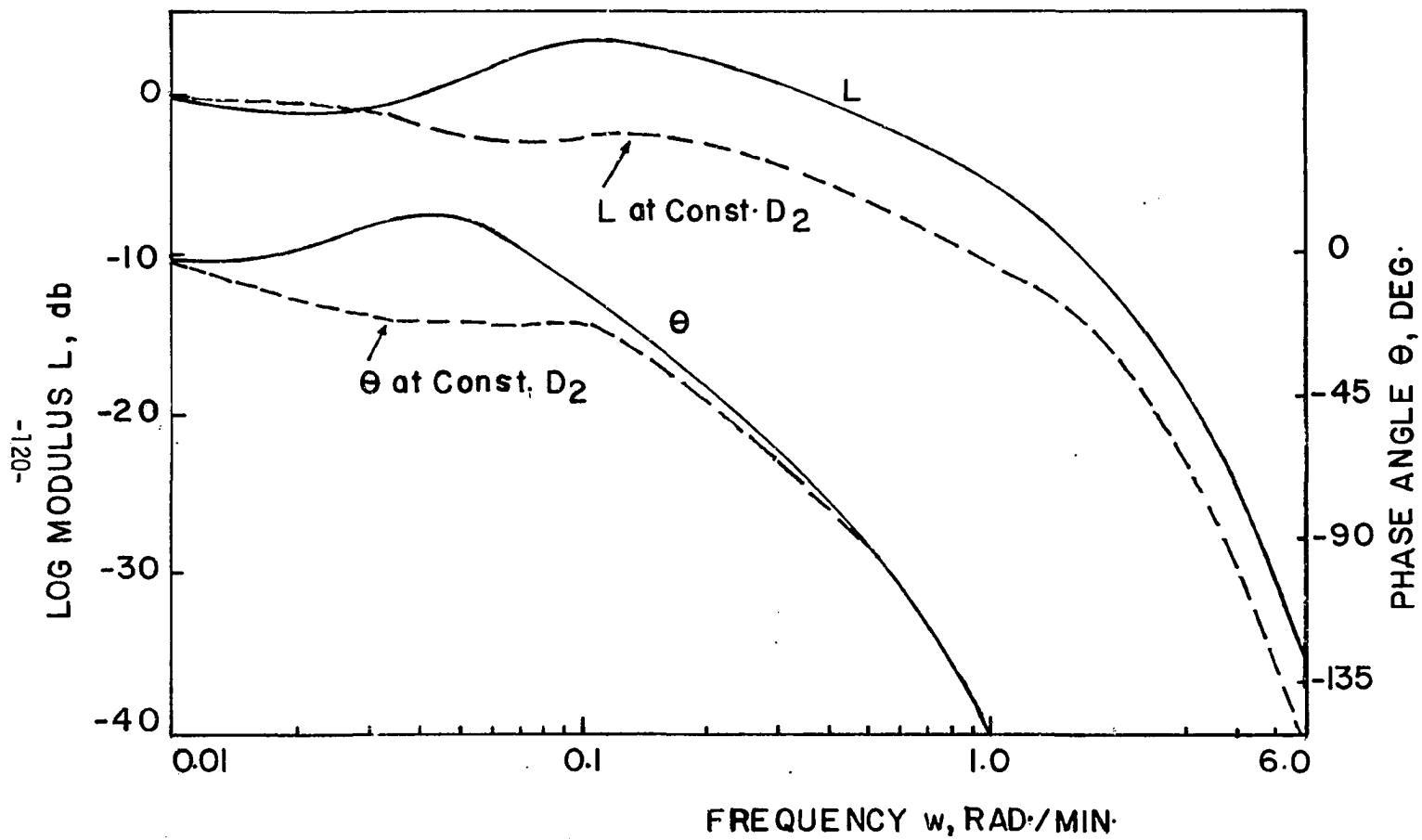

Figure (9-10) - Bode Plot for Control-Tray Temperature Transfer Function of Column 1 for a 10% Pulse Change in D_1

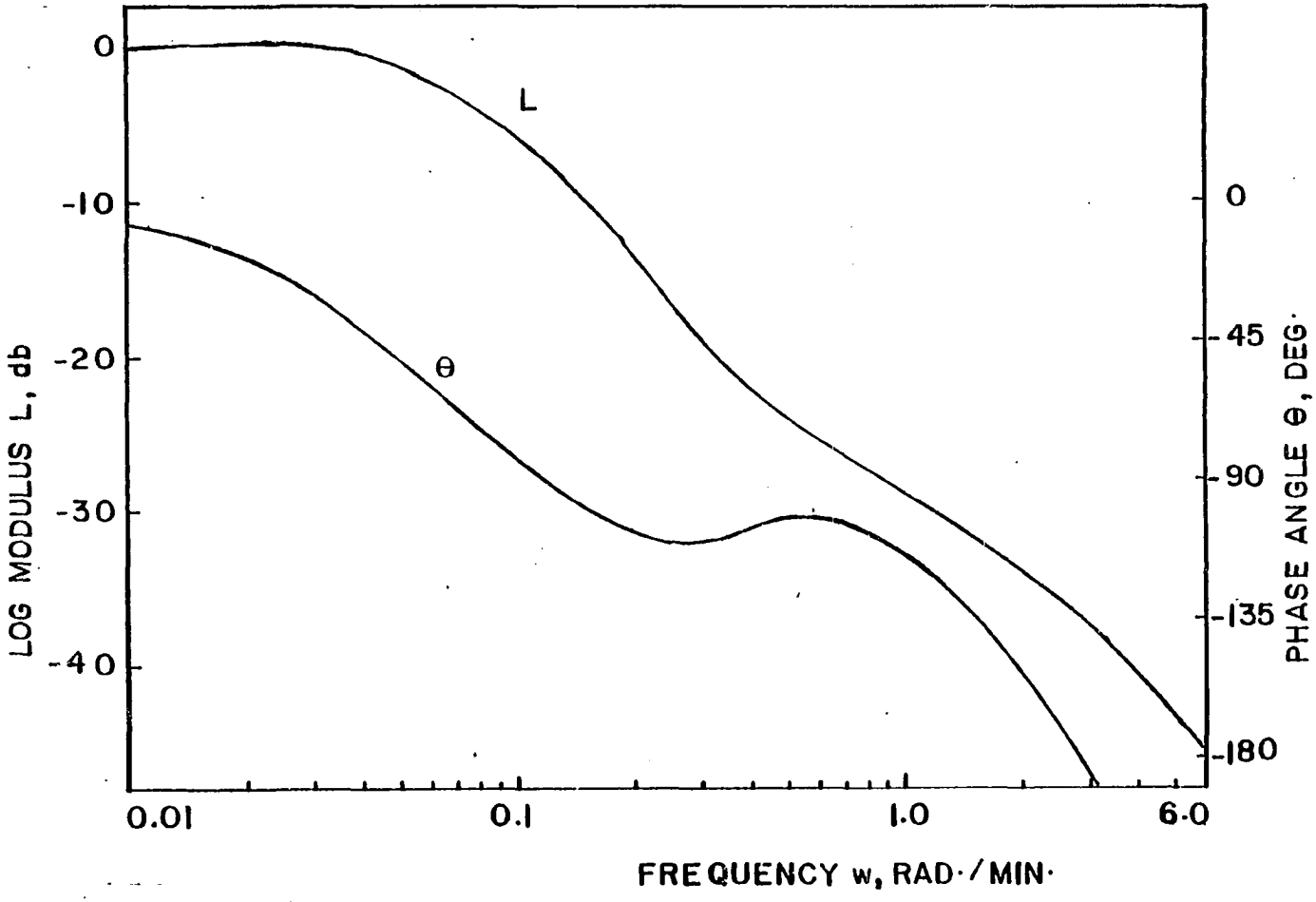

Figure (9-11) - Bode Plot for Control-Tray Temperature Transfer Function of Column 2 for a 10% Pulse Change in D_2

TABLE (9-2): Open-Loop Transfer Functions for Schemes 1 and 3

a - Scheme 1

$$\frac{T_1(2)}{Q_{R1}} = \frac{12.857\ e^{-.1048s}}{(2.22s+1)}$$

$$\frac{T_2(6)}{Q_{R2}} = \frac{4.864\ e^{-.1495s}}{(14.3s+1)}$$

b - Scheme 3

$$\frac{T_1(2)}{D_1} = \frac{1.117(22.22s+1)\ e^{-1.468s}}{(.49s+1)(100s^2+12s+1)}$$

$$\frac{T_2(6)}{D_2} = \frac{1.4815\ e^{-.557s}}{(18.15s+1)}$$

For $T_i(j)$: i refers to column number,

j refers to control tray number

respectively. As shown in Figure (9-10) the response of the transfer function relating the control-tray temperature and distillate flow rate for column 1 is underdamped at a breakpoint frequency of about 0.1 rad/min (τ_p = 10 min) and has a damping coefficient of 0.6. See solid L-curve in Figure (9-10). Also, as shown by the solid θ-curve of the same figure, the transfer function has a lead at a frequency of 0.55 rad/min. (τ_Z = 18.15 min). The transfer functions for this

scheme are listed in Table (9-2.b). Summary of the pulse test results and controllers settings are shown in Table (9-3).

TABLE (9-3) Summary of Pulse Test Results and Controllers Settings for Scheme 3

	Column 1	Column 2
Process gain, k_p, dimensionless	1.117	1.482
Process time constant, τ_p, min	0.49	18.15
Process dead time, min	1.468	0.557
Process damping coefficient, ζ	0.6	-
Process lead time constant, τ_Z,min	22.22	-
Ultimate gain, k_u	2.197	47.785
Ultimate frequency, ω_u, rad/min	1.28	2.82
Ultimate period, P_u, min	4.909	2.228

PI - Controller settings	k_c	τ_I,min	k_c	τ_I,min
Ziegler - Nichols	0.989	4.091	21.50	1.857
Design	1.410	11.194	15.82	0.55

The extraordinary behavior of this system (underdamped and having a lead) was attributed to changes in the recycle stream flow rate, D_2. When the distillate fed from column 1 to column 2, D_1, was changed, the recycle stream flow rate, D_2, would also change and affect the first column. To prove this, D_2 was fixed and the pulse test of D_1 was repeated. The results of this are as shown by the dotted L- and θ curves in Figure (9-10). In this case, both the underdampness and lead were elminated.

9.5 Evaluation of the Control Scheme

The three control schemes described above were tested on the non-linear dynamic model. The system was disturbed (by three different disturbances) to evaluate the performance of these schemes.

I. Feed Rate Disturbance: At time = 0 feed rate was changed by 25% (from $2x10^6$ to $2.5x10^6$ or $2x10^6$ to $1.5x10^6$ gmol/hr).

II. Feed Composition Disturbance: THF in the feed was changed by 50% (from 0.06 to .09 or .06 to .03).

III. Periodic Disturbance in Feed Composition: Recovery of THF from mixtures with air is usually carried by adsorption on activated carbon beds [5]. When one adsorber becomes saturated with solvent, the vapor-air flow is switched to another bed. This typically occurs every hour. Solvent is then removed from the saturated unit by passing low pressure steam through the bed where steam vaporizes the solvent and carries it from the adsorber. The effluent from the adsorber is fed to a tank before being fed to the separation unit. Assuming constant holdup in the tank (flow in = flow out) of 3 hours, a typical shape of the input and output curves of the feed composition is shown in Figure (9-12). This periodic change in feed composition will be used to examine the behavior of control scheme 1.

9.6 Comparison of the Control Schemes

In making these comparisons we have to remember that we want to

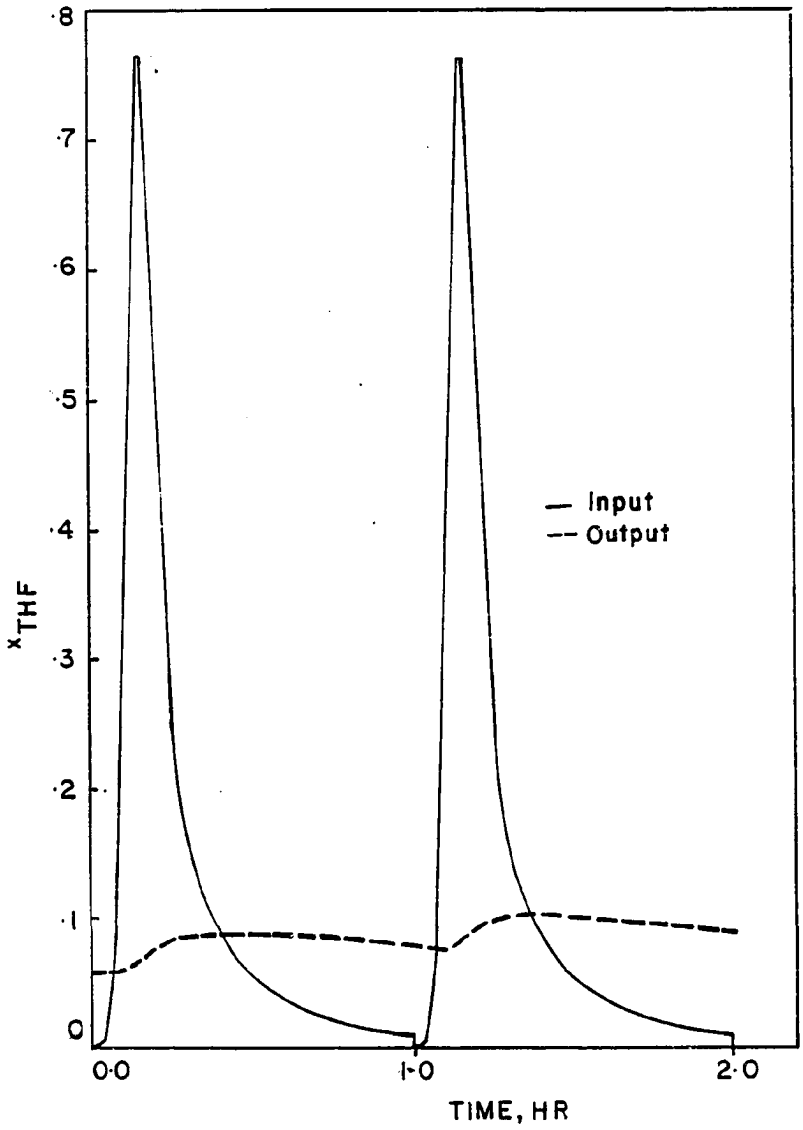

Figure (9-12) - Periodic Change in Feed Composition In and Out of the Feed Tank

keep no more than 10-100 ppm THF ($1x10^{-5}$ - $1x10^{-4}$) in column 1 bottom product and up to 500 ppm H_2O ($5x10^{-4}$) in column 2 bottom product. At the same time, we want to keep the distillate compositions near their optimum in order to minimize total energy required.

Figures (9-13) through (9-15) show the response of the three control schemes described earlier, for a 25% increase in feed rate. All schemes gave satisfactory performance. For a 100% increase in feed rate, scheme 2 had almost the same performance as scheme 1 but it required 7.8% more energy. Scheme 3 had similar energy requirement as scheme 1 but its deviation from steady state were bigger and lasted longer.

When a 50% decrease in feed composition was applied on the three schemes, the results are as shown in Figures (9-16) and (9-17) for schemes 1 and 2, respectively. Here, both schemes showed satisfactory performance, but again, the total energy required for scheme 1 is about 15% less than that required by scheme 2. Scheme 3 could not handle that much decrease in feed composition because a sharp decrease was noticed in the liquid flowing from trays 4 and 5 of column 1, as shown in Table (9-4) for a 25% decrease in feed composition. This was the maximum disturbance in feed composition that this scheme could handle without having the trays being dried. The performance of this scheme is shown in Figure (9-18).

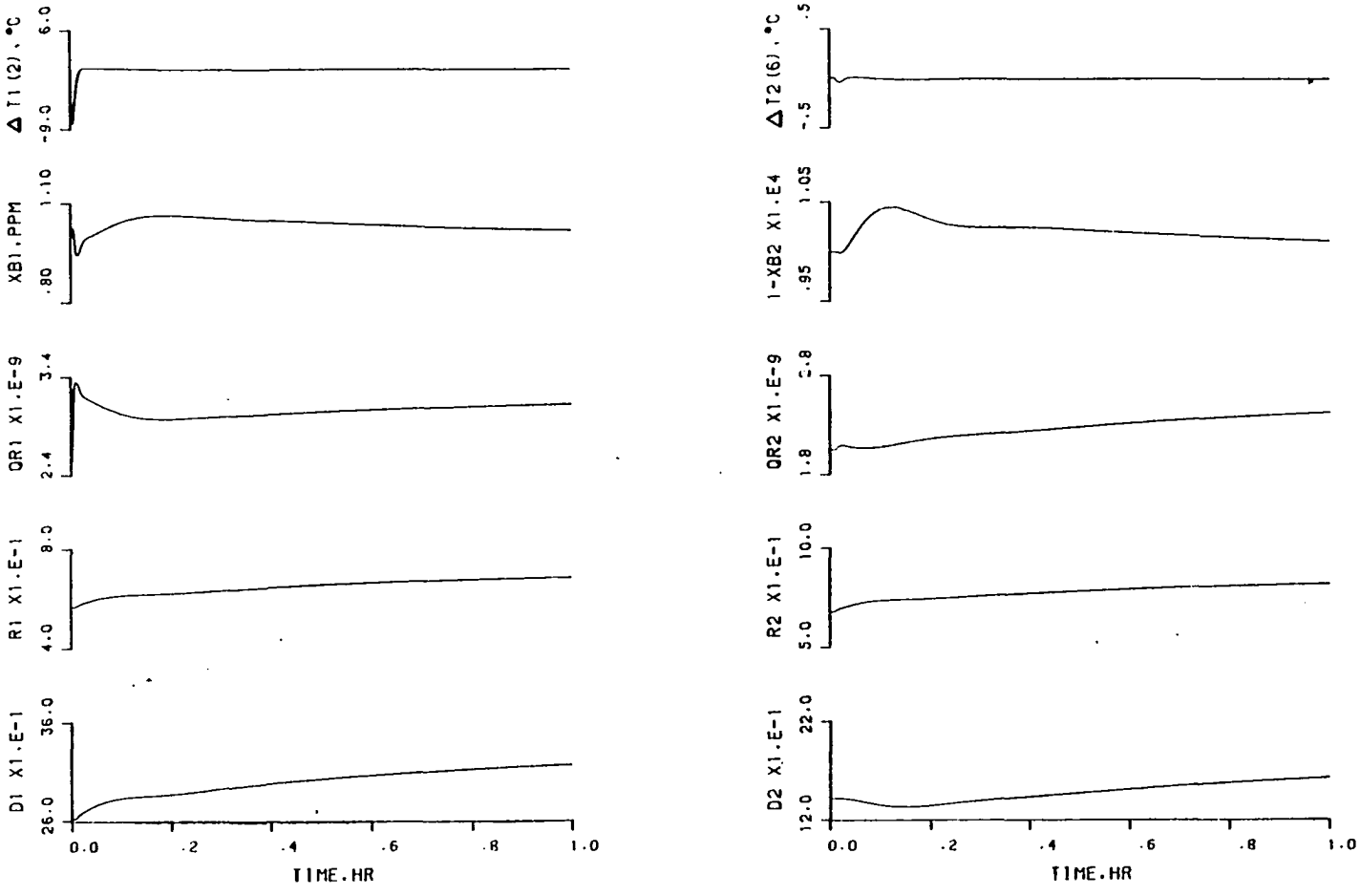

Figure (9-13) - Response of the Two-Column System to +25% Change in Feed Rate Using Scheme 1

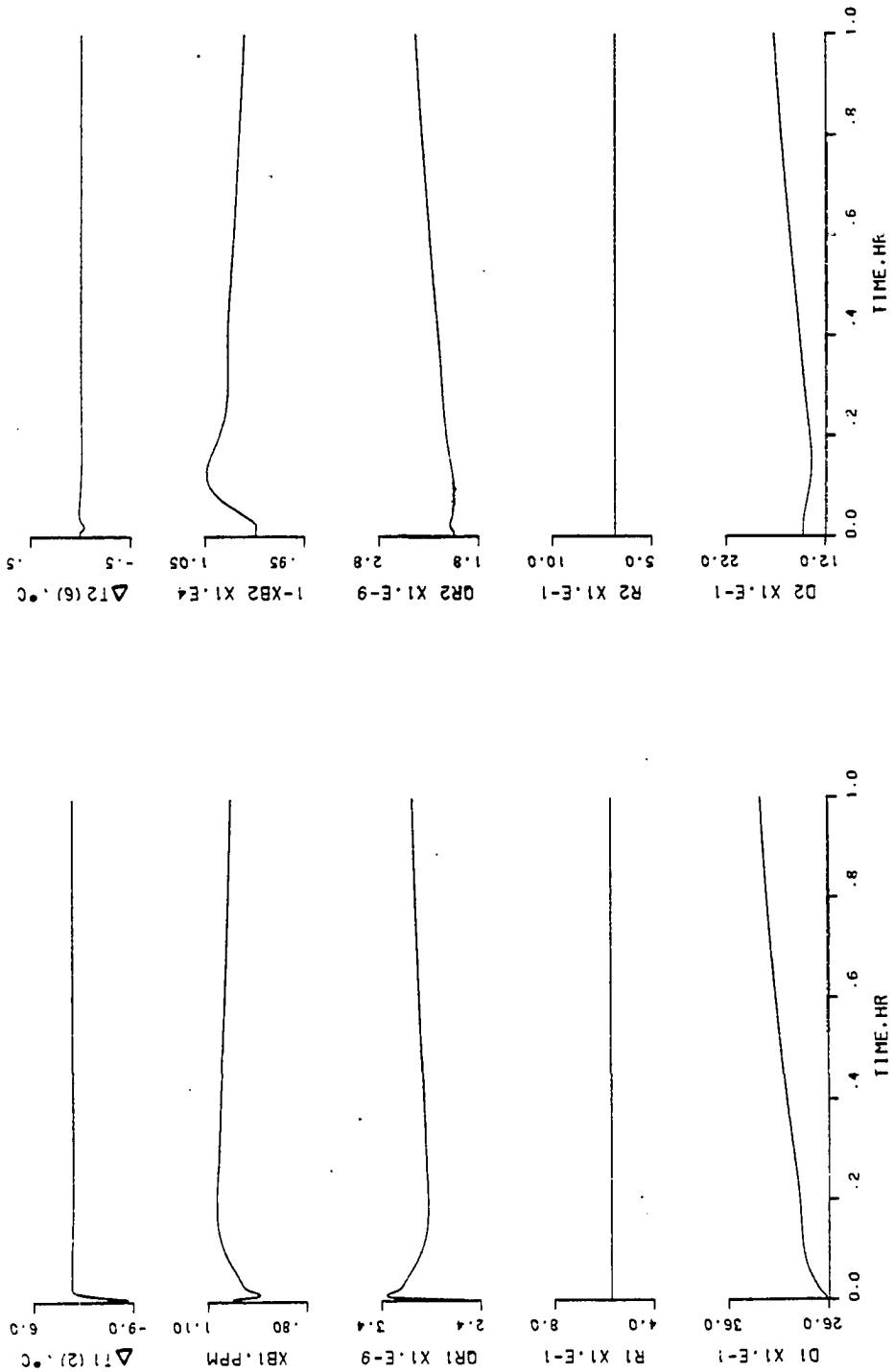

Figure (9-14) - Response of the Two-Column System to +25% Change in Feed Rate Using Scheme 2

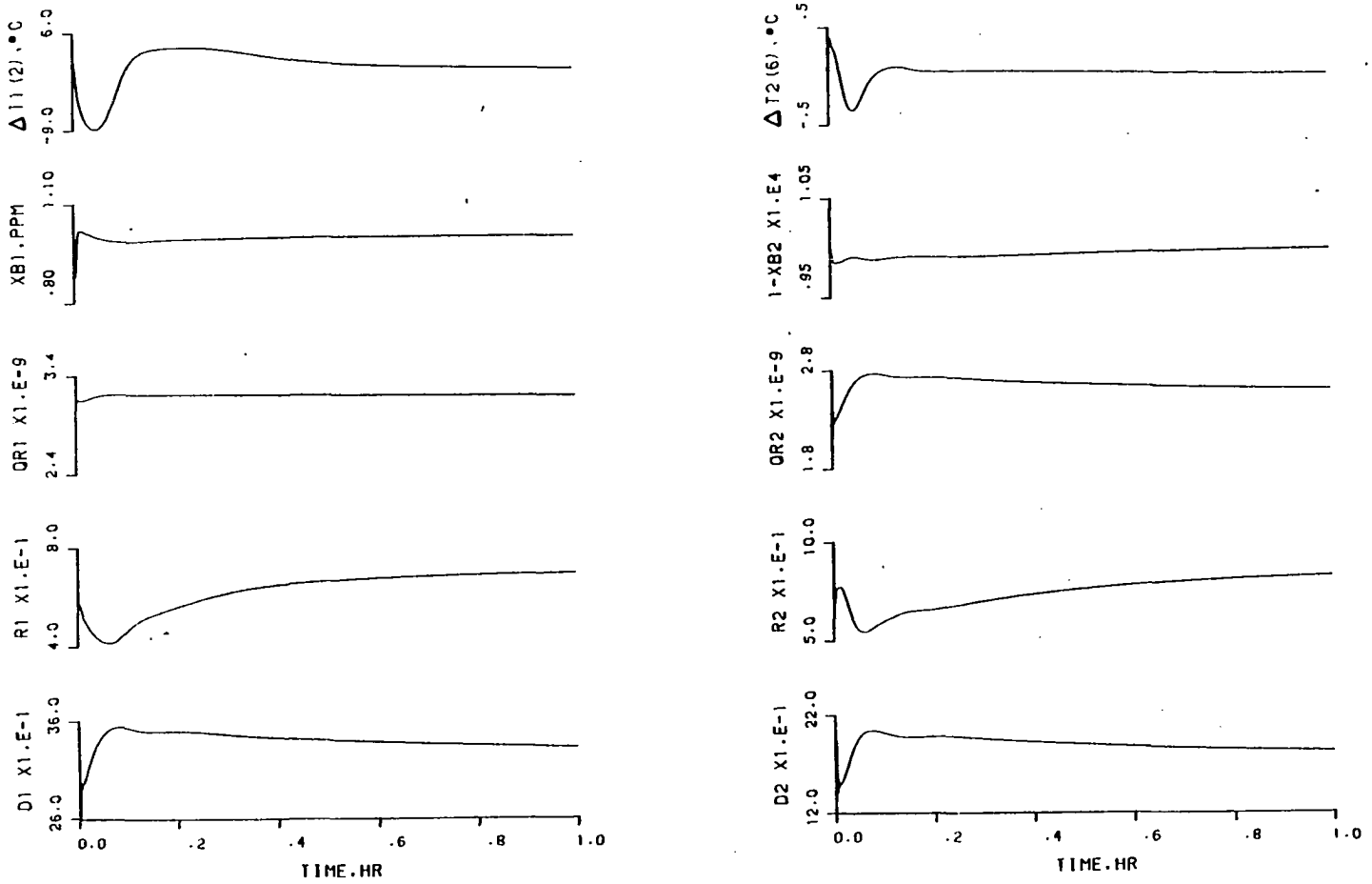

Figure (9-15) - Response of the Two-Column System to +25% Change in Feed Rate Using Scheme 3

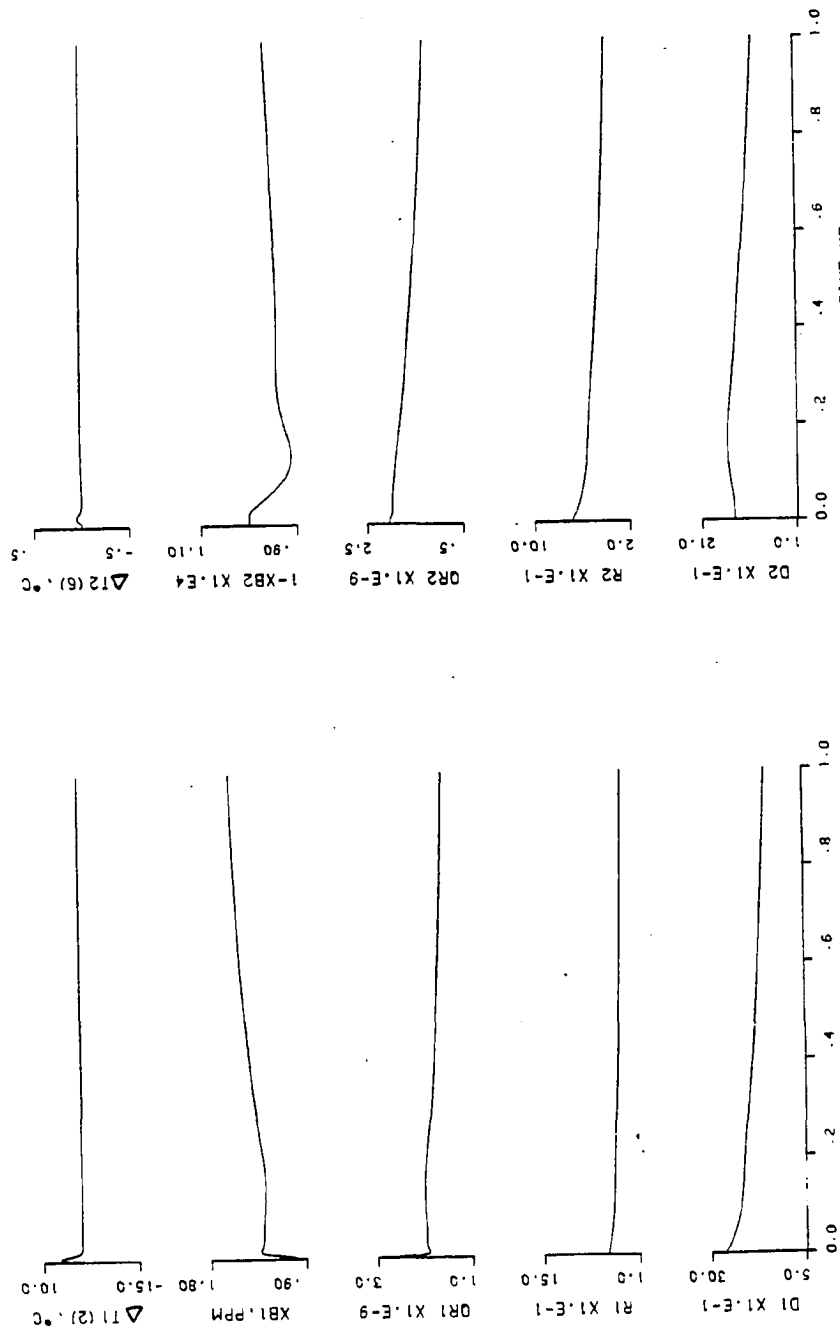

Figure (9-16) - Response of the Two-Column System to -50% Change in Feed Composition Using Scheme 1

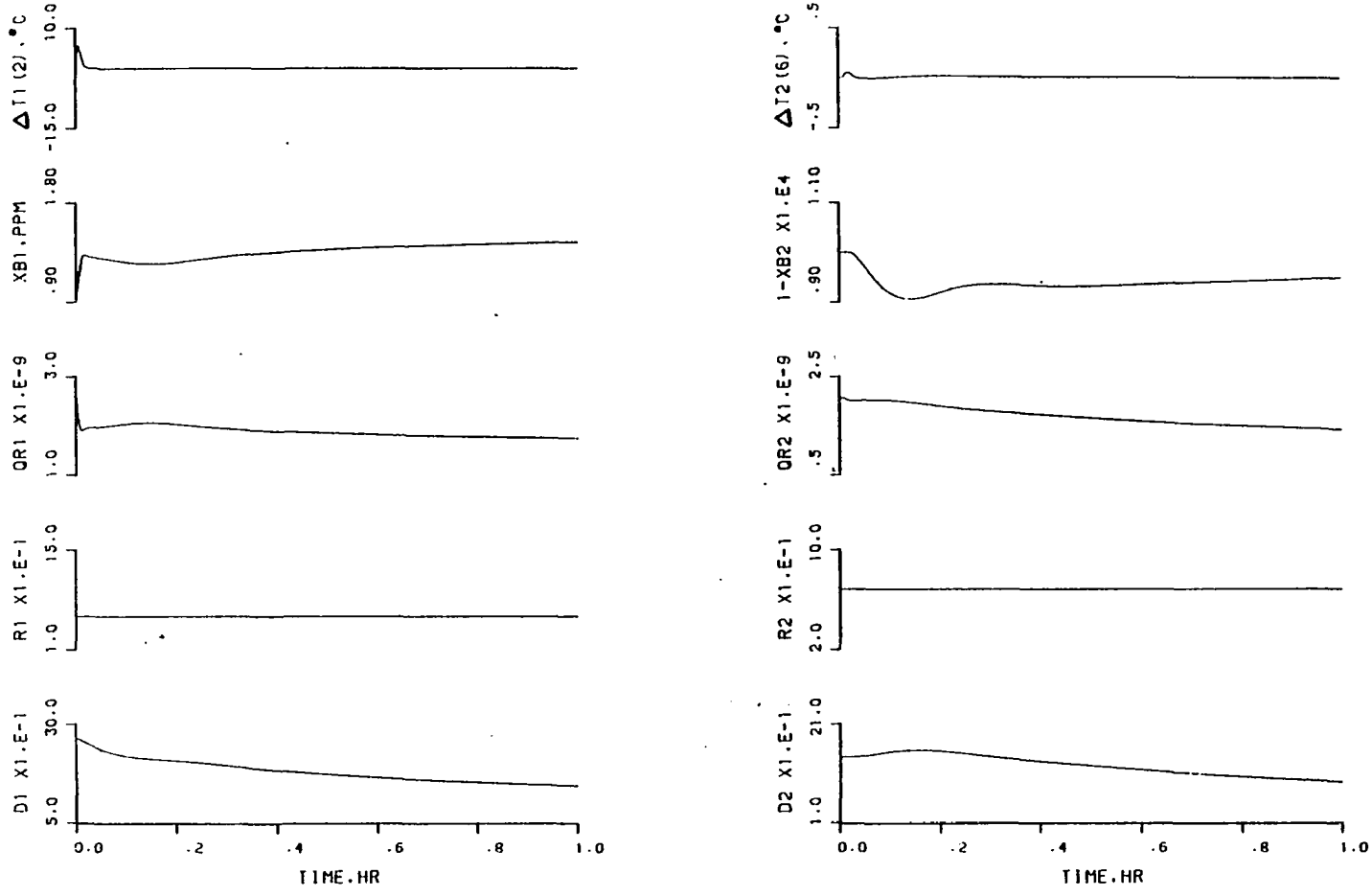

Figure (9-17) - Response of the Two-Column System to -50% Change in Feed Composition Using Scheme 2

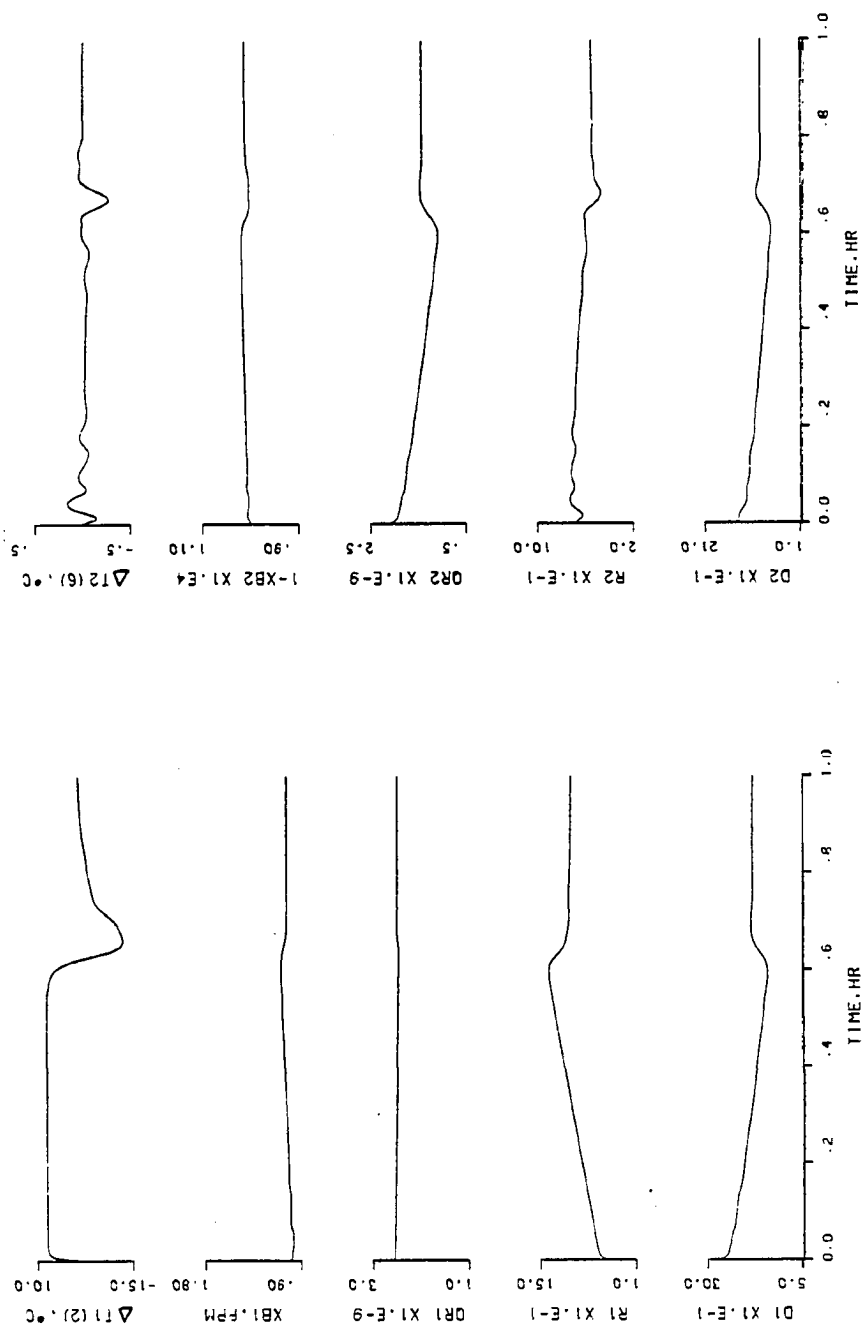

Figure (9-18) - Response of the Two-Column System to -25% Change in Feed Composition Using Scheme 3

TABLE (9-4): Variation of Liquid Flow Rate From Trays 4 and 5 of Column 1 for Control Schemes 1 and 3, for a 25% Decrease in Feed Composition

	Liquid flow rate, Kgmol/hr			
	Scheme 1		Scheme 3	
Time, min	Tray 4	Tray 5	Tray 4	Tray 5
0.0	148.77	60.60	148.77	60.60
0.6	142.99	60.92	95.09	58.77
1.2	150.19	60.99	55.80	58.15
1.8	149.67	60.39	42.43	63.53
2.4	148.96	59.80	42.58	67.89
3.0	148.80	59.39	45.69	67.47
3.6	148.94	59.13	71.04	51.03
4.2	149.18	58.93	88.07	23.83
4.8	149.42	58.76	80.90	13.46
5.4	149.63	58.61	75.25	8.56
6.0	149.79	58.48	71.71	5.96
12.0	- -	- -	104.80	45.88
24.0	- -	- -	136.42	82.89

The constant reflux scheme was tested using a proportional-integral level controller (K_C = .5, τ_I = 5.0 min.), instead of the proportional-only level controller, on the reflux drum of both columns. The response of the system is as shown in Figure (9-19). In this case, the system becomes more oscillatory and the deviations lasts longer. Compare Figures (9-17) and (9-19).

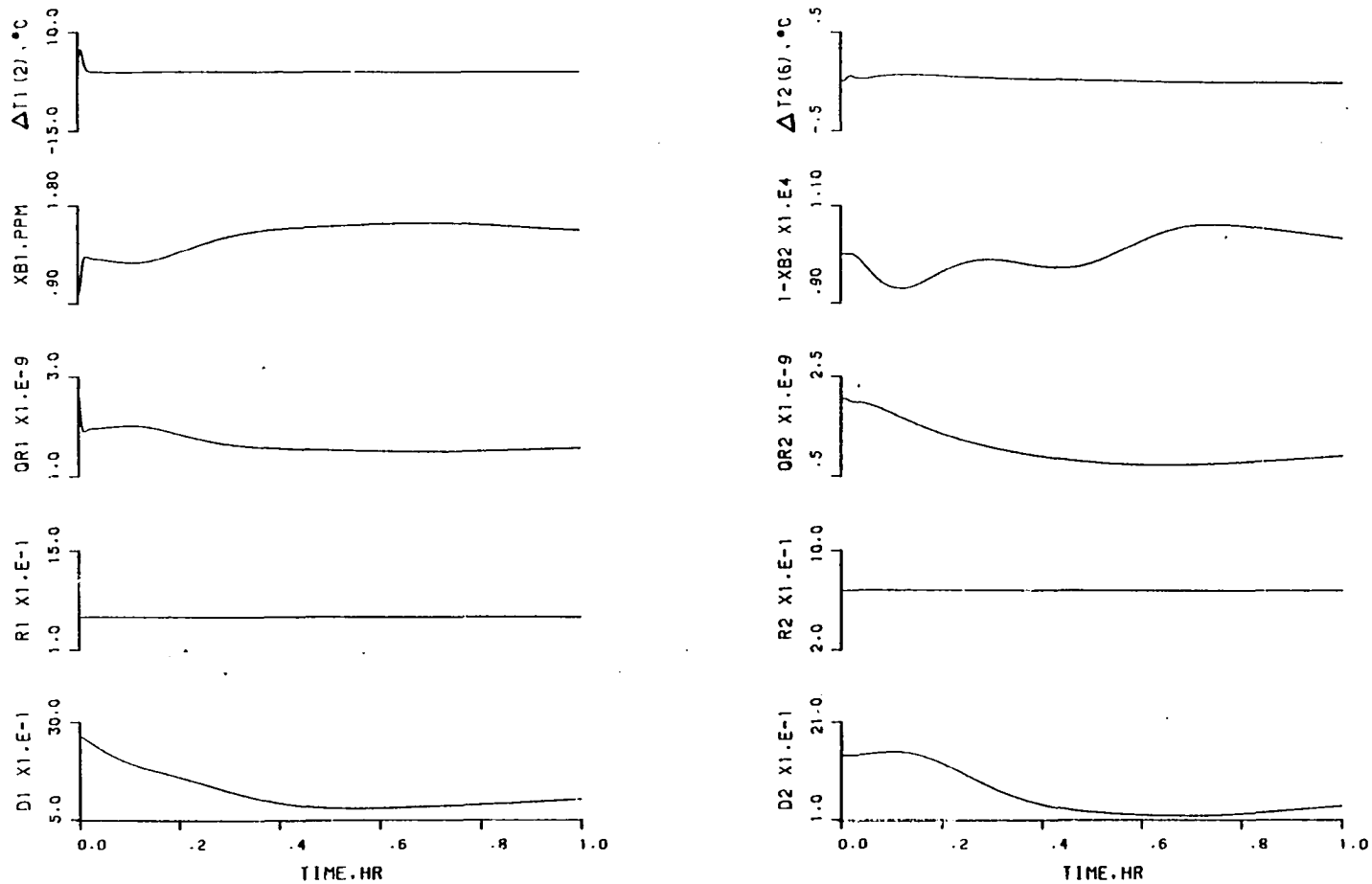

Figure (9-19) - Response of the Two-Column System with a PI-Level Controller on Reflux-Drum Level to -50% Change in Feed Composition Using Scheme 2

Lastly, the performance of scheme 1 was tested by introducing a periodic change in feed composition for 4 cycles (hours). This was done for a feed tank holdup of 3 and 1.5 hours, and proved satisfactory. See Figures (9-20) and (9-21). This means that we can use a smaller tank if necessary.

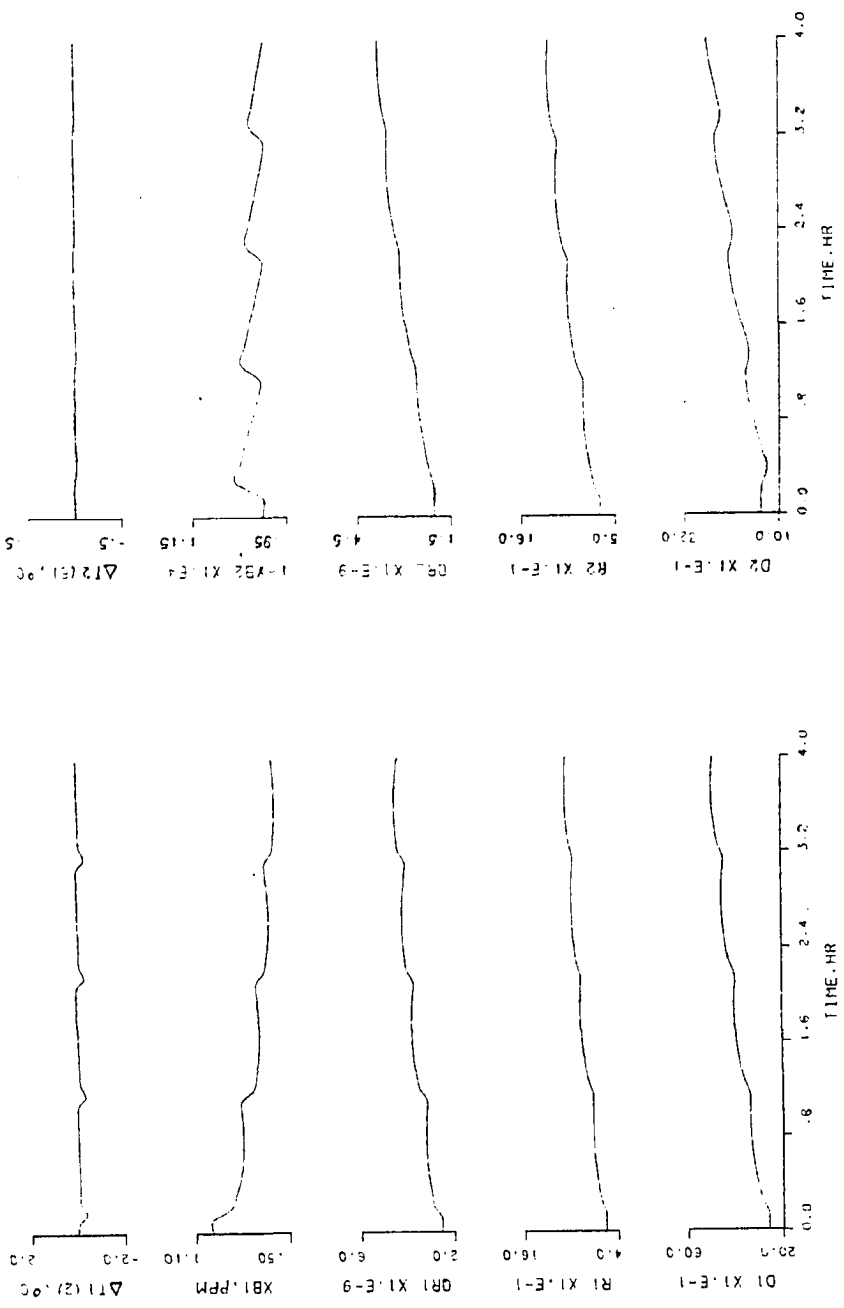

Figure (9-20) - Response of the Two-Column System to a Periodic Change in Feed Composition Using Scheme 1 (For a Feed Tank Holdup of 3 Hrs.)

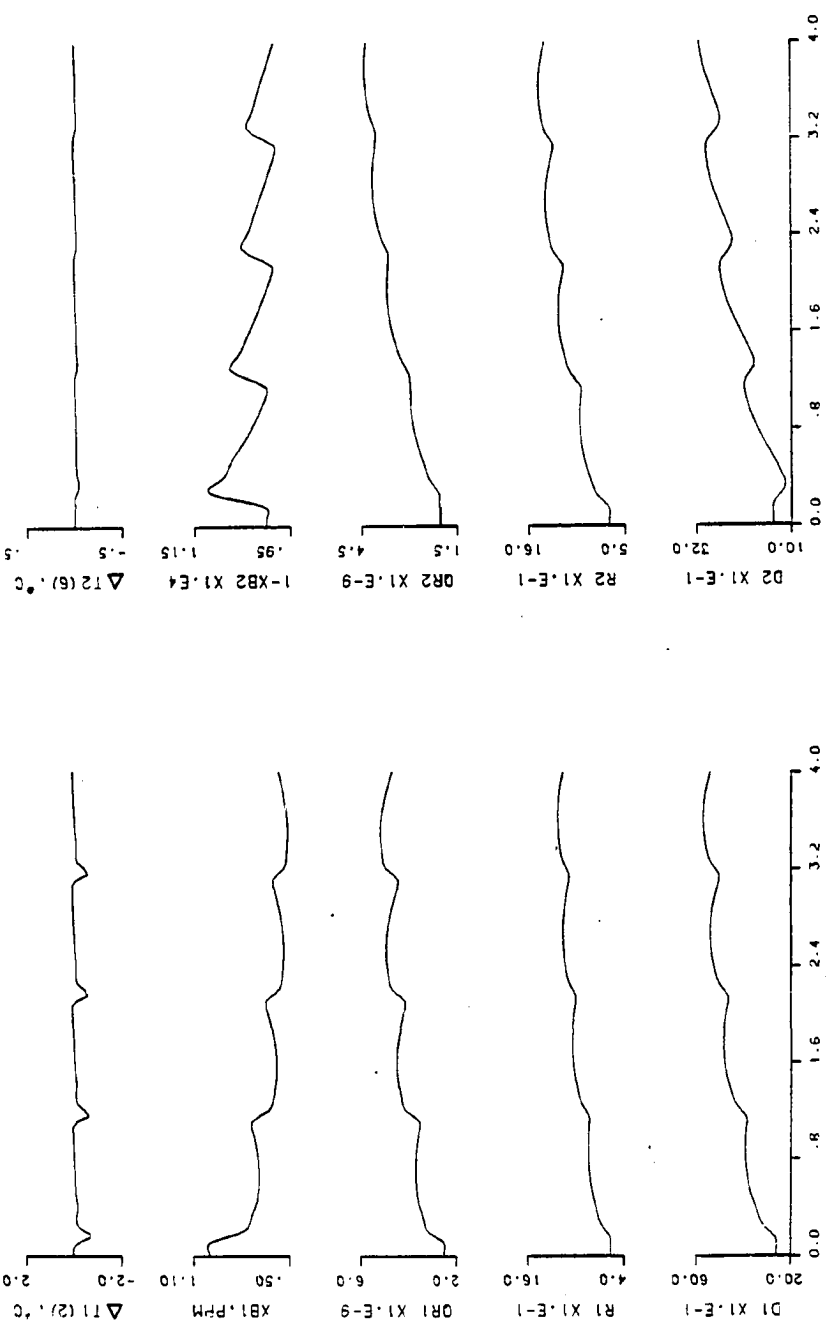

Figure (9-21) - Response of the Two-Column System to a Periodic Change in Feed Composition Using Scheme 1 (For a Feed Tank Holdup of 1.5 Hrs.)

CHAPTER 10

CONCLUSIONS AND RECOMMENDATIONS

This study has primarily been concerned with the steady-state design aspects and the dynamics and control of a two-column system operating at two different pressures used for the separation of minimum-boiling homogenous binary azeotropes. The tetrahydrofuran-water mixture was studied as an example. The vapor-liquid equilibria for the THF-water system was predicted using Wilson's equations for activity coefficients.

The results of the steady-state investigation lead to the following conclusions:

a) The low-pressure column is more sensitive to changes in design parameters, such as reflux ratio and distillate composition, than the high pressure column due to the presence of a pinch in its VLE curve.

b) Reducing the first column pressure and/or increasing that of the other, reduces the total energy requirement.

c) At fixed columns' pressure, there is an optimum distillate composition where the total energy required is minimized. This optimum is flat and has much less effect on the system, compared with that of pressure.

d) Preheating the feeds of the columns via hot product streams saves up to 10% of the total energy required.

e) Using the second column overhead vapor to reboil column 1 saves up to 30% of the total energy required.

f) There is always a combination of the columns pressures that minimizes the total energy required by the system. The lowest pressure that can be used in column 1 while still being able to use cooling water in the overhead condensers is 350 mmHg. This corresponds to 150 psig in the second column.

g) The optimum pressure case with energy integration and heat economizers [II.4] consumes up to 55% less energy than the base case [I.1] and the annual capital cost is about 20% less than the base case.

h) Operating the columns at a reflux ratio of 1.2 times the minimum was confirmed to be a good choice by economic evaluation.

Dynamically, the control scheme developed, using the steady-state energy conservation aspects, was to control the ratios of reflux to distillate in the first column and reflux to feed in the second column, and to control temperatures in each column on chosen tray locations by heat inputs. The performance of the system was examined and proved satisfactory. It handled big distrubances in feed rate and composition and periodic changes in feed composition for tank holdups of 1.5 and 3 hrs. It was better and more energy efficient than the constant reflux scheme and Shinskey's material-balance scheme.

Lastly, the optimum pressure scheme with energy integration and heat economizers (Case II.4) is recommended to be used in building new THF-water separation plants. Its energy consumption is much less than the standard configuration currently used in industry.

BIBLIOGRAPHY

[1] Billet, R., 1979. Distillation Engineering. Chemical Publishing Co., New York.

[2] Buckley, P. S., 1974. Material Balance Control in Distillation Columns, AIChE Workshop on Industrial Process Control, November.

[3] Buckley, P. S. 1981. Control of Heat-Integrated Distillation Columns, Engineering Foundation Conference on Chemical Process Control, Sea Island, Georgia, Jan. 18-23.

[4] Cigna, R. and Sebastiani, E., 1964. Ann. Chim. (Rome), 54:1048.

[5] E. I. du Pont de Nemours and Co., 1962. Electrochemical Department, Wilmington, Delaware.

[6] Fuentes, C., 1980. Control of High Purity Distillation Columns. Ph.D. Dissertation, Lehigh University, Bethlehem, PA.

[7] Glew, D. N. and Watts, H., 1973. Can. J. Chem., 51:1933.

[8] Gmehling, J. and Onken, U., 1977. VLE Data Collection, Aqueous Organic Systems, Vol. 1, Part 1, Dechema, W. Germany.

[9] Hayduk, W., Landie, H. and Smith, O.H., 1973. J. Chem. Eng. Data, 18(4):373.

[10] Hirata, M., Ohe, S. and Nagahama, K., 1975. Computer Aided Book of Vapor-Liquid Equilibria. Kodansha Ltd., Tokyo, Japan.

[11] Hoffman, E. J., 1964. Azeotropic and Extractive Distillation. John Wiley and Sons, New York.

[12] King. C. J., 1971. Separation Processes. McGraw-Hill, New York.

[13] Kiyohara, O., D'Arcy, P. J. and Benson, G. C., 1979. Can. J. Chem., 57:1006.

[14] Kiyohara, O., D'Arcy, P. J. and Benson, G. C., 1978, Can. J. Chem., 56:2803.

[15] Kiyohara, O. and Benson, G. C., 1977. Can. J. Chem., 55:1354.

[16] Kudchadker, A. P., Kudchadker, S. A. and Wilhoit, R. C., 1978. Key Chemicals Data Book, Furan, Dihydrofuran and Tetrahydrofuran. Thermodynamic Research Center, Texas A&M University, May.

[17] Lampa, J., Matous, J., Novak, J. P. and Pick, J., 1980. Coll. Czech. Chem. Commun., 45:1162.

[18] Lebedev, B. V., Rabinovich, I. B., Milov, V. I. and Lityagov, V. Ya, 1978. J. Chem. Thermodynamics, 10:321.

[19] Luyben, W. L. , 1973. Process Modeling, Simulation and Control for Chemical Engineers, McGraw-Hill, New York.

[20] Luyben, W. L., 1975. Ind. Eng. Chem., Fundam., 14(4):321.

[21] Lybarger, H. M., 1972. Ternary Vapor-Liquid Equilibrium Data Applied to the Separation of a Mixture of Water, Methyl Ethyl Ketone, and Tetrahydrofuran. M.S. Thesis, Univ. of Akron, March.

[22] Madhavan, P. R., Lakshman, C. M. and Laddha, G. S., 1976. Indian J. Tech., 14(10):461.

[23] Matous, J., Novak, J. P., Sobr, J. and Pick, J., 1972. Coll. Czech. Chem. Commun. 37:2653.

[24] Matous, J., Henrick, J., Novak, J. P. and Sobr, J., 1970. Coll. Czech. Chem. Commun., 35:1904.

[25] Miller, J. S. and Kapella, W. A., 1977. Chem. Eng., 84(8):129, April 11.

[26] Modell, M. and Reid, R. C., 1974. Thermodynamics and Its Applications. Prentice-Hall, Inc., New Jersey.

[27] Nakayama, H., 1970. Bull. Chem. Soc. Japan, 43(6):1683.

[28] Nakayama, H. and Shinoda, K., 1971. J. Chem. Thermodynamics, 3:401.

[29] Orye, R. V. and Prausnitz, J. M., 1965. Ind. Eng. Chem., 57(5):18.

[30] Perry, J. H., 1950. Chemical Engineer's Handbook, 3rd ed., McGraw-Hill, New York.

[31] Peters, M. S. and Timmerhaus, K. D., 1980. Plant Design and Economics for Chemical Engineers, 3rd. ed., McGraw-Hill, New York.

[32] Pinder, K. L., 1973. J. Chem. Eng. Data, 18(3):275.

[33] Private Communication, 1980. From R. B. Akell and R. E. Vallerschamp

[34] Robinson, C. S. and Gilliland, E. R., 1950. Elements of Fractional Distillation. McGraw-Hill, New York.

[35] Scheiman, A. D., 1969. Hydrocarbon Proc., 48:187, September.

[36] Scott, D. W., 1970. J. Chem. Thermodynamics, 2:833.

[37] Shinskey, F. G., 1977. Distillation Control. McGraw-Hill, New York,

[38] Shnitko, V. A. and Kogan, V. B., 1968. J. Appl. Chem. of USSR, 41:1236.

[39] Signer, R., Arm, H. and Daeniker, H., 1969. Helv. Chim. Acta, 52:2347.

[40] Smith, B. D., 1963. Design of Equilibrium Stage Processes, McGraw-Hill, New York.

[41] Smith, J. M. and Van Ness, H. C., 1975. Introduction to Chemical Engineering Thermodynamics. 3rd ed., McGraw-Hill, New York.

[42] Tolliver, T. L. and McCune, L. C., 1978. ISA Transactions, 17(3):3.

[43] Treybal, R. E., 1968. Mass Transfer Operations. 2nd ed., McGraw-Hill, New York.

[44] Tsuboka, T. and Katayama, T., 1975. J. Chem. Eng. Japan, 8(3):181.

[45] van Winkle, M., 1967. Distillation. McGraw-Hill, New York.

[46] Wilson, G. C., 1964. Am. Chem. Soc., 86:127.

[47] Yoshida, S., Miyajima, M., Ito, M., Sudo, N. and Saito, T., 1979. Mitsubishi Chemical Industries Co., Ltd., Japan. Chemical Abstract, 90:598.

APPENDIX

TABLE 1: Physical Properties of Tetrahydrofuran (THF)

Chemical Formula

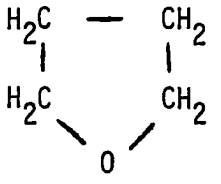

Molecular weight		72.108
Specific gravity 20°/4° °C		0.888
Boiling point (at 760 mmHg), °C		66.0
Specific heat:	liquid at 20°C	0.470
	liquid at 50°C	0.496
	vapor at 66°C	0.370
Latent heat of vaporization (at 760 mmHg),cal/g		98.1
Critical temperature, °C		268.0
Critical pressure , atm		51.2
Solubility parameter		9.1 , 9.52
Miscibility:	Water; esters; ketones; alcohols; diethylether; aliphatic; aromatic and chlorinated hydrocarbons	∞

TABLE 2: Physical Properties of Water

Chemical Formula	H - O - H
Molecular weight	18.016
Specific gravity 4°/4° °C	1.0
Boiling poing, °C	100.0
Specific heat: liquid at 100°C	1.007
vapor at 110°C	0.481
Latent heat of vaporization (at 760 mmHg)cal/g	539.55
Critical temperature, °C	374.4
Critical pressure, atm	218.3
Solubility parameter	23.5

VITA

Name: Samir Ibraheem Abu-Eishah

Date of Birth: October 28, 1951

Place of Birth: Anabta, West Bank - Jordan

Parents: Ibraheem and Najeebah Abu-Eishah

Education:

	Degree	Date
Cairo University, Cairo, Egypt	B.Sc.	July, 1975
Iowa State University, Ames, Iowa	M.S.	June, 1979

Experience:

Jordanian Petroleum Refinery Co., Zerqa-Jordan

October 1975 - August 1977